

Bosonic Spectral Function in HTSC Cuprates: Part I - Experimental Evidence for Strong Electron-Phonon Interaction

¹E. G. Maksimov, ^{2,3}M. L. Kulić, ⁴O. V. Dolgov

¹ *Lebedev Physical Institute, 119991 Moscow, Russia*

² *Goethe-Universität Frankfurt, Theoretische Physik,
60054 Frankfurt/Main, Germany*

³ *Max-Born-Institut für Nichtlineare Optik und Kurzzeitspektroskopie,
12489 Berlin, Germany*

⁴ *Max-Planck-Institut für Festkörperphysik,
70569 Stuttgart, Germany*

(Dated: September 12, 2021)

In *Part I* we discuss accumulating experimental evidence related to the structure and origin of the bosonic spectral function $\alpha^2 F(\omega)$ in high-temperature superconducting (HTSC) cuprates near optimal doping. Some global properties of $\alpha^2 F(\omega)$, such as number and positions of peaks, are extracted by combining optics, neutron scattering, ARPES and tunnelling measurements. These methods give convincing evidence for strong electron-phonon interaction (EPI) with $1 < \lambda \lesssim 3$ in cuprates near optimal doping. Here we clarify how these results are in favor of the Eliashberg-like theory for HTSC cuprates near optimal doping. We argue that the neglect of EPI in some previous studies of HTSC was based on a number of deceptive prejudices related to the strength of EPI, on some physical misconceptions and misleading interpretation of experimental results.

In *Part II* we discuss some theoretical ingredients which are necessary to explain the experimental results related to pairing mechanism in optimally doped cuprates. These comprise the Migdal-Eliashberg theory for EPI in strongly correlated systems which give rise to the forward scattering peak. The latter is due to the combined effects of the weakly screened Madelung interaction in the ionic-metallic structure of layered cuprates and many body effects of strong correlations. While EPI is responsible for the strength of pairing the residual Coulomb interaction (by including spin fluctuations) triggers the d-wave pairing.

PACS numbers:

I. INTRODUCTION

In spite of an unprecedentedly intensive experimental and theoretical study after the discovery of high-temperature superconductivity (HTSC) in cuprates there is, even twenty-two years after, no consensus on the pairing mechanism in these materials. At present there are two important experimental facts which are not under dispute: (1) the critical temperature T_c in cuprates is high, with the maximum $T_c^{\max} \sim 160$ K; (2) the pairing in cuprates is d-wave like, i.e. $\Delta(\mathbf{k}, \omega) \approx \Delta_s(k, \omega) + \Delta_d(\omega)(\cos k_x - \cos k_y)$ with $\Delta_s < 0.1\Delta_d$. On the contrary there is a dispute concerning the scattering mechanism which governs normal state properties and pairing in cuprates. To this end, we stress that in the HTSC cuprates, a number of properties can be satisfactorily explained by assuming that the quasi-particle dynamics is governed by some electron-boson scattering and in the superconducting state bosonic quasi-particles are gluing electrons in Cooper pairs. Which bosonic quasi-particles are dominating in the cuprates is the subject which will be discussed in this work. It is known that the electron-boson (phonon) scattering is well described by the Migdal-Eliashberg theory if the adiabatic parameter $A_B \equiv \lambda(\omega_B/W_b)$ fulfills the condition $A_B \ll 1$, where λ is the electron-boson coupling constant, ω_B is the characteristic bosonic energy and W_b is the electronic band width. The important characteristic of the

electron-boson scattering is the Eliashberg spectral function $\alpha^2 F(\mathbf{k}, \mathbf{k}', \omega)$ (or its average $\alpha^2 F(\omega)$) which characterizes scattering of quasi-particle from \mathbf{k} to \mathbf{k}' by exchanging bosonic energy ω . Therefore, in systems with electron-boson scattering the knowledge of this function is of crucial importance. There are at least two approaches differing in assumed gluing bosons. The first one is based on the electron-phonon interaction (EPI) [1], [2], [4], [5], [3] where mediating bosons are *phonons* and where the the average spectral function $\alpha^2 F(\omega)$ is similar to the phonon density of states $F_{ph}(\omega)$. Note, $\alpha^2 F(\omega)$ is not the product of two functions although sometimes one defines the function $\alpha^2(\omega) = \alpha^2 F(\omega)/F(\omega)$ which should approximate the energy dependence of the strength of the EPI coupling. There are numerous experimental evidence in cuprates which support the dominance of the EPI scattering mechanism with a rather large coupling constant $1 < \lambda^{ep} \lesssim 3$ and which will be discussed in detail below. In the EPI approach $\alpha^2 F(\omega)$ is extracted from tunnelling measurements in conjunction with IR optical measurements. We stress again that the Migdal-Eliashberg theory is well justified framework for EPI since in most superconductors the condition $A_{ph} \ll 1$ is fulfilled. The HTSC are on the borderline and it is a natural question - under which condition can high T_c be realized in the non-adiabatic limit $A_{ph} \sim 1$? The second approach [6] assumes that EPI is too weak to be responsible for high T_c in cuprates and it is

based on a phenomenological model for spin-fluctuation interaction (*SFI*) as the dominating scattering mechanism, i.e. it is a non-phononic mechanism. In this approach the spectral function is proportional to the imaginary part of the spin susceptibility $\text{Im} \chi(\mathbf{k} - \mathbf{k}', \omega)$, i.e. $\alpha^2 F(\mathbf{k}, \mathbf{k}', \omega) \sim \text{Im} \chi(\mathbf{k} - \mathbf{k}', \omega)$. NMR spectroscopy and magnetic neutron scattering give that in HTSC cuprates $\chi(\mathbf{q}, \omega)$ is peaked at the antiferromagnetic wave vector $Q = (\pi/a, \pi/a)$ and this property is favorable for d-wave pairing. The *SFI* theory roots basically on the strong electronic repulsion on Cu atoms, which is usually studied by the Hubbard model or its (more popular) derivative the t-J model. Regarding the possibility to explain high T_c solely by strong correlations, as it is reviewed in [7], we stress two facts. First, at present there is no viable theory which can justify these (non-phononic) mechanisms of pairing. Second, the central question in this approach is - do models based on the Hubbard Hamiltonian show up superconductivity at sufficiently high critical temperatures ($T_c \sim 100 K$)? A number of numerical studies of these models offer a negative answer. For instance, the sign-free variational Monte Carlo algorithm in the 2D repulsive ($U > 0$) Hubbard model gives no evidence for HTSC, neither the BCS- nor Berezinskii-Kosterlitz-Thouless (BKT)-like [8]. At the same time, similar calculations show that there is a strong tendency to superconductivity in the attractive ($U < 0$) Hubbard model for the same strength of U , i.e. at finite temperature in the 2D model with $U < 0$ the BKT superconducting transition is favored. Concerning HTSC in the *t-J* model, various numerical calculations such as Monte Carlo calculations of the Drude spectral weight [9] and high temperature expansion [10] have shown that there is no superconductivity at temperatures characteristic for cuprates and if it exists T_c must be rather low - few Kelvins. These numerical results tell us that the lack of high T_c (even in 2D BKT phase) in the repulsive ($U > 0$) single-band Hubbard model and in the *t-J* model is not only due to thermodynamical 2D-fluctuations (which at finite T suppress and destroy superconducting phase coherence in large systems) but it is mostly due to an *inherent ineffectiveness of strong correlations to produce solely high T_c in cuprates*. These numerical results certainly mean that the simple single-band Hubbard, as well as its derivative the t-J model, are insufficient to explain the pairing mechanism in cuprates and some other ingredients must be included. Having in mind these facts there is no room at present for any kind of celebration of the victory of non-phononic mechanisms of pairing as some prefer to do.

Since *EPI* is as a rule strong in oxides, then it is plausible that it should be accounted for in cuprates at least in the normal metallic state. As it will be argued later on, the experimental support for the importance of *EPI* comes from optics, tunnelling, and recent ARPES measurements [11]. It is worth mentioning that recent ARPES activity was a strong impetus for renewed experimental and theoretical studies of *EPI* in cuprates.

However, in spite of accumulating experimental evidence for importance of *EPI* with $\lambda^{ep} > 1$, there are occasionally reports which doubt its importance in cuprates. This is the case with recent interpretation of some optical measurements in terms of *SFI* only [12] and with LDA band structure calculations [13], [14], where both claim that *EPI* is negligibly small, i.e. $\lambda^{ep} < 0.3$.

The paper is organized as follows. There are two parts - in *Part I* we will mainly discuss experimental results in *cuprates near optimal doping* and minimal theoretical explanations which are related to the spectral function $\alpha^2 F(\omega)$ as well to the transport spectral function $\alpha_{tr}^2 F(\omega)$ and how these are related to *EPI* in cuprates. In this work we consider mainly those direct one-particle and two-particles probes of low energy quasi-particle excitations (by including gap and pseudogap) and scattering rates which give informations on the structure of the spectral functions $\alpha^2 F(\mathbf{k}, \mathbf{k}', \omega)$ and $\alpha_{tr}^2 F(\omega)$ in systems near optimal doping. These are angle-resolved photoemission (*ARPES*), various arts of tunnelling spectroscopies such as superconductor/insulator/normal metal (*SIN*) junctions and break junctions, scanning-tunnelling microscope spectroscopy (*STM*), infrared (*IR*) and Raman optics, inelastic neutron scattering (*INS*) etc. We shall argue that these direct probes give evidence for a rather strong *EPI* in cuprates as dominating scattering mechanism of quasi-particles. Some other experiments on *EPI* are also discussed in order to complete the arguments for the importance of *EPI* in cuprates. The detailed contents of Part I is the following. In *Section II* we discuss some prejudices related to *EPI* and the Fermi-liquid behavior of HTSC cuprates. We argue that any non-phononic mechanism of pairing should have very large bare critical temperature $T_{c0} \gg T_c$ in the presence of the large *EPI* coupling constant, $\lambda^{ep} \geq 1$, if its spectral function is weakly momentum dependent, i.e. if $\alpha^2 F(\mathbf{k}, \mathbf{k}', \omega) \approx \alpha^2 F(\omega)$. The fact that *EPI* is large in the normal state of cuprates and the condition that it must conform with d-wave pairing implies inevitably that *EPI* in cuprates must be *strongly momentum dependent*. In *Section III* we discuss direct and indirect experimental evidence for the importance of *EPI* and for the weakness of *SFI* in cuprates. These are:

(A) *Magnetic neutron scattering measurements* - These measurements provide dynamic spin susceptibility $\chi(\mathbf{q}, \omega)$ which is in the *SFI* phenomenological approach [6] related to the Eliashberg spectral function, i.e. $\alpha^2 F_{sf}(\mathbf{k}, \mathbf{k}', \omega) \sim \text{Im} \chi(\mathbf{q} = \mathbf{k} - \mathbf{k}', \omega)$. We stress that such an approach can be qualitatively justified only in the weak coupling limit, $g_{sf} \ll W_b$, where W_b is the band width. Here we discuss experimental results which give evidence for strong rearrangement (with respect to ω) of $\text{Im} \chi(\mathbf{Q}, \omega)$ by doping toward the optimal doped HTSC [16]. It turns out that in the optimally doped cuprates with $T_c = 92.5 K$ $\text{Im} \chi(\mathbf{Q}, \omega)$ is drastically suppressed compared to that in slightly underdoped ones with $T_c = 91 K$, and this is strong evidence for the smallness of the *SFI* coupling constant.

(B) Optical conductivity measurements - From these measurements one can extract the transport relaxation rate $\gamma_{tr}(\omega)$ and indirectly an approximative shape of the transport spectral function $\alpha^2 F_{tr}(\omega)$. In that respect we discuss: (i) the misleading concept concerning the relation between the optical relaxation rate $\gamma_{tr}(\omega)$ and the quasi-particle relaxation rate $\gamma(\omega)$. This (misleading) concept has been appearing repeatedly in the last twenty years despite the fact that this controversy is resolved many years ago [17], [18], [19], [1], [2], [44]; (ii) some methods of extraction of the optical spectral function $\alpha_{tr}^2 F(\omega)$ from optical reflectivity measurements. It turns out that the width and the shape of the extracted $\alpha_{tr}^2 F(\omega)$ favor EPI; (iii) the restricted sum-rule for the optical weight as a function of temperature which can also be explained by strong EPI [20], [21]; (iv) good agreement with experiments of the temperature dependence of the resistivity $\rho(T)$ calculated with the extracted $\alpha_{tr}^2 F(\omega)$. Recent femtosecond time-resolved optical spectroscopy in $La_{2-x}Sr_xCuO_4$ gives additional evidence for importance of EPI and ineffectiveness of SFI [22].

(C) ARPES measurements and EPI - From these measurements one can extract the self-energy $\Sigma(\mathbf{k}, \omega)$ from which one can extract some properties of $\alpha^2 F(\mathbf{k}, \mathbf{k}', \omega)$. Here we discuss the following items: (i) appearance of the nodal and anti-nodal kinks in optimally and slightly underdoped cuprates, as well as the structure of the ARPES self-energy ($\Sigma(\mathbf{k}, \omega)$) and its isotope dependence, which are all due to EPI; (ii) appearance of different slopes of $\Sigma(\mathbf{k}, \omega)$ at low ($\omega \ll \omega_{ph}$) and high energies ($\omega \gg \omega_{ph}$) which can be explained with strong EPI; (iii) formation of small polarons in the undoped HTSC which is due to strong EPI - this gives rise to phonon side bands which are clearly seen in ARPES of undoped HTSC.

(D) Tunnelling spectroscopy - It is well known that this method is of an immense importance in obtaining the spectral function $\alpha^2 F(\omega)$ from tunnelling conductance. In this part we discuss the following items: (i) extraction of the Eliashberg spectral function $\alpha^2 F(\omega)$ with $\lambda = 2-4$ from the tunnelling conductance of break-junctions [23]-[29] which gives that the maxima of $\alpha^2 F(\omega)$ coincide with the maxima in the phonon density of states; (ii) the presence of the dip in dI/dV in STM which shows the pronounced oxygen isotope effect and important role of these phonons; (iii) the presence of fine and doping independent structure in $I(V)$ characteristics due to phonon emission by the Josephson current in layered HTSC cuprates with intrinsic Josephson junctions.

(E) Phonon neutron scattering measurements - From these experiments one can extract the phonon density of state $F_{ph}(\omega)$ and strengths of the quasi-particle coupling with various phonon modes. Here we argue, that the large softening and broadening of the half-breathing Cu-O bond-stretching phonon, of apical oxygen phonons and of oxygen B_{1g} buckling phonons (in LSCO, BISCO, YBCO) cannot be explained by LDA. It is curious that the magnitude of softening can be partially

obtained by LDA but the calculated widths of some important modes are an order of magnitude smaller than the neutron scattering data show. This remarkable fact implies *the inadequacy of LDA in strongly correlated systems* and a more sophisticated many body theory for EPI is needed. This problem will be discussed in more details in *Part II* [15]. In *Section IV* brief summary of the *Part I* is given. Since *we are dealing with electron-boson scattering in cuprate near optimal doping*, then in *Section V - Appendix* we introduce the reader briefly into the Migdal-Eliashberg theory for superconductors (and normal metals) where the quasi-particle spectral function $\alpha^2 F(\mathbf{k}, \mathbf{k}', \omega)$ and the transport spectral function $\alpha_{tr}^2 F(\omega)$ are defined.

Finally, at the end of the day one poses a question - do the experimental results of the above enumerated spectroscopic methods allow a building of a satisfactory and physically reasonable microscopic theory for basic scattering and pairing mechanism in cuprates? The posed question is very modest compared with a much stringent request for the *theory of everything* - which would be able to explain all properties of HTSC materials. Such an ambitious project is not realized even in those low-temperature conventional superconductors where it is definitely proved that the pairing is due to EPI and many properties are well accounted for by the Migdal-Eliashberg theory. Let us mention only two examples. First, the experimental value for the coherence peak in the microwave response $\sigma_s(T < T_c)$ at 17 GHz in Nb is much higher than the theoretical value obtained by the Migdal-Eliashberg theory [31]. So to say, the theory explains the coherence peak at 17 GHz in Nb qualitatively but not quantitatively. However, the measurements at higher frequency ~ 60 GHz are in agreement with the Migdal-Eliashberg theory [32]. Second, the experimental boron (B) isotope effect in MgB_2 (with $T_c \approx 40$ K) is much smaller than the theoretical value, i.e. $\alpha_B^{exp} \approx 0.3 < \alpha_B^{th} = 0.5$, although the pairing is due solely by EPI for boron vibrations [33]. Since the theory of everything is impossible in the complex materials such as HTSC cuprates in *Part I* and *II* we shall not discuss those phenomena which need much more microscopic details and/or more sophisticated many-body theory. These are selected by chance: (i) peculiarities of the coherence peak in the microwave response $\sigma(T)$ in HTSC cuprates, which is peaked at T much smaller than T_c , contrary to the case of LTSC where it occurs near T_c ; (ii) T_c dependence on the number of CuO_2 in the unit cell; (iii) temperature dependence of the Hall coefficient; (iv) distribution of states in the vortex core, etc. However, in a separate paper - *Part II* [15] we shall discuss some minimal theoretical concepts which can explain at least qualitatively and semi-quantitatively results related to the above enumerated spectroscopic methods. Due to the presence of strong correlations and quasi-2D electronic structure some of these concepts go beyond the LDA approach. In our opinion at this stage of the HTSC physics some *important ingredients* of the fu-

ture theory are already recognized. These are: (1) very peculiar quasi-2D ionic-metallic structure with a rather weak screening along the c -axis, which is a prerequisite for strong EPI; (2) strong Coulomb interaction and correlations which are responsible for strong magnetism in undoped cuprates and for important renormalizations of EPI. Since both ingredients belong to the class of strong coupling problems, at present there is no quantitative theory and therefore we must rely on approximative and model theories. Even these approaches allow us qualitative (and semi-quantitative) explanations of some important properties which are due to the interplay of EPI and strong correlations. The latter two cause the appearance of momentum dependent EPI - peaked at small transfer momenta [2]. Based on such an approach we are able to explain (understand) at least qualitatively some very puzzling experimental results, for instance: (a) why is d -wave pairing realized in the presence of strong EPI? (b) why is the transport coupling constant (λ_{tr}) smaller than the pairing one λ , i.e. $\lambda_{tr} \lesssim \lambda/3$? (c) Why is the mean-field (one-body) LDA approach unable to give reliable values for the EPI coupling constant in cuprates and how many-body effects help; (d) why is d -wave pairing robust in presence of non-magnetic impurities and defects? (e) why the ARPES nodal and antinodal kinks are differently renormalized in the superconducting states?

In real materials there are numerous experimental evidence for nanoscale inhomogeneities in HTSC oxides. For instance recent STM experiments show rather large gap dispersion at least on the surface of BISCO crystals [30] giving rise for a pronounced inhomogeneity of the superconducting order parameter, i.e. $\Delta(\mathbf{k}, \mathbf{R})$ where \mathbf{k} is the relative momentum of the Cooper pair and \mathbf{R} is the center of mass of Cooper pairs. One possible reason for the inhomogeneity of $\Delta(\mathbf{k}, \mathbf{R})$ and disorder on the atomic scale can be due to extremely high doping level of $\sim (10 - 20) \%$ in HTSC cuprates which is many orders of magnitude larger than in standard semiconductors (10^{21} vs 10^{15} carrier concentration). There are some claims that high T_c is exclusively due to these inhomogeneities (of an extrinsic or intrinsic origin) which may increase EPI [34], while other try to explain high T_c within the inhomogeneous Hubbard or t - J model. In *Part II* [15] we argue that the concept of an increase of T_c by inhomogeneity is ill-defined, since the increase of T_c is defined with respect to the average value \bar{T}_c . However, the latter quantity is experimentally not well defined and an alleged increase of T_c by the material inhomogeneity cannot be tested at all.

II. EPI VS NON-PHONONIC MECHANISMS - FACTS VS PREJUDICES

Concerning the high T_c in cuprates, one of the central questions is - which interaction(s) is(are) responsible for strong quasi-particle scattering in the normal state and for the superconducting pairing? In the last twenty-two

years, the scientific community was overwhelmed by all kinds of (im)possible proposed pairing mechanisms, most of which are hardly verifiable in any material, if at all. This trend is still continuing nowadays (although with smaller slope), in spite of the fact that the accumulated experimental results eliminate all but few.

A. Fermi vs non-Fermi liquid in cuprates

After discovery of HTSC in cuprates there was a large amount of evidence on strong scattering of quasi-particles which contradicts the canonical (popular but narrow) definition of the Fermi liquid, thus giving rise to numerous proposals of the so called non-Fermi liquids, such as Luttinger liquid, RVB theory, marginal Fermi liquid, etc. In our opinion there is no need for these radical approaches in explaining basic physics in cuprates at least in optimally, slightly underdoped and overdoped metallic and superconducting HTSC cuprates. This subject will be discussed more in *Part II* and here we give some clarifications related to the dilemma of Fermi vs non-Fermi liquid. The definition of the *canonical Fermi liquid* (based on the Landau work) in interacting Fermi systems comprises the following properties: (1) there are quasi-particles with charge $q = \pm e$, spin $s = 1/2$ and low-laying energy excitations $\xi_{\mathbf{k}} (= \epsilon_{\mathbf{k}} - \mu)$ which are much larger than their inverse life-times, i.e. $\xi_{\mathbf{k}} \gg 1/\tau_{\mathbf{k}} \sim \xi_{\mathbf{k}}^2/W_b$. Since the level width $\Gamma = 2/\tau_{\mathbf{k}}$ of the quasi-particle is negligibly small, this means that the excited states of the Fermi liquid are placed in one-to-one correspondence with the excited states of the free Fermi gas; (2) at $T = 0$ K there is an energy level with the Fermi surface at which $\xi_{\mathbf{k}_F} = 0$ and the Fermi quasi-particle distribution function $n_F(\xi_{\mathbf{k}})$ has finite jump; (3) the number of quasi-particles under the Fermi surface is equal to the total number of conduction particles (we omit here other valence and core electrons) - the Luttinger theorem; (4) the interaction between quasi-particles are characterized with a few (Landau) parameters which describe low-temperature thermodynamics and transport properties. Having this definition in mind one can say that if fermionic quasi-particles interact with some bosonic excitation (for instance with phonons) and if the coupling is sufficiently strong, then the former are not described by the canonical Fermi liquid since at energies and temperatures of the order of the Debay temperature $k_B\Theta_D (\equiv \hbar\omega_D)$ (more precisely $\sim \Theta_D/5$), i.e. for $\xi_{\mathbf{k}} \sim \Theta_D$ one has $\tau_{\mathbf{k}}^{-1} \gtrsim \xi_{\mathbf{k}}$ and the quasi-particle picture (in the sense of the Landau definition) is broken down. In that respect an electron-boson system can be classified as a *non-canonical Fermi liquid* for sufficiently strong electron-boson coupling. It is nowadays well known that for instance Al, Zn are weak coupling systems since for $\xi_{\mathbf{k}} \sim \Theta_D$ one has $\tau_{\mathbf{k}}^{-1} \ll \xi_{\mathbf{k}}$ and they are well described by the Landau theory. However, the electron-phonon system is satisfactory described by the Migdal-Eliashberg theory and the Boltzmann theory, where thermodynamic and transport properties depend on the spectral function $\alpha^2 F_{sf}(\mathbf{k}, \mathbf{k}', \omega)$ and its higher momenta. Since in HTSC cuprates the electron-boson (phonon) coupling is rather

strong and T_c is large, i.e. of the order of characteristic boson energies (ω_B), $T_c \sim \omega_B/4$, then it is natural that in the normal state (at $T > T_c$) we deal inevitably with a strong interacting non-canonical Fermi liquid which is at least qualitatively and semi-quantitatively described by the Migdal-Eliashberg theory. In order to justify this statement we shall in the following elucidate some properties in more details by studying optical, ARPES, tunnelling and other experiments.

B. Prejudice on the limitation of the strength of EPI

In spite of reach experimental evidence in favor of strong EPI in HTSC oxides there was a disproportion in the research activity (especially theoretical) in the past, since the investigation of the SFI mechanism of pairing prevailed in the literature. This retrograde trend was partly due to an incorrect statement in [35] on the possible upper limit of T_c in the phonon mechanism of pairing. Since in the past we have discussed this problem thoroughly in numerous papers - for the recent one see [36], we shall outline here the main issue and results only.

It is well known that in an electron-ion crystal, besides the attractive EPI, there is also repulsive Coulomb interaction. In case of an isotropic and homogeneous system with weak quasi-particle interaction, the effective potential $V_{eff}(\mathbf{k}, \omega)$ in the leading approximation looks like as for two external charges (e) embedded in the medium with the *total longitudinal dielectric function* $\varepsilon_{tot}(\mathbf{k}, \omega)$ (\mathbf{k} is the momentum and ω is the frequency) [37], i.e.

$$V_{eff}(\mathbf{k}, \omega) = \frac{V_{ext}(\mathbf{k})}{\varepsilon_{tot}(\mathbf{k}, \omega)} = \frac{4\pi e^2}{k^2 \varepsilon_{tot}(\mathbf{k}, \omega)}. \quad (1)$$

In case of strong interaction between quasi-particles, the state of embedded quasi-particles changes significantly due to interaction with other quasi-particles, giving rise to $V_{eff}(\mathbf{k}, \omega) \neq 4\pi e^2/k^2 \varepsilon_{tot}(\mathbf{k}, \omega)$. In that case V_{eff} depends on other (than $\varepsilon_{tot}(\mathbf{k}, \omega)$) response functions. However, in the case when Eq.(1) holds, i. e. when the weak-coupling limit is realized, T_c is given by $T_c \approx \bar{\omega} \exp(-1/(\lambda^{ep} - \mu^*))$ [118], [37]). Here, λ^{ep} is the EPI coupling constant, $\bar{\omega}$ is an average phonon frequency and μ^* is the Coulomb pseudo-potential, $\mu^* = \mu/(1 + \mu \ln E_F/\bar{\omega})$ (E_F is the Fermi energy). The couplings λ^{ep} and μ are expressed by $\varepsilon_{tot}(\mathbf{k}, \omega = 0)$

$$\begin{aligned} \mu - \lambda^{ep} &= \langle N(0) V_{eff}(\mathbf{k}, \omega = 0) \rangle \\ &= N(0) \int_0^{2k_F} \frac{k dk}{2k_F^2} \frac{4\pi e^2}{k^2 \varepsilon_{tot}(\mathbf{k}, \omega = 0)}, \end{aligned} \quad (2)$$

where $N(0)$ is the density of states at the Fermi surface and k_F is the Fermi momentum - see more in [1]. In [35] it was claimed that lattice stability of the system with respect to the charge density wave formation implies the condition $\varepsilon_{tot}(\mathbf{k}, \omega = 0) > 1$ for all \mathbf{k} . If this was correct then from Eq.(2) it follows that $\mu > \lambda^{ep}$, which limits the maximal value of T_c to the value $T_c^{\max} \approx E_F \exp(-4 - 3/\lambda^{ep})$. In typical metals

$E_F < (1 - 10) eV$ and if one accepts the statement in [35], i.e. that $\lambda^{ep} \leq \mu \leq 0.5$, one obtains $T_c \sim (1 - 10) K$. The latter result, if it would be true, means that EPI is ineffective in producing not only high- T_c superconductivity but also low-temperature superconductivity (LTS). However, this result is apparently in conflict first of all with experimental results in LTSC, where in numerous systems $\mu \leq \lambda^{ep}$ and $\lambda^{ep} > 1$. For instance, $\lambda^{ep} \approx 2.6$ is realized in *PbBi* alloy which is definitely much higher than $\mu (< 1)$.

Moreover, the basic theory tells us that $\varepsilon_{tot}(\mathbf{k} \neq 0, \omega)$ is not the response function [37]. Namely, if a small external potential $\delta V_{ext}(\mathbf{k}, \omega)$ is applied to the system it induces screening by charges of the medium and the total potential is given by $\delta V_{tot}(\mathbf{k}, \omega) = \delta V_{ext}(\mathbf{k}, \omega)/\varepsilon_{tot}(\mathbf{k}, \omega)$ which means that $1/\varepsilon_{tot}(\mathbf{k}, \omega)$ is the response function. The latter obeys the Kramers-Kronig dispersion relation which implies the following stability condition: $1/\varepsilon_{tot}(\mathbf{k}, \omega = 0) < 1$ for $\mathbf{k} \neq 0$, i.e. either $\varepsilon_{tot}(\mathbf{k} \neq 0, \omega = 0) > 1$ or $\varepsilon_{tot}(\mathbf{k} \neq 0, \omega = 0) < 0$. This important theorem invalidates the above restriction on the maximal value of T_c in the EPI mechanism. We stress that the condition $\varepsilon_{tot}(\mathbf{k} \neq 0, \omega = 0) < 0$ is not in conflict with the lattice instability. For instance, in inhomogeneous systems such as crystal, the total longitudinal dielectric function is matrix in the space of reciprocal lattice vectors (\mathbf{Q}), i.e. $\hat{\varepsilon}_{tot}(\mathbf{k} + \mathbf{Q}, \mathbf{k} + \mathbf{Q}', \omega)$, and $\varepsilon_{tot}(\mathbf{k}, \omega)$ is defined by $\varepsilon_{tot}^{-1}(\mathbf{k}, \omega) = \hat{\varepsilon}_{tot}^{-1}(\mathbf{k} + \mathbf{0}, \mathbf{k} + \mathbf{0}, \omega)$. It is well known that in dense metallic systems with one ion per cell (such as metallic hydrogen) and with the electronic dielectric function $\varepsilon_{el}(\mathbf{k}, 0)$, one has [38]

$$\varepsilon_{tot}(\mathbf{k}, 0) = \frac{\varepsilon_{el}(\mathbf{k}, 0)}{1 - 1/\varepsilon_{el}(\mathbf{k}, 0)G_{ep}(\mathbf{k})}. \quad (3)$$

At the same time the frequency of the longitudinal phonon $\omega_l(\mathbf{k})$ is given by

$$\omega_l^2(\mathbf{k}) = \frac{\Omega_p^2}{\varepsilon_{el}(\mathbf{k}, 0)} [1 - \varepsilon_{el}(\mathbf{k}, 0)G_{ep}(\mathbf{k})], \quad (4)$$

where Ω_p^2 is the ionic plasma frequency, G_{ep} is the local (electric) field correction - see Ref. [38]. The real condition for lattice stability requires that $\omega_l^2(\mathbf{k}) > 0$, which implies that for $\varepsilon_{el}(\mathbf{k}, 0) > 0$ one has $\varepsilon_{el}(\mathbf{k}, 0)G_{ep}(\mathbf{k}) < 1$. The latter condition gives automatically $\varepsilon_{tot}(\mathbf{k}, 0) < 0$. Furthermore, the calculations [38] show that in the metallic hydrogen crystal, $\varepsilon_{tot}(\mathbf{k}, 0) < 0$ for all $\mathbf{k} \neq \mathbf{0}$. Moreover, the analyzes of crystals with more ions per unit cell [38] gives that $\varepsilon_{tot}(\mathbf{k} \neq \mathbf{0}, 0) < 0$ is *more a rule than an exception* - see Fig. 1. The physical reason for $\varepsilon_{tot}(\mathbf{k} \neq \mathbf{0}, 0) < 0$ are local field effects described above by $G_{ep}(\mathbf{k})$. Whenever the local electric field \mathbf{E}_{loc} acting on electrons (and ions) is different from the average electric field \mathbf{E} , i.e. $\mathbf{E}_{loc} \neq \mathbf{E}$, there are corrections to $\varepsilon_{tot}(\mathbf{k}, 0)$ (and to $\varepsilon_e(\mathbf{k}, 0)$) which may lead to $\varepsilon_{tot}(\mathbf{k}, 0) < 0$.

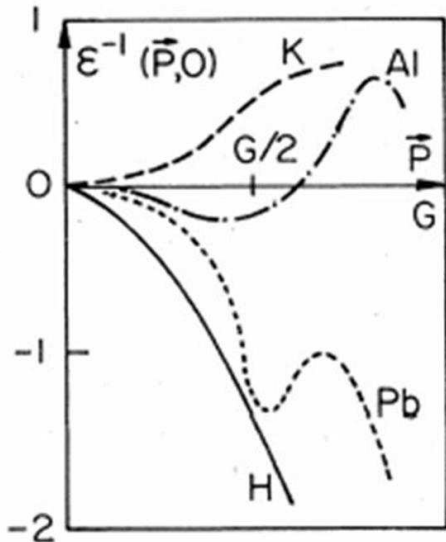


FIG. 1: Inverse total static dielectric function $\epsilon^{-1}(\mathbf{p})$ for normal metals (K, Al, Pb and metallic H) in $\mathbf{p} = (1, 0, 0)$ direction. \mathbf{G} is the reciprocal lattice vector.

The above analysis tells us that in real crystals $\epsilon_{tot}(\mathbf{k}, 0)$ can be negative in the large portion of the Brillouin zone giving rise to $\lambda^{ep} - \mu > 0$ in Eq.(2). This means that the dielectric function ϵ_{tot} does not limit T_c in the phonon mechanism of pairing. This result does not mean that there is no limit on T_c at all - see more in [36] and references therein. We mention in advance that the local field effects play important role in HTSC oxides, due to their layered structure with very *unusual ionic-metallic binding*, thus giving rise to large *EPI* - see more in the subsequent sections. It is pertinent to note that one of the author of [35] recognizes the possibility $\epsilon_{tot}(\mathbf{k}, 0) < 0$ and in [39] even makes interesting proposals for compounds with large *EPI* and $T_c > 100$ K, while the other author [40] still ignores rigors of scientific arguments and negates importance of *EPI* in HTSC cuprates.

In conclusion we point out that there are no theoretical and experimental arguments for ignoring *EPI* in HTSC cuprates. To this end it is necessary to answer several important questions which are related to experimental findings in HTSC cuprates (oxides): (1) if *EPI* is responsible for pairing in HTSC cuprates and if superconductivity is of *d-wave* type, how are these two facts compatible? (2) why is the transport *EPI* coupling constant λ_{tr} (entering resistivity) much smaller than the pairing *EPI* coupling constant $\lambda^{ep} (> 1)$ (entering T_c), i.e. why one has $\lambda_{tr} (\approx 0.4 - 1.2) \ll \lambda^{ep} (\sim 2 - 4)$? (3) is high T_c possible for a moderate *EPI* coupling constant, let say for $\lambda^{ep} \leq 1$, and under which conditions? (4) if *EPI* is ineffective for pairing in HTSC oxides, inspite of $\lambda^{ep} > 1$, why it is so?

C. Is a non-phononic pairing realized in HTSC?

Regarding *EPI* one can pose a question - whether it contributes significantly to *d-wave* pairing in cuprates? Surprisingly, despite numerous experiments in favor of *EPI*, a number of researchers still believe that *EPI* is irrelevant for pairing [6]. This belief is mainly based: (i) on the, previously discussed, incorrect lattice stability criterion, which implies small *EPI*; (ii) on the well established experimental fact that *d-wave* pairing is realized in cuprates [41], which is believed to be incompatible with *EPI*. Having in mind that *EPI* in HTSC is strong with $1 < \lambda^{ep} < 3$ (see below), we assume for the moment that the leading pairing mechanism in cuprates, which gives *d-wave* pairing, is due to some non-phononic mechanism, like the *exitonic* one, with the high energy gluing boson ($\Omega_{nph} \gg \omega_{ph}$) and with the bare critical temperature T_{c0} and look for the effect of *EPI*. If *EPI* is *isotropic*, like in most LTSC materials, then it would be very detrimental for *d-wave* pairing - the pair breaking effect. In the case of dominating *isotropic* *EPI* in the normal state and the *exitonic-like* pairing, then near T_c the linearized Eliashberg equations have an approximate form for *weak* non-phonon interaction (with the characteristic frequency Ω_{nph})

$$Z(\omega_n)\Delta(\mathbf{k}, \omega_n) = \pi T_c \sum_{n'} \sum_{\mathbf{q}} V_{nph}(\mathbf{k}, \mathbf{q}, n, n') \frac{\Delta(\mathbf{q}, \omega_{n'})}{|\omega_{n'}|}$$

$$Z(\omega_n) \approx 1 + \Gamma_{ep}/\omega_n. \quad (5)$$

For pure *d-wave* pairing one has $V_{nph}(\mathbf{k}, \mathbf{q}, n, n') = V_{nph} \Theta(\Omega_{nph} - |\omega_n|) \Theta(\Omega_{nph} - |\omega_{n'}|) \times (\cos k_x - \cos k_y)(\cos q_x - \cos q_y)$ and $\Delta(\mathbf{k}, \omega_n) = \Delta_d \Theta(\Omega_{nph} - |\omega_n|)(\cos k_x - \cos k_y)$ which gives the equation for T_c - see [1]

$$\ln \frac{T_c}{T_{c0}} = \Psi\left(\frac{1}{2}\right) - \Psi\left(\frac{1}{2} + \frac{\Gamma_{ep}}{2\pi T_c}\right). \quad (6)$$

Here Ψ is the di-gamma function. At temperatures near T_c one has $\Gamma_{ep} \approx 2\pi \lambda_{ep} T_c$ and the solution of Eq. (6) is approximately $T_c \approx T_{c0} \exp\{-\lambda^{ep}\}$, which means that for $T_c^{\max} \sim 160$ K and $\lambda^{ep} > 1$ the bare T_{c0} due to the non-phononic interaction must be very large, i.e. $T_{c0} > 500$ K.

Concerning other non-phononic mechanisms, such as the *SFI* one, the effect of the *isotropic* *EPI* in the framework of Eliashberg equations was studied numerically in [42]. The latter is based on Eqs.(42-44) in Appendix A. with kernels

$$\lambda_{\mathbf{kp}}^Z(i\nu_n) = \lambda_{\mathbf{kp}}^{sf}(i\nu_n) + \lambda_{\mathbf{kp}}^{ep}(i\nu_n) \quad (7)$$

$$\lambda_{\mathbf{kp}}^\Delta(i\nu_n) = \lambda_{\mathbf{kp}}^{ep}(i\nu_n) - \lambda_{\mathbf{kp}}^{sf}(i\nu_n), \quad (8)$$

where $\lambda_{\mathbf{kp}}^{sf}(i\nu_n)$ is taken in the *FLEX* approximation [43]. The calculations [42] confirm the very detrimental effect

of the isotropic EPI on the d-wave pairing due to SFI. For the bare SFI $T_{c0} \sim 100$ K and $\lambda^{ep} > 1$ the calculations give very small $T_c \ll 100$ K. These results tell us that a more realistic pairing interaction must be operative in cuprates and that EPI is *strongly momentum dependent* [45]. Only in that case is strong EPI conform with d-wave pairing, either as its main cause or as a supporter of a non-phononic mechanism. In *Part II* we shall argue that the strongly momentum dependent EPI is the main player in cuprates providing the strength of the pairing mechanism, while the residual Coulomb interaction and SF, although weaker, trigger it to d-wave pairing.

III. EXPERIMENTAL EVIDENCE FOR STRONG EPI AND WEAK SFI

In the following we discuss some important experiments which give evidence for strong EPI in cuprates. Before doing it; we shall discuss some magnetic neutron scattering measurements in cuprates whose results are against the SFI mechanism of pairing. The experimental results related to the pronounced imaginary part of the susceptibility $Im\chi(\mathbf{k}, k_z, \omega)$ at the AF wave vector $\mathbf{k} = \mathbf{Q} = (\pi, \pi)$ were interpreted in a number of papers as a support for the SFI mechanism for pairing [6]. We briefly explain *inadequacy* of such an interpretation.

A. Magnetic neutron scattering and the spin fluctuation spectral function

A. SFI affects T_c very little

Before discussing experimental results in cuprates on the imaginary part of the spin susceptibility $Im\chi(\mathbf{k}, \omega)$ we point out that in theories based on spin fluctuations the effective pairing potential $V_{sf}(\mathbf{k}, \omega)$, which is repulsive, is assumed in the form [6]

$$V_{sf}(\mathbf{q}, \omega + i0^+) = g_{sf}^2 \int_{-\infty}^{\infty} \frac{d\nu}{\pi} \frac{Im\chi(\mathbf{q}, \nu + i0^+)}{\nu - \omega}. \quad (9)$$

This form of V_{sf} can be theoretically justified in the weak coupling limit ($U \ll W_b$) only. This mechanism of pairing could be effective in cuprates only if the spin susceptibility (spectral function) $Im\chi(\mathbf{q}, \omega)$ is strongly peaked at the AF wave vector $\mathbf{Q} = (\pi/a, \pi/a)$. What is the experimental situation? The breakthrough came from magnetic neutron scattering experiments on $YBa_2Cu_3O_{6+x}$ by Bourges group [16]. They showed that $Im\chi^{(odd)}(\mathbf{q}, \omega)$ (the odd part of the spin susceptibility in the bilayer system) at $\mathbf{q} = \mathbf{Q} = (\pi, \pi)$ is strongly dependent on the hole doping as it is shown in Fig. 2.

By varying doping there is a huge rearrangement of $Im\chi^{(odd)}(\mathbf{Q}, \omega)$ in the frequency interval which is important for superconducting pairing, let say 5 meV $< \omega < 60$ meV as it is seen in the last two curve in Fig. 2(top). At the same time there is only a small variation of the

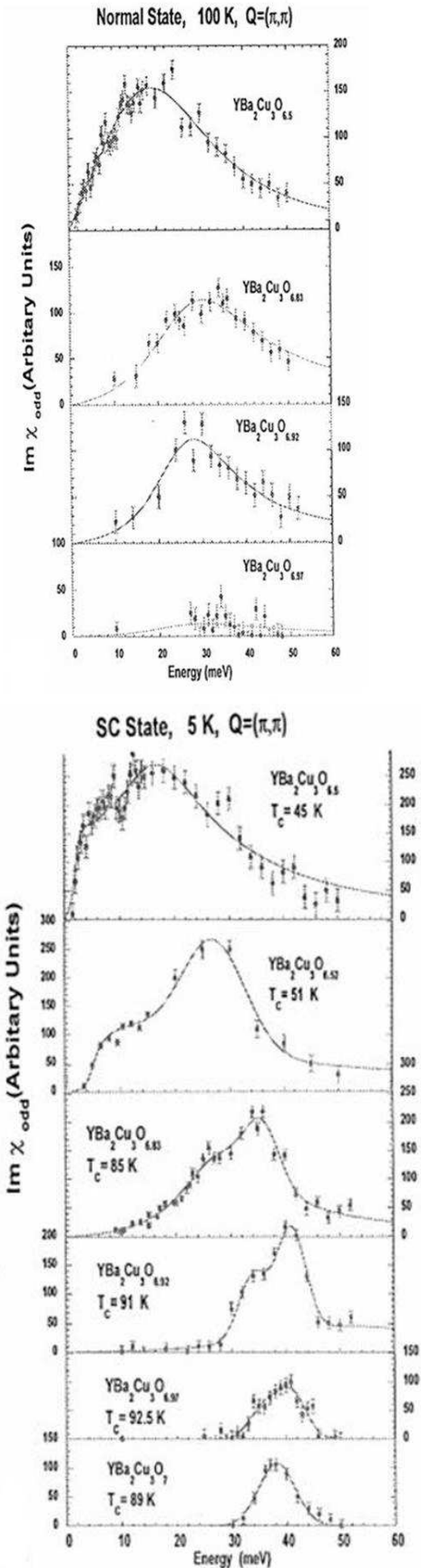


FIG. 2: Magnetic spectral function $Im\chi^{(-)}(\mathbf{k}, \omega)$ in $YBa_2Cu_3O_{6+x}$. (Top) In the normal state at $T = 100$ K and at $Q = (\pi, \pi)$. 100 counts in the vertical scale corresponds to $\chi_{max}^{(-)} \approx 350\mu_B^2/eV$. (Bottom) In the superconducting state at $T = 5$ K and at $Q = (\pi, \pi)$. From Ref. [16].

corresponding critical temperature T_c ! For instance, in the underdoped $YBa_2Cu_3O_{6.92}$ crystal $\text{Im}\chi^{(odd)}(\mathbf{Q}, \omega)$, and $S(\mathbf{Q}) = N(\mu)g_{sf}^2 \int_0^{60} d\omega \text{Im}\chi^{(odd)}(\mathbf{Q}, \omega) \sim \lambda^{sf} \cdot \langle \omega \rangle$, is much larger than that in the near optimally doped $YBa_2Cu_3O_{6.97}$, i.e. $S_{6.92}(\mathbf{Q}) \gg S_{6.97}(\mathbf{Q})$, although the difference in the corresponding critical temperatures T_c is very small, i.e. $T_c^{(6.92)} = 91 \text{ K}$ (in $YBa_2Cu_3O_{6.92}$) and $T_c^{(6.97)} = 92.5 \text{ K}$ (in $YBa_2Cu_3O_{6.97}$). This *pronounced rearrangement and decrease* of $\text{Im}\chi^{(odd)}(\mathbf{Q}, \omega)$ by doping, but a negligible change in T_c in YBCO is clearly seen in Fig. 2(top), which is *strong evidence* against the SFI mechanism of pairing. These results in fact mean that the SFI coupling constant $\lambda^{sf} (\sim g_{sf}^2)$ is small, i.e. $\lambda_{sf}^{(exp)} \ll 1$, and the SFI pairing mechanism is ineffective in cuprates. We stress that in the phenomenological theory of the SFI pairing [6], an unrealistically large coupling $g_{sf} > 0.7 \text{ eV}$ was assumed which gives $\lambda^{sf} \sim 2$. The latter value cannot be justified neither experimentally nor theoretically. Let us add that the *anti-correlation* between the decrease of $\text{Im}\chi(\mathbf{Q}, \omega)$ and increase of T_c by increasing doping toward the optimal value is also present in the NMR spectral function $I_{\mathbf{Q}} = \lim_{\omega \rightarrow 0} \text{Im}\chi(\mathbf{Q}, \omega)/\omega$ which determines the longitudinal relaxation rate $1/T_1$ - see [2]. This result additionally disfavors the SFI model of pairing [6], i.e. the strength of pairing interaction is little affected by SFI. As we shall discuss below the role of SFI together with the stronger direct Coulomb interaction is to trigger d-wave pairing.

A less direct argument for *smallness of the SFI coupling constant*, i.e. $g_{sf} \leq 0.2 \text{ eV}$ and $\lambda^{sf} \sim 0.2 - 0.3$ comes from other experiments related to the magnetic resonance peak in the superconducting state, and this will be discussed next.

B. Ineffectiveness of the magnetic resonance peak

In the superconducting state of optimally doped YBCO and BISCO, $\text{Im}\chi(\mathbf{Q}, \omega)$ is significantly suppressed at low frequencies except near the resonance energy $\omega_{res} \approx 41 \text{ meV}$ where a pronounced narrow peak appears - the *magnetic resonance peak*. We stress that there is no magnetic resonance peak in LSCO and consequently one can question the importance of the resonance peak in the scattering processes. The relative intensity of this peak (compared to the total one) is small, i.e. $I_0 \sim (1 - 5)\%$ - see Fig 2 (bottom). In underdoped cuprates this peak is present also in the normal state as it is seen in Fig 2 (top). After the discovery of the resonance peak there were attempts to relate it: (i) to the origin of the superconducting condensation energy and (ii) to the kink in the energy dispersion or the peak-dimp structure in the ARPES spectral function. In order that the property (i) holds it is necessary that the peak intensity I_0 is small [46]. I_0 is obtained by equating the condensation energy E_{con} with the change of the magnetic energy in the superconducting state, i.e. $\delta E_{mag} \approx 4I_0 E_{mag}$, where

$$E_{con} \approx N(0)\Delta^2/2$$

$$E_{mag} = J \iint \frac{d\omega d^2k}{(2\pi)^3} (1 - \cos k_x - \cos k_y) S(\mathbf{k}, \omega). \quad (10)$$

By taking $2\Delta \approx 4T_c$ and the realistic value $N(0) \sim 1/(10J) \sim 1 \text{ states/eV} \cdot \text{spin}$, one obtains $I_0 \sim 10^{-1}(T_c/J)^2 \sim 10^{-3}$. However, such a small intensity cannot be responsible for the anomalies in ARPES and optical spectra since it gives rise to small coupling constant λ^{res} for the interaction of holes with the resonance peak, i.e. $\lambda^{res} \approx (2I_0 N(0)g_{sf}^2/\omega_{res}) \ll 1$. Such a small coupling does not affect superconductivity. Moreover, by studying the width of the resonance peak one can extract the SFI coupling constant g_{sf} . Thus, the magnetic resonance disappears in the normal state of the optimally doped YBCO, which can be qualitatively understood by assuming that its broadening scales with the resonance energy ω_{res} , i.e. $\gamma^{res} < \omega_{res}$, where the line-width is given by $\gamma^{res} = 4\pi(N(0)g_{sf})^2\omega_{res}$ [46]. This limits to $g_{sf} < 0.2 \text{ eV}$. We stress that the obtained g_{sf} is much smaller than the one assumed in the phenomenological spin-fluctuation theory [6] where $g_{sf} \sim 0.6 - 0.7 \text{ eV}$, but much larger than in [46] (where $g_{sf} < 0.02 \text{ eV}$). The smallness of g_{sf} comes out also from the analysis of the antiferromagnetic state in underdoped metals of LSCO and YBCO [47], where the small magnetic moment $\mu (< 0.1 \mu_B)$ points to an itinerant antiferromagnetism with small coupling constant $g_{sf} \leq 0.2 \text{ eV}$. The conclusion is that the magnetic resonance in the optimally doped YBCO is a consequence of the onset of superconductivity and not its cause.

There is also a principal reason against the pairing due to the resonance peak at least in optimally doped cuprates. Since its intensity near T_c is vanishingly small, though not affecting pairing at the second order phase transition at T_c , then if it would be the origin for superconductivity the phase transition at T_c would be *first order*, contrary to experiments. Recent ARPES experiments give evidence that the magnetic resonance cannot be related to the kinks in ARPES spectra [48], [49] - see the discussion below.

We shall argue below that despite its smallness, spin fluctuations can, together with other contributions of the residual Coulomb interaction, *trigger* d-wave pairing, while the *strength of pairing is due to EPI* which is peaked at small transfer momenta - see more below and in [2], [44].

B. Optical conductivity and EPI

Optical spectroscopy gives information on *optical conductivity* $\sigma(\omega)$ and on two-particle excitations, from which one can indirectly extract the transport spectral function $\alpha_{tr}^2 F(\omega)$. Since this method probes bulk sample (on the skin depth), contrary to ARPES and tunnelling methods which probe tiny regions ($10 - 15 \text{ \AA}$) near the sample surface, this method is very indispensable. However, $\sigma(\omega)$ is *not a directly measured*

quantity but it is derived from the reflectivity $R(\omega) = \left| \frac{(\sqrt{\varepsilon_{ii}(\omega)} - 1)}{(\sqrt{\varepsilon_{ii}(\omega)} + 1)} \right|^2$ with the transversal dielectric tensor $\varepsilon_{ii}(\omega) = \varepsilon_{ii,\infty} + \varepsilon_{ii,latt} + 4\pi i \sigma_{ii}(\omega)/\omega$. Here, $\varepsilon_{ii,\infty}$ is the high frequency dielectric function, $\varepsilon_{ii,latt}$ describes the contribution of the lattice vibrations and $\sigma_{ii}(\omega)$ describes the optical (dynamical) conductivity of conduction carriers. $R(\omega)$ was usually measured in the limited frequency interval $\omega_{\min} < \omega < \omega_{\max}$. Therefore, some physical modelling for $R(\omega)$ is needed in order to guess it outside this range - see more in reviews [1], [2]. This was the reason for numerous inadequate interpretations of optic measurements in cuprates, as well as the misconceptions and misinterpretations that will be uncovered below. An illustrative example for this claim is large dispersion in the reported value of ω_{pl} - from 0.06 to 25 eV, i.e. almost three orders of magnitude - see discussion in [50]. This tells us also that in some periods science suffers from a lack of rigorousness and objectiveness. However, it turns out that IR measurements of $R(\omega)$ in conjunction with ellipsometric measurements of $\varepsilon_{ii}(\omega)$ at high frequencies allows reliable determination of $\sigma(\omega)$.

1. Transport and quasiparticle relaxation rates

The widespread misconception in studying the quasiparticle scattering in cuprates was an ad hoc assumption that the *transport relaxation rate* $\gamma_{tr}(\omega)$ is equal to the *quasi-particle relaxation rate* $\gamma(\omega)$, in spite of the well known fact that $\gamma_{tr}(\omega) \neq \gamma(\omega)$ [17]. This incorrect assumption led to the abandoning of EPI as relevant scattering mechanism in cuprates. Although we have discussed this problem several times before, we want to do it again, since the correct understanding of the scattering mechanism in cuprates will take us forward in understanding of the pairing mechanism.

The dynamical conductivity $\sigma(\omega)$ consists of two parts, i.e. $\sigma(\omega) = \sigma^{inter}(\omega) + \sigma^{intra}(\omega)$ where $\sigma^{inter}(\omega)$ describes *interband transitions* which contribute at higher frequencies, while $\sigma^{intra}(\omega)$ is due to *intra-band transitions* which are relevant at low frequencies $\omega < 1$ eV. (In IR measurements the frequency is usually given in cm^{-1} , where the following conversion holds: $1cm^{-1} = 29.98$ GHz = 0.123985 meV = 1.44 K.) The experimental data for $\sigma(\omega) = \sigma_1 + i\sigma_2$ in cuprates are usually processed by the generalized (extended) Drude formula [17], [51], [18], [19]

$$\sigma(\omega) = \frac{\omega_p^2}{4\pi} \frac{1}{\gamma_{tr}(\omega) - i\omega m_{tr}(\omega)/m_\infty} \equiv \frac{1}{\tilde{\omega}_{tr}(\omega)}, \quad (11)$$

which is a useful representation for systems with single band electron-boson scattering which is justified in HTSC cuprates - see the discussion below. (The usefulness of introducing the optic relaxation $\tilde{\omega}_{tr}(\omega)$ will be discussed in Appendix B.) Here, $i = a, b$ enumerates the plane axis, ω_p , $\gamma_{tr}(\omega, T)$ and $m_{op}(\omega)$ are the electronic plasma frequency, the transport (optical) scattering rate and the optical mass, respectively. Very frequently, the quantity $\gamma_{tr}^*(\omega, T) = \gamma_{tr}(\omega, T)(m_\infty/m_{tr}(\omega)) =$

$\text{Im} \sigma(\omega)/\omega \text{Re} \sigma(\omega)$ [51], which is determined from the half-width of the Drude-like expression for $\sigma(\omega)$, was analyzed since it is independent of ω_p^2 . In the weak coupling limit $\lambda^{ep} < 1$, the formula for conductivity given in Eqs. (64-67) can be written in the form of Eq.(11) where γ_{tr} reads [18]-[19]

$$\gamma_{tr}(\omega, T) = \pi \sum_l \int_0^\infty d\nu \alpha_{tr,l}^2 F_l(\nu) [2(1 + 2n_B(\nu)) - 2\frac{\nu}{\omega} - \frac{\omega + \nu}{\omega} n_B(\omega + \nu) + \frac{\omega - \nu}{\omega} n_B(\omega - \nu)]. \quad (12)$$

Here $n_B(\omega)$ is the Bose distribution function. (For the explicit form of the transport mass $m_{tr}(\omega)$ see [17], [18], [19], [1], [2].) In the presence of impurity scattering one should add γ_{tr}^{imp} to γ_{tr} . It turns out that Eq.(12) holds within a few percents also for large $\lambda^{ep} (> 1)$. Note, that $\alpha_{tr,l}^2 F_l(\nu) \neq \alpha_l^2 F_l(\nu)$ and the index l enumerates all scattering bosons - phonons, spin fluctuations, etc. For comparison, we give the quasi-particle scattering rate $\gamma(\omega, T)$

$$\gamma(\omega, T) = 2\pi \int_0^\infty d\nu \alpha^2 F(\nu) \{2n_B(\nu) + n_F(\nu + \omega) + n_F(\nu - \omega)\} + \gamma^{imp}, \quad (13)$$

where n_F is the Fermi distribution function. By comparing Eq.(13) and Eq.(12), it is seen that γ_{tr} and γ are different quantities, $\gamma_{tr} \neq \gamma$, i.e. the former describes the relaxation of Bose particles (electron-hole pairs) while the latter one the relaxation of Fermi particles. This difference persists also at $T = 0$ K where one has (due to simplicity we omit in the following summation over l) [17]

$$\gamma_{tr}(\omega) = \frac{2\pi}{\omega} \int_0^\omega d\nu (\omega - \nu) \alpha_{tr}^2(\nu) F(\nu) \quad (14)$$

and

$$\gamma(\omega) = 2\pi \int_0^\omega d\nu \alpha^2(\nu) F(\nu). \quad (15)$$

In the case of EPI, the above equations give that $\gamma^{ep}(\omega) = \text{const}$ for $\omega > \omega_{ph}^{\max}$ while $\gamma_{tr}^{ep}(\omega)$ (as well as γ_{tr}^*) is monotonic growing for $\omega > \omega_{ph}^{\max}$, where ω_{ph}^{\max} is the maximal phonon frequency. This is clearly seen by comparing $\gamma(\omega, T)$, $\gamma_{tr}(\omega, T)$ and γ_{tr}^* which are calculated for the EPI spectral function $\alpha_{ep}^2(\omega) F_{ph}(\omega)$ extracted from tunnelling experiments in YBCO (with $\omega_{ph}^{\max} \sim 80$ meV) [23] - see Fig. 3.

The results shown in Fig. 3 clearly demonstrate the physical difference between two scattering rates γ^{ep} and γ_{tr}^{ep} . It is also seen that $\gamma_{tr}^*(\omega, T)$ is more a linear function of ω than $\gamma_{tr}(\omega, T)$. From these calculations one concludes that the quasi-linearity of $\gamma_{tr}(\omega, T)$ (and γ_{tr}^*) is

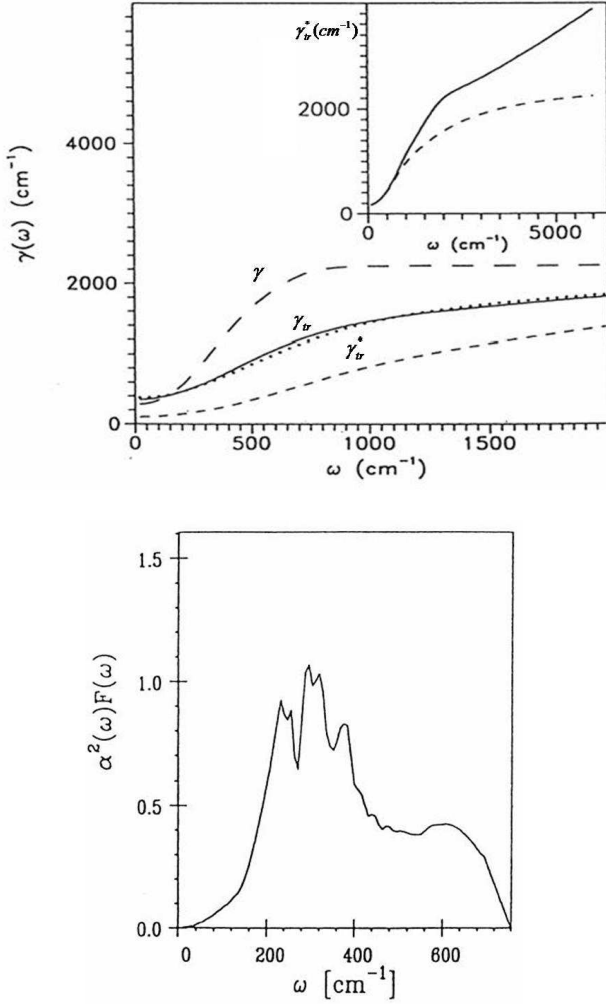


FIG. 3: (a) Scattering rates $\gamma(\omega, T)$, $\gamma_{tr}(\omega, T)$ and γ_{tr}^* - from top to bottom, for the Eliashberg function in (b). From [18]. (b) Eliashberg spectral function $\alpha_{ep}^2(\omega)F_{ph}(\omega)$ obtained from tunnelling experiments on break junctions [23]. Inset shows γ_{tr}^* with (full line) and without (dashed line) interband transitions protect[1].

not in contradiction with the EPI scattering mechanism but it is in fact a natural consequence of EPI. We stress that such behavior of γ^{ep} and γ_{tr}^{ep} , shown in Fig. 3, is in fact not exceptional for HTSC cuprates but it is generic for many metallic systems, for instance 3D metallic oxides, low temperature superconductors such as *Al*, *Pb*, etc. - see more in [1], [2].

Let us discuss briefly the experimental results for $R(\omega)$ and $\gamma_{tr}^*(\omega, T)$ and compare these with theoretical predictions obtained by using a single band model and $\alpha_{ep}^2(\omega)F_{ph}(\omega)$ from tunnelling data with the EPI coupling $\lambda = 2$ [23]. In the case of YBCO the agreement between measured and calculated $R(\omega)$ is very good up to frequencies $\omega < 6000 \text{ cm}^{-1}$ which confirms the importance of EPI in scattering processes. For higher frequencies, where a mead infrared peak appears, it is nec-

essary to account for interband transitions [1]. In optimally doped *Bi2Sr2CaCu2O6* [52] the experimental results for $\gamma_{tr}^*(\omega, T)$ are explained theoretically by assuming that the EPI spectral function $\alpha_{ep}^2(\omega)F(\omega) \sim F_{ph}(\omega)$, where $F_{ph}(\omega)$ is the phononic DOS in BISCO while $\alpha_{ep}^2(\omega) \sim \omega^{1.6}$, $\lambda = 1.9$ and $\gamma_{im} \approx 320 \text{ cm}^{-1}$ - see Fig. 4(a). The agreement is rather good. At the same time the fit of $\gamma_{tr}^*(\omega, T)$ by the marginal Fermi liquid fails as it is evident in Fig. 4(b).

Now we will comment on the so called pronounced linear behavior of $\gamma_{tr}(\omega, T)$ (and $\gamma_{tr}^*(\omega, T)$) which served in the past for numerous inadequate conclusions. We stress that the measured quantity is reflectivity $R(\omega)$ and derived ones are $\sigma(\omega)$, $\gamma_{tr}(\omega, T)$ and $m_{tr}(\omega)$, which are very sensitive to the value of the dielectric constant ϵ_∞ . This is clearly demonstrated in Fig. 5 for Bi2212 where it is seen that $\gamma_{tr}(\omega, T)$ (and $\gamma_{tr}^*(\omega, T)$) for $\epsilon_\infty = 1$ is linear up to much higher ω than in the case $\epsilon_\infty > 1$.

In some experiments [53], [54] $\gamma_{tr}(\omega, T)$ (and $\gamma_{tr}^*(\omega, T)$) is linear up to very high ω which means that the ion background and interband transitions (contained in ϵ_∞) are not properly taken into account since it is assumed too small ϵ_∞ . The recent ellipsometric measurements on YBCO [55] give the reliable value for $\epsilon_\infty \approx 4 - 6$. The latter gives rise to a much less spectacular linearity in the relaxation rates than it was the case immediately after the discovery of HTSC cuprates.

Furthermore, we would like to comment on two points concerning σ , γ_{tr} , γ and their interrelations. First, the parametrization of $\sigma(\omega)$ with the generalized Drude formula in Eq.(11) and its relation to the transport scattering rate $\gamma_{tr}(\omega, T)$ and the transport mass $m_{tr}(\omega, T)$ is useful if we deal with electron-boson scattering in a single band problem. In [19] it is shown that $\sigma(\omega)$ of a two-band model with only elastic impurity scattering can be represented by the generalized (extended) Drude formula with ω and T dependence of effective parameters $\gamma_{tr}^{eff}(\omega, T)$, $m_{tr}^{eff}(\omega, T)$ despite the fact that the inelastic electron-boson scattering is absent. To this end we stress that the single-band approach is fully justified for a number of HTSC cuprates such as LSCO, BISCO etc. Second, at the beginning we said that $\gamma_{tr}(\omega, T)$ and $\gamma(\omega, T)$ are physically different quantities and it holds $\gamma_{tr}(\omega, T) \neq \gamma(\omega, T)$. In order to give the physical picture and qualitative explanation we assume that $\alpha_{tr}^2 F(\nu) \approx \alpha^2 F(\nu)$. In that case the renormalized frequencies, the quasi-particle one $\tilde{\omega}(\omega) = Z(\omega)\omega = \omega - \Sigma(\omega)$ (for the definition of $Z(\omega)$ see Appendix A.) and the transport one $\tilde{\omega}_{tr}(\omega)$ - defined above, are related and at $T = 0$, they are given by [17], [19]

$$\tilde{\omega}_{tr}(\omega) = \frac{1}{\omega} \int_0^\omega d\omega' 2\tilde{\omega}(\omega'). \quad (16)$$

It gives the relation between $\gamma_{tr}(\omega)$ and $\gamma(\omega)$, $m_{tr}(\omega)$ and $m^*(\omega)$ respectively

$$\gamma_{tr}(\omega) = \frac{1}{\omega} \int_0^\omega d\omega' \gamma(\omega') \quad (17)$$

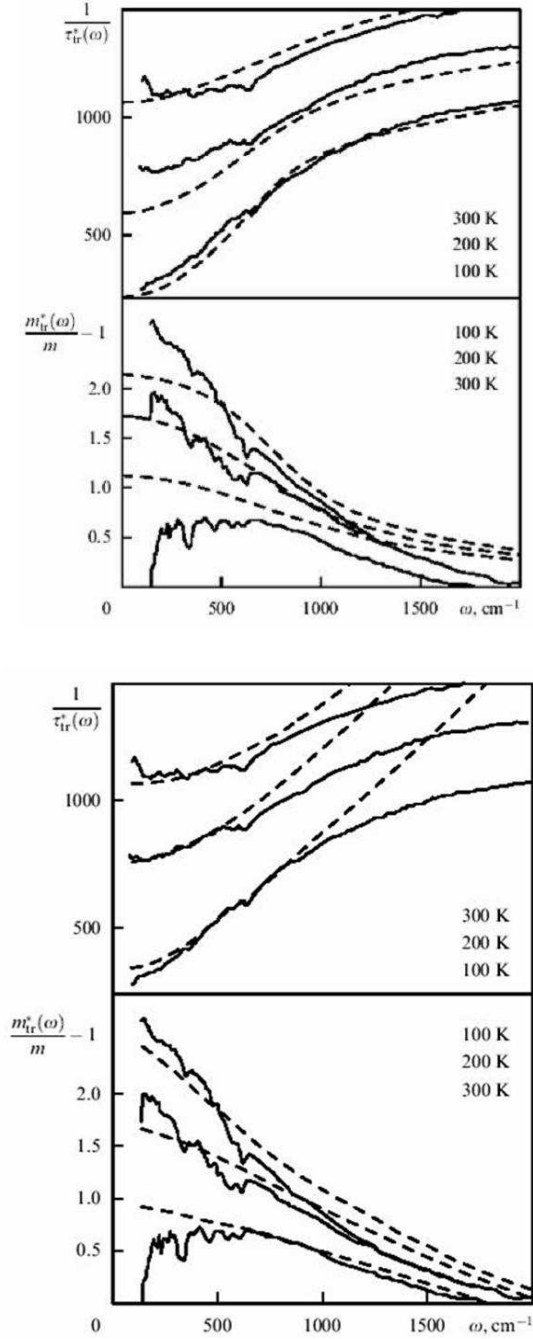


FIG. 4: (Top) Experimental transport scattering rate γ_{tr}^* (solid lines) for BiSCO and the theoretical curve by using Eq. (64) and transport mass m_{tr}^* with $\alpha^2 F(\omega)$ described in text (dashed lines). (Bottom) Comparison with the marginal Fermi liquid theory - dashed lines. From [1]

$$\omega m_{tr}(\omega) = \frac{1}{\omega} \int_0^\omega d\omega' 2\omega' m^*(\omega'). \quad (18)$$

The physical meaning of Eq.(16) is the following: in optical measurements one photon with the energy ω is absorbed and two excited particles (electron and hole) are

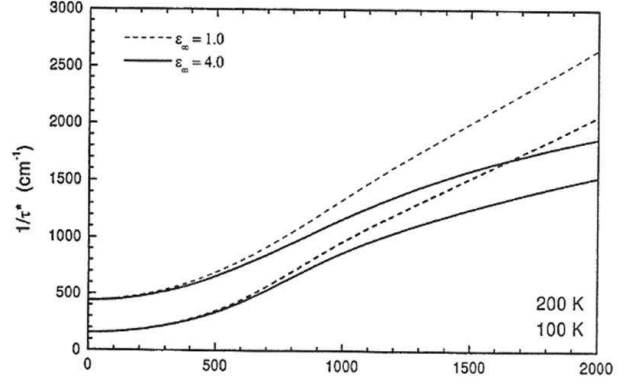


FIG. 5: Dependence of $\gamma_{tr}^*(\omega, T)$ on ϵ_∞ in $Bi_2Sr_2CaCu_2O_8$ on different temperatures for $\epsilon_\infty = 4$ (solid lines) and $\epsilon_\infty = 1$ (dashed lines). From [56].

created above and below the Fermi surface. If the electron has energy ω' and the hole $\omega - \omega'$, then they relax as quasi-particles with the renormalized $\tilde{\omega}$. Since ω' takes values $0 < \omega' < \omega$ then the optical relaxation $\tilde{\omega}_{tr}(\omega)$ is the energy-averaged $\tilde{\omega}(\omega)$ according to Eq.(16). The factor 2 is due to the two quasi-particles, electron+hole. At finite T , the generalization reads [17], [19]

$$\tilde{\omega}_{tr}(\omega) = \frac{1}{\omega} \int_0^\omega d\omega' [1 - n_F(\omega') - n_F(\omega - \omega')] 2\tilde{\omega}(\omega'). \quad (19)$$

2. Inversion of the optical data and $\alpha_{tr}^2(\omega)F(\omega)$

In principle, the transport spectral function $\alpha_{tr}^2(\omega)F(\omega)$ can be precisely extracted from $\sigma(\omega)$, i.e. $\gamma_{tr}(\omega)$, only at $T = 0$ K, which follows from Eq.(14)

$$\begin{aligned} \alpha_{tr}^2(\omega)F(\omega) &= \frac{1}{2\pi} \frac{\partial^2}{\partial \omega^2} (\omega \gamma_{tr}(\omega)) \\ &= \frac{\omega_p^2}{8\pi^2} \frac{\partial^2}{\partial \omega^2} [\omega \text{Re} \frac{1}{\sigma(\omega)}] |_{T=0}. \end{aligned} \quad (20)$$

However, real measurements are performed at finite T (and also at $T > T_c$) and the inversion procedure is in principle an ill-posed problem since $\alpha_{tr}^2(\omega)F(\omega)$ is the deconvolution of the inhomogeneous Fredholm integral equation of the first kind with the temperature dependent Kernel $K_2(\omega, \nu, T)$ in Eq.(12). An ill-posed mathematical problem, like this one, is very sensitive to input since experimental data contain less information than one needs. This can cause the fine structure of $\alpha_{tr}^2(\omega)F(\omega)$ gets blurred in the extraction procedures and it can be temperature dependent even when the true $\alpha_{tr}^2(\omega)F(\omega)$ is T independent. In the context of HTSC cuprates, this problem was first studied in [18], [19] with the following results: (1) the extracted shape of $\alpha_{tr}^2(\omega)F(\omega)$ in $YBa_2Cu_3O_{7-x}$ is not unique and it is temperature dependent, i.e. at higher $T > T_c$ the peak structure is

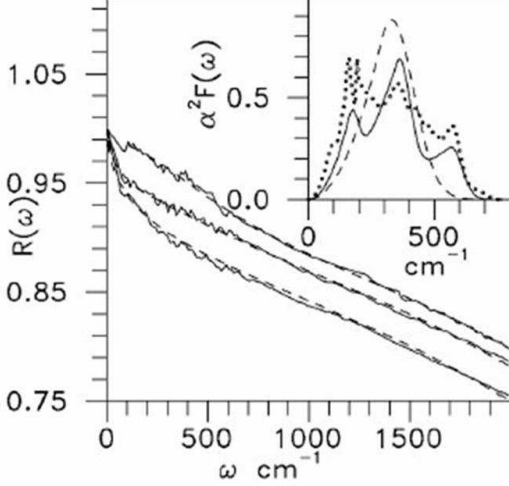


FIG. 6: Experimental (solid lines) and calculated (dashed lines) of $R(\omega)$ in optimally doped YBCO [57] at $T=100, 200, 300$ K (from top to bottom). Inset: the two reconstructed $\alpha_{tr}^2(\omega)F(\omega)$ at $T=100$ K. The phonon density of states $F(\omega)$ - dotted line. From [18]

smearred and only a single peak (slightly shifted to higher ω) is present. For instance, the experimental data of $R(\omega)$ in YBCO were reproduced by two different spectral functions $\alpha_{tr}^2(\omega)F(\omega)$, one with single peak and the other with three peaks structure as it is shown in Fig. 6. The similar situation is realized in optimally doped BISCO as it is seen in Fig. 7. It is important to stress that the width of the extracted $\alpha_{tr}^2(\omega)F(\omega)$ in both compounds coincide with the width of the phonon density of states $F_{ph}(\omega)$ [18], [19], [56]; (2) the upper energy bound for $\alpha_{tr}^2(\omega)F(\omega)$ can be extracted with certainty and it coincides approximately with the maximal phonon frequency in cuprates $\omega_{ph}^{max} \lesssim 80$ meV as it is seen in Figs. 6-7.

These results undoubtedly demonstrate the importance of EPI in cuprates [18], [19], [1]. We point out that the width of $\alpha_{tr}^2(\omega)F(\omega)$ which is extracted from the optical measurements [18], [19], [1] coincides with the width of the quasi-particle spectral function $\alpha^2(\omega)F(\omega)$ obtained in tunneling and ARPES spectra (which we shall discuss below), i.e. both functions are spread over the energy interval $0 < \omega < \omega_{ph}^{max} (\lesssim 80$ meV). Since in cuprates this interval coincides with the width in the phononic density of states $F(\omega)$ and since the maxima of $\alpha^2(\omega)F(\omega)$ and $F(\omega)$ almost coincide, this is further strong evidence for the dominance of EPI.

To this end, we would like to comment on two important points. *First*, in some reports [59],[12], [60] it was assumed that $\alpha_{tr}^2(\omega)F(\omega)$ of cuprates can be extracted also in the superconducting state by using Eq. (20). However, Eq. (20) holds exclusively in the normal state (at $T=0$) since $\sigma(\omega)$ can be described by the

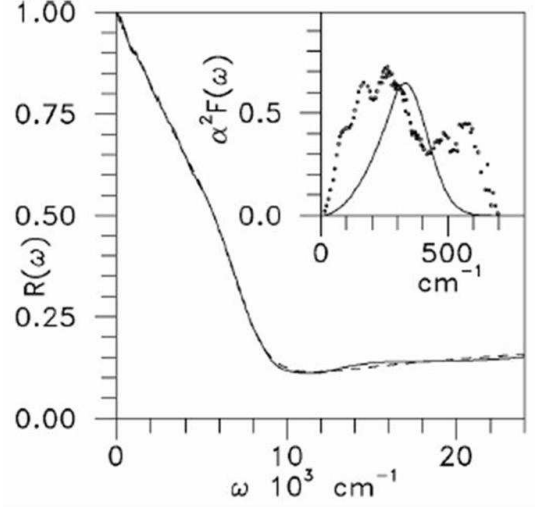


FIG. 7: Experimental (solid line) and calculated (dashed line) of $R(\omega)$ in optimally doped BISCO [58] at $T=100$ K. Inset: the reconstructed $\alpha_{tr}^2(\omega)F(\omega)$ - solid line. The phonon density of states $F(\omega)$ - dotted line. From [18]

generalized (extended) Drude formula in Eq. (11) only in the normal state. Such an approach apparently does not hold in the superconducting state since the dynamical conductivity depends not only on the electron-boson scattering but also on coherence factors and on the momentum and energy dependent order parameter $\Delta(\mathbf{k}, \omega)$. In such a case it is unjustified to extract $\alpha_{tr}^2(\omega)F(\omega)$ from Eq. (20). *Second*, if $R(\omega)$ (and $\sigma(\omega)$) in cuprates are due to some other bosonic scattering which is pronounced up to much higher energies $\omega_c \gg \omega_{ph}^{max}$, this should be seen in the extracted spectral function $\alpha_{tr}^2(\omega)F(\omega)$. Such an assumption is made, for instance, in the phenomenological spin-fluctuation approach [6] where it is assumed that $\alpha^2(\omega)F(\omega) = g_{sf}^2 \text{Im}\chi(\omega)$ where $\text{Im}\chi(\omega)$ is extended up to the large energy cutoff $\omega_c \approx 400$ meV. This assumption is apparently in conflict with the above theoretical and experimental analysis which shows that solely EPI can describe $R(\omega)$ very well and that the contribution from higher energies $\omega \gg \omega_{ph}^{max}$ must be small and therefore irrelevant for pairing [18], [19], [56]. This is also confirmed by tunnelling measurements - see below.

Despite the experimentally established facts for the importance of EPI, some reports appeared recently claiming that SFI dominates and that $\alpha_{tr}^2(\omega)F(\omega) \approx g_{sf}^2 \text{Im}\chi(\omega)$ where $\text{Im}\chi(\omega) = \int d^2k \chi(\mathbf{k}, \omega)$ [12], [60]. This claim is based on reanalyzing some old IR measurements [12], [60]. The transport spectral function $\alpha_{tr}^2(\omega)F(\omega)$ is extracted in [12] by using the maximum entropy method in solving the Fredholm equation. However, in order to exclude negative values in the extracted $\alpha_{tr}^2(\omega)F(\omega)$ they imply a biased condition that $\alpha_{tr}^2(\omega)F(\omega)$ has a rather large tail at large energies - up to 400 meV. Then it is

not surprising at all that their extracted $\alpha_{tr}^2(\omega)F(\omega)$ at large ω resembles qualitatively $\text{Im}\chi(\omega)$ obtained by the magnetic neutron scattering on $La_{2-x}Sr_xCuO_4$ [61]. In other words one obtains as output what is assumed in the input. It turns out that even such a biased assumption in [12] by extracting $\alpha_{tr}^2(\omega)F(\omega)$ does not reproduce the experimental curve $\text{Im}\chi(\omega)$ [61] in some important respects. (1) The relative heights of the two peaks in the extracted spectral function $\alpha_{tr}^2(\omega)F(\omega)$ at lower temperatures are opposite to that in $\text{Im}\chi(\omega)$ [61] - see Fig. 1 in [12]. (2) The strong temperature dependence of the extracted $\alpha_{tr}^2(\omega)F(\omega)$, found in [12], [60] is in fact not the intrinsic property of the spectral function but it is due to the high sensitivity of the extraction procedure on temperature. As we already explained before, this is due to the ill-posed problem of solving the Fredholm integral equation of the first kind with strong T -dependent kernel. (3) The extracted spectral weight $\alpha_{tr}^2(\omega)F(\omega)$ in [12] has much smaller values at larger frequencies ($\omega > 100 \text{ meV}$) than it is the case for the measured $\text{Im}\chi(\omega)$, i.e. $(I(\omega > 100 \text{ meV})/I(\omega_{\text{max}})) \ll \text{Im}\chi(\omega > 100 \text{ meV})/\text{Im}\chi(\omega_{\text{max}})$ - see Fig. 1 in [12]. In spite of the fact that the main weight of the extracted $\alpha_{tr}^2(\omega)F(\omega)$ [12] lies in the range of phononic frequencies, $0 < \omega < \omega_{\text{max}}^{\text{ph}}$ it is not in agreement with that obtained in tunnelling and ARPES measurements. (4) To this end it is suspicious that the transport coupling constant λ_{tr} extracted in [12] is so large, i.e. $\lambda_{tr} > 3$ contrary to the previous findings that $\lambda_{tr} < 1.5$ [18], [19], [56]. Since in HTSC one has $\lambda > \lambda_{tr}$ this would probably give $\lambda \approx 6$ that is not confirmed by other experiments. It is necessary to stress that the estimated λ_{tr} depends strongly on the value of plasma frequency, i.e. on ω_{pl}^2 - see Fig. 12 below, and it might be that for the latter the larger value is assumed in [12]. (5) The interpretation of $\alpha_{tr}^2(\omega)F(\omega)$ in LSCO and BISCO solely in terms of $\text{Im}\chi(\omega)$ is in contradiction with the magnetic neutron scattering in the optimally doped and slightly underdoped YBCO [16] - that was discussed above, where in the former $\text{Im}\chi(\mathbf{Q}, \omega)$ is small in the normal state - it is even below the experimental noise. This means that if the assumption that $\alpha_{tr}^2(\omega)F(\omega) \approx g_{sf}^2 \text{Im}\chi(\omega)$ were correct then the contribution to $\text{Im}\chi(\omega)$ from the momenta $0 < k < Q$ would be dominant and very detrimental for d-wave superconductivity and T_c would be rather low. Since the results of magnetic neutron scattering in YBCO [16] are very convincing and trustful, then the conclusion is that the SFI coupling constant $\lambda^{sf} (\sim g_{sf}^2)$ must be small, i.e. $g_{sf} < 0.2 \text{ eV}$ and $\lambda^{sf} < 0.2$. The latter is in accordance with other independent estimates (discussed also above) of $\lambda^{sf} (\ll 2)$.

Finally, we point out that very similar (to cuprates) properties, of $\sigma(\omega)$, $R(\omega)$ (and $\rho(T)$ and electronic Raman spectra) were observed in 3D isotropic metallic oxides $La_{0.5}Sr_{0.5}CoO_3$ and $Ca_{0.5}Sr_{0.5}RuO_3$ which are non-superconducting [62] and in $Ba_{1-x}K_xBiO_3$ which superconducts at $T_c \simeq 30 \text{ K}$ at $x = 0.4$. This means that in all of them, the scattering mechanism might be of simi-

lar origin. Since in these compounds there are no signs of antiferromagnetic fluctuations (which are present in cuprates), then EPI plays important role.

3. Restricted optical sum-rule

The *restricted optical sum-rule* was studied intensively in HTSC cuprates. It shows peculiarities not present in low-temperature superconductors. It turns out that the restricted spectral weight $W(\Omega_c, T)$ is strongly temperature dependent in the normal and superconducting state, that was interpreted either to be due to EPI [20], [21] or to some non-phononic mechanisms [63]. In the following we demonstrate that the temperature dependence of $W(\Omega_c, T) = W(0) - \beta T^2$ in the normal state can be explained in a natural way by the T -dependence of the EPI transport relaxation rate $\gamma_{tr}^{ep}(\omega, T)$ [20], [21]. Since the problem of the restricted sum-rule attracted much interest, it will be considered here in some details. In fact there are two kinds of sum rules related to $\sigma(\omega)$. The first one is the *total sum rule* which in the normal state reads

$$\int_0^\infty \sigma_1^N(\omega) d\omega = \frac{\omega_{pl}^2}{8} = \frac{\pi n e^2}{2m}, \quad (21)$$

while in the *superconducting state* it is given by the Tinkham-Ferrell-Glover (TFG) sum-rule

$$\int_0^\infty \sigma_1^S(\omega) d\omega = \frac{c^2}{8\lambda_L^2} + \int_{+0}^\infty \sigma_1^S(\omega) d\omega = \frac{\omega_{pl}^2}{8}. \quad (22)$$

Here, n - the total electron density, e - the electron charge, m - the bare electron mass and λ_L - the London penetration depth. The first (singular) term $c^2/8\lambda_L^2$ is due to the superconducting condensate which contributes $\sigma_{1,cond}^S(\omega) = (c^2/4\lambda_L^2)\delta(\omega)$. The total sum rule represents the fundamental property of matter - the conservation of the electron number, and to calculate it one should use the total Hamiltonian $\hat{H}_{tot} = \hat{T}_e + \hat{H}_{int}$ where all electrons, bands and their interactions \hat{H}_{int} (Coulomb, EPI, with impurities, etc.) are accounted for. Here, T_e is the *kinetic energy of bare electrons*

$$\hat{T}_e = \sum_{\sigma} \int d^3x \hat{\psi}_{\sigma}^{\dagger}(x) \frac{\hat{\mathbf{p}}^2}{2m} \hat{\psi}_{\sigma}(x) = \sum_{\mathbf{p}, \sigma} \frac{\mathbf{p}^2}{2m_e} \hat{c}_{\mathbf{p}\sigma}^{\dagger} \hat{c}_{\mathbf{p}\sigma}. \quad (23)$$

The *partial sum rule* is related to the energetics in the *conduction (valence) band* which is described by the Hamiltonian of the valence (band) electrons

$$\hat{H}_v = \sum_{\mathbf{p}, \sigma} \epsilon_{\mathbf{p}} \hat{c}_{v, \mathbf{p}\sigma}^{\dagger} \hat{c}_{v, \mathbf{p}\sigma} + \hat{V}_{v, Coul}. \quad (24)$$

It contains the band-energy with the dispersion $\epsilon_{\mathbf{p}}$ and the effective Coulomb interaction of the valence electrons $\hat{V}_{v, Coul}$. In this case the *partial sum-rule* in the normal state reads [64] (for general form of $\epsilon_{\mathbf{p}}$)

$$\int_0^\infty \sigma_{1,v}^N(\omega) d\omega = \frac{\pi e^2}{2V} \sum_{\mathbf{p}} \frac{\langle \hat{n}_{v, \mathbf{p}} \rangle_{H_v}}{m_{\mathbf{p}}} \quad (25)$$

where the number operator $\hat{n}_{v,\mathbf{p}} = \sum_{\sigma} \hat{c}_{\mathbf{p}\sigma}^{\dagger} \hat{c}_{\mathbf{p}\sigma}$; $1/m_{\mathbf{p}} = \partial^2 \epsilon_{\mathbf{p}} / \partial p_x^2$ is the reciprocal mass and V is volume. In practice measurements are performed up to finite frequency and the integration over ω goes up to some cutoff frequency Ω_c (of the order of the band plasma frequency). In this case the restricted sum-rule has the form

$$\begin{aligned} W(\Omega_c, T) &= \int_0^{\Omega_c} \sigma_{1,v}^N(\omega) d\omega \\ &= \frac{\pi}{2} [K^d + \Pi(0)] - \int_0^{\Omega_c} \frac{\text{Im}\Pi(\omega)}{\omega} d\omega. \end{aligned} \quad (26)$$

where K^d is the diamagnetic Kernel and $\Pi(\omega)$ is the paramagnetic (current-current) response function - see more in [20], [21]. In the case when the interband gap E_g is the largest scale in the problem, i.e. when $W_b < \Omega_c < E_g$, in this region one has approximately $\text{Im}\Pi(\omega) \approx 0$ and the limit $\Omega_c \rightarrow \infty$ in Eq.(26) is justified. In that case one has $\Pi(0) \approx \int_0^{\Omega_c} (\text{Im}\Pi(\omega)/\omega) d\omega$ which gives the approximate formula for $W(\Omega_c, T)$

$$\begin{aligned} W(\Omega_c, T) &= \int_0^{\Omega_c} \sigma_{1,v}^N(\omega) d\omega \approx \frac{\pi}{2} K^d \\ &= e^2 \pi \sum_{\mathbf{p}} \frac{\partial^2 \epsilon_{\mathbf{p}}}{\partial \mathbf{p}^2} n_{\mathbf{p}}, \end{aligned} \quad (27)$$

where $\epsilon_{\mathbf{p}}$ is the band-energy and $n_{\mathbf{p}} = \langle \hat{n}_{v,\mathbf{p}} \rangle$ is the quasiparticle distribution function in the interacting system. Note that the right hand side of Eq.(27) does not depend on the cutoff energy Ω_c . So one should be careful not to interpret blindly the experimental result in cuprates by this formula and for that reason the best way is to calculate $W(\Omega_c, T)$ by using the exact result in Eq.(26) which apparently depends on Ω_c . However, Eq.(27) is useful for appropriately chosen Ω_c , since it allows us to get semi-quantitative and qualitative results. In most papers related to the restricted sum-rule in HTSC, it was assumed, due to simplicity, the *tight-binding model with nearest neighbors* (n.n.) with the energy $\epsilon_{\mathbf{p}} = -2t(\cos p_x a + \cos p_y a)$ and $1/m_{\mathbf{p}} = -2ta^2 \cos p_x a$. It is straightforward to show that in this case one has

$$\begin{aligned} W(\Omega_c, T) &= \int_0^{\Omega_c} \sigma_{1,v}^N(\omega) d\omega \\ &\approx \frac{\pi e^2 a^2}{2V} \langle -T_v \rangle, \end{aligned} \quad (28)$$

where $\langle T_v \rangle_{H_v} = \sum_{\mathbf{p}} \epsilon_{\mathbf{p}} \langle n_v \rangle_{H_v}$ is the averaged kinetic energy of the band electrons and $\omega_{pl,v}$ is the (band) plasma frequency. In this approximation $W(\Omega_c, T)$ is a direct

measure of the averaged kinetic energy. In the *superconducting state* the partial sum-rule reads

$$\begin{aligned} W_s(\Omega_c, T) &= \frac{c^2}{8\lambda_L^2} + \int_{+0}^{\Omega_c} \sigma_{1,v}^S(\omega) d\omega \\ &= \frac{\pi e^2 a^2}{2} \langle -T_v \rangle_s. \end{aligned} \quad (29)$$

In order to introduce the reader to the complexity of the problem of T-dependence of $W(\Omega_c, T)$, let us consider the electronic system in the normal state and in absence of quasi-particle interaction. In that case one has $n_{\mathbf{p}} = f_{\mathbf{p}}$ ($f_{\mathbf{p}}$ is the Fermi distribution function) and $W_n(\Omega_c, T)$ increases with the decrease temperature, i.e. $W_n(\Omega_c, T) = W_n(0) - \beta_b T^2$ where $\beta_b \sim 1/W_b$. To this end, let us mention in advance that the experimental value β_{exp} is much larger than β_b , i.e. $\beta_{\text{exp}} \gg \beta_b$ thus telling us that the simple Sommerfeld-like smearing of $f_{\mathbf{p}}$ by the temperature effects cannot explain the T-dependence of $W(\Omega_c, T)$ as it was put forward in some papers. We stress that the smearing of $f_{\mathbf{p}}$ by temperature lowers the spectral weight compared to that at $T = 0$, i.e. $W_n(\Omega_c, T) < W_n(\Omega_c, 0)$. In that respect it is not surprising at all that there is a lowering of $W_s(\Omega_c, T)$ in the BCS superconducting state, $W_s^{BCS}(\Omega_c, T = 0) < W_n(\Omega_c, 0)$ since $f_{\mathbf{p}}$ is smeared due to the appearance of the superconducting gap, $2f_{\mathbf{p}} = 1 - (\xi_{\mathbf{p}}/E_{\mathbf{p}}) \text{th}(E_{\mathbf{p}}/2T)$, $E_{\mathbf{p}} = \sqrt{\xi_{\mathbf{p}}^2 + \Delta^2}$, $\xi_{\mathbf{p}} = \epsilon_{\mathbf{p}} - \mu$, and the maximal decrease of $W_s(\Omega_c, T)$ is at $T = 0$.

Let us enumerate and analyze the *main experimental results in cuprates*. **1.** In the *normal state* ($T > T_c$) of most cuprates, one has $W_n(\Omega_c, T) = W_n(0) - \beta_{\text{ex}} T^2$ with $\beta_{\text{exp}} \gg \beta_b$, i.e. $W_n(\Omega_c, T)$ is increasing by decreasing T , even at T below the opening of the pseudogap. The change of $W_n(\Omega_c, T)$ from room temperature down to T_c is no more than 5%. **2.** In the *superconducting state* ($T < T_c$) of some underdoped and optimally doped Bi-2212 compounds [66], [65] (and underdoped Bi-2212 films [72]) there is an *effective increase* of $W_s(\Omega_c, T)$ with respect to that in the normal state, i.e. $W_s(\Omega_c, T) > W_n(\Omega_c, T)$ for $T < T_c$. This is non-BCS behavior shown in Fig. 8.

In some optimally doped and in most overdoped cuprates, there is decreasing of $W_s(\Omega_c, T)$ at $T < T_c$ which is the BCS-like behavior [67] as it is seen in Fig. 9

We stress that the non-BCS behavior of $W_s(\Omega_c, T)$ for underdoped and optimally doped systems was obtained by assuming that $\Omega_c \approx (1 - 1.2) eV$. However, in Ref. [55] these results have been questioned and the conventional BCS-like behavior was observed ($W_s(\Omega_c, T) < W_n(\Omega_c, T)$) in the optimally doped YBCO and slightly underdoped Bi-2212 by using larger cutoff energy $\Omega_c = 1.5 eV$. Although the results obtained in [55] looks very trustfully, it is fair to say that the issue of the reduced spectral weight in the superconducting state of cuprates is still unsettled and under dispute. In overdoped Bi-2212 films, the BCS-like behavior $W_s(\Omega_c, T) <$

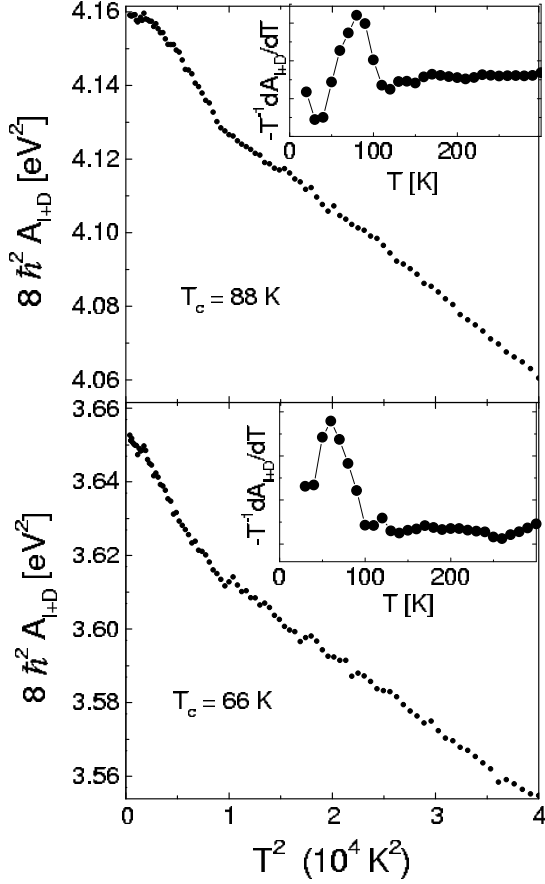


FIG. 8: Measured spectral weight $W_s(\Omega_c, T)$ for $\omega_c \approx 1.25 eV$ in two underdoped *Bi2212* (with $T_c = 88 K$ and $T_c = 66 K$). From [66].

$W_n(\Omega_c, T)$ was observed, while in LSCO it was found that $W_s(\Omega_c, T) \approx const$, i.e. $W_s(\Omega_c, T < T_c) \approx W_n(\Omega_c, T_c)$.

How to explain the strong temperature dependence of $W(\Omega_c, T)$ in the normal and superconducting state? In [20], [21] it was shown that the EPI relaxation $\gamma^{ep}(T)$ plays the main role in the T -dependence of $W(\Omega_c, T)$. The main theoretical results of [20], [21] are the following. (1) The calculations based on the exact formula in Eq.(27) give that for $\Omega_c \gg \Omega_D$, the difference in spectral weights of the normal and superconducting state is small, i.e. $W_n(\Omega_c, T) \approx W_s(\Omega_c, T)$ (in the following we call it W) since $W_n(\Omega_c, T) - W_s(\Omega_c, T) \sim \Delta^2/\Omega_c^2$. In the case of large Ω_c based on the approximate formula Eq.(27), one obtains

$$W(\Omega_c, T) \approx \frac{\omega_{pl}^2}{8} \left[1 - \frac{\gamma(T)}{W_b} - \frac{\pi^2 T^2}{2 W_b^2} \right]. \quad (30)$$

In the case of EPI, one has $\gamma = \gamma^{ep}(T) + \gamma^{imp}$ where $\gamma^{ep}(T) = \int_0^\infty dz \alpha^2(z) F(z) \coth(z/2T)$. It turns out that for $\alpha^2(\omega)F(\omega)$ shown in Fig. 3, one obtains: (i) $\gamma^{ep}(T) \sim T^2$ in the temperature interval 100

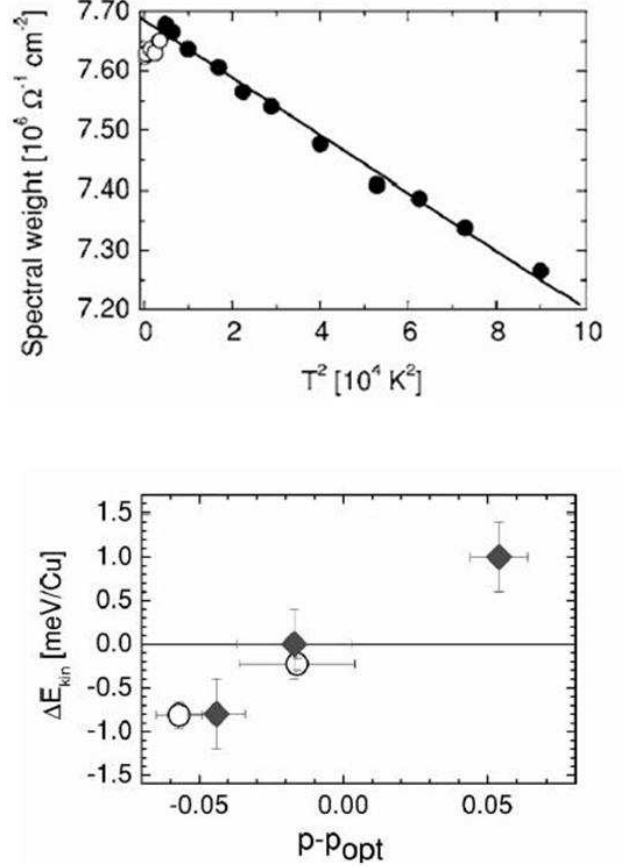


FIG. 9: (Top) Spectral weight $W_n(\Omega_c, T)$ of the overdoped *Bi2212* for $\Omega_c = 1 eV$. Closed symbols - normal state. Open symbols - superconducting state. (Bottom) Change of the kinetic energy $\Delta E_{kin} = E_{kin,S} - E_{kin,N}$ in *meV* per Cu site vs the charge p per Cu with respect to the optimal value p_{opt} . From [67].

$K < T < 200 K$ as it is seen in Fig. 10, [20], [21]; (ii) the second term in Eq.(30) is much larger than the last one (the Sommerfeld-like term). For the EPI coupling constant $\lambda_{tr}^{ep} = 1.5$ one obtains rather good agreement with experiments. At lower temperatures, $\gamma^{ep}(T)$ deviates from the T^2 behavior and the deviation depends on the structure of the spectrum in $\alpha^2(\omega)F(\omega)$. It is seen in Fig. 10 that for a softer Einstein spectrum (with $\Omega_E = 200 K$), $W(\Omega_c, T)$ lies above the curve with the T^2 asymptotic, while the one with a harder phononic spectrum (with $\Omega_E = 400 K$) lies below it. This result means that different behavior of $W(\Omega_c, T)$ in the superconducting state of cuprates for different doping might be simply related to different contributions of low and high frequency phonons. We stress that such

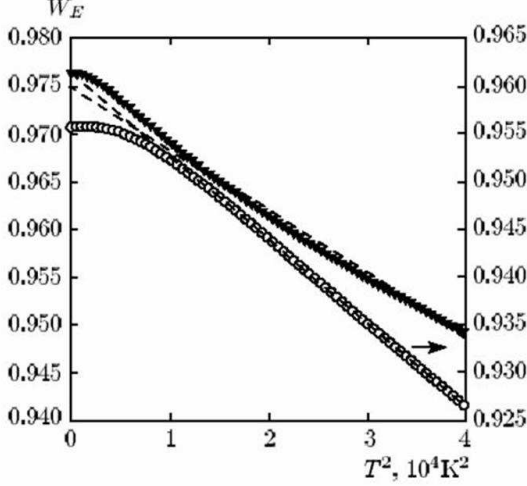


FIG. 10: Spectral weight $W(\Omega_c, T)$ for Einstein phonons with $\Omega_E = 200$ K (full triangles) and $\Omega_E = 400$ K (open circles, left axis). Dashed lines is T^2 asymptotic. From [21].

a behavior of $W(\Omega_c, T)$ was observed in experiments [66], [65], [55] and the above analysis tells us that the theory based on EPI explains in a consistent way the strange temperature behavior of $W(\Omega_c, T)$ above and below T_c and that there is no need to invoke exotic scattering mechanisms.

4. Resistivity $\rho(T)$

The temperature dependence of the in-plane resistivity $\rho_{ab}(T)$ in cuprates is a direct consequence of the quasi-2D motion of quasi-particles and of the inelastic scattering which they experience. At present, there is no consensus on the origin of the linear temperature dependence of the in-plane resistivity $\rho_{ab}(T)$ in the normal state and there is rather widespread believe that it can not be due to EPI. The inadequacy of this belief was already demonstrated by analyzing the dynamic conductivity $\sigma(\omega)$ which is successfully explained by EPI. Since $\rho(T) = 1/\sigma(\omega = 0)$

$$\rho(T) = \frac{4\pi}{\omega_p^2} \gamma_{tr}(T) + \rho_{imp} \quad (31)$$

$$\gamma_{tr}(T) = \frac{\pi}{T} \int_0^\infty d\omega \frac{\omega}{\sin^2(\omega/2T)} \alpha_{tr}^2(\omega) F(\omega). \quad (32)$$

It is quite natural that in some temperature region, $\rho(T)$ in cuprates can be explained by EPI as it is shown in Fig. 11. It turns out that $\gamma_{tr}(T) \sim T$ for $T > \alpha\Theta_D$, $\alpha < 1$ depending on the shape of $\alpha_{tr}^2(\omega)F(\omega)$. In case of the Debye spectrum, it is realized for $T > \Theta_D/5$ i.e.

$$\rho(T) \simeq 8\pi^2 \lambda_{tr}^{ep} \frac{k_B T}{\hbar \omega_p^2} = \rho' T. \quad (33)$$

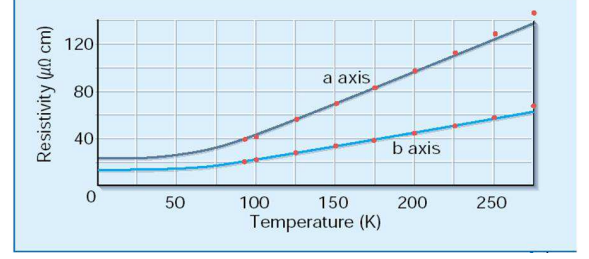
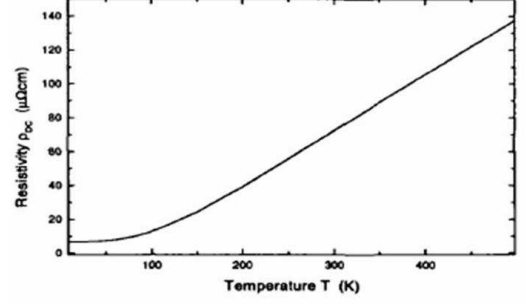


FIG. 11: (a) Calculated resistivity $\rho(T)$ for the EPI spectral function $\alpha_{tr}^2(\omega)F(\omega)$ in [68]. (b) Measured resistivity in a(x)- and b(y)-crystal direction of YBCO [70] and calculated Bloch-Grüneisen curve for $\lambda^{ep} = 1$, [71].

There is an experimental constraint on λ_{tr} , i.e.

$$\lambda_{tr} \approx 0.25 \omega_{pl}^2 (eV) \rho' (\mu\Omega\text{cm}/K), \quad (34)$$

which imposes a limit on it. For instance, for $\omega_{pl} \approx (2-3)$ eV [62] and $\rho' \approx 0.6$ in the oriented YBCO films and $\rho' \approx 0.3-0.4$ in single crystals of BSCO, one obtains $\lambda_{tr} \approx 0.4-1.2$. In case of YBCO single crystals, there is a pronounced anisotropy in $\rho_{a,b}(T)$ [70] which gives $\rho'_x(T) = 0.6 \mu\Omega\text{cm}/K$ and $\rho'_y(T) = 0.25 \mu\Omega\text{cm}/K$. According to Eq.(34), one obtains $\lambda_{tr}(\omega_{pl})$ which is shown in Fig.12, where the plasma frequency ω_{pl} which enters Eqs.(31-33) can be calculated by LDA and also extracted from the width ($\sim \omega_{pl}^*$) of the Drude peak at small frequencies, where $\omega_{pl} = \sqrt{\epsilon_\infty} \omega_{pl}^*$.

We shall argue below that from tunnelling experiments [23]-[28] one obtains in the framework of the Eliashberg theory that the EPI coupling constant is large $\lambda^{ep} \approx 2-3$ which implies that $\lambda_{tr} \sim (\lambda/3)$, i.e. EPI is reduced in transport properties due to some reasons that shall be discussed in *Part II*. Such a large reduction of λ_{tr} cannot be obtained within the LDA band structure calculations which means that λ^{ep} and λ_{tr} contain renormalization which do not enter in the *LDA* theory. In *Part II* we shall argue that the strong suppression of λ_{tr} may have its origin in strong electronic correlations and the long-range Madelung energy [45], [73].

4. Femtosecond time-resolved optical spectroscopy

The *femtosecond time-resolved optical spectroscopy* (FTROS) has been developed intensively in the last couple of years and applied successfully to HTSC cuprates.

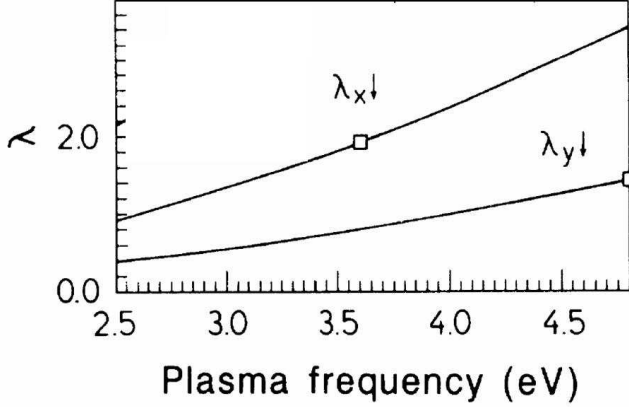


FIG. 12: Transport EPI spectral function coupling constant in YBCO as a function of plasma frequency ω_p as derived from the experimental slope of resistivity $\rho'(T)$ in Eq.(34). λ_x for $\rho'_x(T) = 0.6\mu\Omega\text{cm}/K$ and λ_y for $\rho'_y(T) = 0.25\mu\Omega\text{cm}/K$ [70]. Squares are LDA values [69].

In this method a femtosecond ($1fs = 10^{-15}$ sec) laser pump excites in materials electron-hole pairs via inter-band transitions. These hot carriers release their energy via electron-electron (with the relaxation time τ_{ee}) and electron-phonon scattering reaching states near the Fermi energy within $10 - 100 fs$ - see [74]. The typical energy density of the laser pump pulses with the wavelength $\lambda \approx 810 nm$ ($1.5 eV$) was around $F \sim 1\mu J/cm^2$ (the *excitation fluenc* F) which produces approximately 3×10^{10} carriers per puls (by assuming that each photon produces $\hbar\omega/\Delta$ carriers, Δ is the superconducting gap). By measuring photoinduced changes of the reflectivity in time, i.e. $\Delta R(t)/R_0$, one can extract information on the further relaxation dynamics of the low-laying electronic excitations. Since $\Delta R(t)$ relax to equilibrium the fit with exponential functions is used

$$\frac{\Delta R(t)}{R_0} = f(t) \left[Ae^{-\frac{t}{\tau_A}} + Be^{-\frac{t}{\tau_B}} + \dots \right], \quad (35)$$

where $f(t) = H(t)[1 - \exp\{-t/\tau_{ee}\}]$ ($H(t)$ is the Heavy-side function) describes the finite rise-time. The parameters A, B depends on the fluenc F . This method was used in studying the superconducting phase of $La_{2-x}Sr_xCuO_4$, with $x = 0.1, 0.15$ and $T_c = 30 K$ and $38 K$ respectively [22]. In that case the signal $A \neq 0$ for $T < T_c$ and $A = 0$ for $T > T_c$, while the signal B was present also at $T > T_c$. It turns out that the signal A is related to the quasi-particle recombination across the superconducting gap $\Delta(T)$ and has a relaxation time of the order $\tau_A > 10 ps$ at $T = 4.5 K$. At the so called threshold fluenc ($F_T = 4.2 \pm 1.7 \mu J/cm^2$ for $x = 0.1$ and $F_T = 5.8 \pm 2.3 \mu J/cm^2$ for $x = 0.15$) occurs the vaporization (destroying) of the superconducting phase, where the parameter A saturates. This vaporization process

takes place at the time scala $\tau_r \approx 0.8 ps$. The external fluenc is distributed in the sample over the *excitation volume* which is proportional to the optical penetration depth $\lambda_{op} (\approx 150 nm$ at $\lambda \approx 810 nm)$ of the pump. The energy densities stored in the excitation volume at the vaporization threshold for $x = 0.1$ and $x = 0.15$ are $U_p = F_T/\lambda_{op} = 2.0 \pm 0.8 K/Cu$ and $2.6 \pm 1.0 K/Cu$, respectively. The important fact is that U_p is much larger than the superconducting condensation energy which is $U_{cond} \approx 0.12 K/Cu$ for $x = 0.1$ and $U_{cond} \approx 0.3 K/Cu$ for $x = 0.15$, i.e. $U_p \gg U_{cond}$. This means that the energy difference $U_p - U_{cond}$ must be stored elsewhere on the time scale τ_r . The only present reservoir which can absorb the difference in energy are the bosonic baths of phonons and spin fluctuations. The energy required to heat the spin reservoir from $T = 4.5K$ to T_c is $U_{sf} = \int_{T_c}^T C_{sf}(T)dT$. The measured $C_{sf}(T)$ in La_2CuO_4 [22] gives very small value $U_{sf} \approx 0.01 K$. In the case of the phonon reservoir one obtains $U_{ph} = \int_{T_c}^T C_{ph}(T)dT = 9 K/Cu$ for $x = 0.1$ and $28 K/Cu$ for $x = 0.15$. Since $U_{sf} \ll U_p - U_{cond}$ the spin reservoir cannot absorb the rest energy $U_p - U_{cond}$. The situation is opposite with phonons since $U_{ph} \gg U_p - U_{cond}$ and phonon can absorb the rest energy in the excitation volume. The complete vaporization dynamics can be described in the framework of the Rothwarf-Taylor model which describes approaching of electrons and phonons to quasi-equilibrium on the time scale of $1 ps$ [75]. We shall not go into details but only summarize, that only phonon-mediated vaporization is consistent with the experiments, thus ruling out spin-mediated quasi-particle recombination and pairing in HTSC cuprates. This is additional proof for the ineffectiveness of the SFI scattering in cuprates.

In conclusion, optics and resistivity measurements in normal state of cuprates are much more in favor of EPI than against it. However, some intriguing questions still remain to be answered: (i) what are the values of λ_{tr} and ω_{pl} ; (ii) what is the reason that $\lambda_{tr} \ll \lambda$ is realized in cuprates; (iii) what is the role of Coulomb scattering in $\sigma(\omega)$ and $\rho(T)$. Later on we shall argue that ARPES measurements in cuprates give evidence for a contribution of Coulomb scattering at higher frequencies, where $\gamma(\omega) \approx \gamma_0 + \lambda_c\omega$ for $\omega > \omega_{max}^{ph}$ with $\lambda_c \approx 0.4$. So, despite the fact that EPI is suppressed in transport properties it can be sufficiently strong in the self-energy in some frequency and temperature range.

C. ARPES and the EPI self-energy

ARPES is nowadays a leading spectroscopy method in the solid state physics [11]. It provides direct information to the one-electron removal spectrum in a complex many system. The method involves shining light (photons) with energies between $5 - 1000 eV$ on the sample and by detecting momentum (\mathbf{k}) - and energy(ω)-distribution of the outgoing electrons. The resolution of ARPES has been significantly increased in the last

decade with the energy resolution of $\Delta E \approx 1 - 2 \text{ meV}$ (for photon energies $\sim 20 \text{ eV}$) and angular resolution of $\Delta\theta \lesssim 0.2^\circ$. The ARPES method is surface sensitive technique, since the average escape depth (l_{esc}) of the outgoing electrons is of the order of $l_{esc} \sim 10 \text{ \AA}$, depending on the energy of incoming photons. Therefore, very good surfaces are needed in order that the results be representative for bulk samples. The most reliable studies were done on the bilayer $Bi_2Sr_2CaCu_2O_8$ ($Bi2212$) and its single layer counterpart $Bi_2Sr_2CuO_6$ ($Bi2201$), since these materials contain weakly coupled BiO planes with the longest inter-plane separation in the cuprates. This results in a *natural cleavage* plane making these materials superior to others in ARPES experiments. After a drastic improvement of sample quality in other families of HTSC materials, the ARPES technique has become a central method in theoretical considerations. Potentially, it gives valuable information on the quasi-particle Green's function, i.e. on the quasi-particle spectrum and life-time effects. The ARPES can indirectly give information on the momentum and energy dependence of the pairing potential. Furthermore, the electronic spectrum of the (above mentioned) cuprates is highly *quasi-2D* which allows an unambiguous determination of the initial state momentum from the measured final state momentum, since the component parallel to the surface is conserved in photoemission. In this case, the ARPES probes (under some favorable conditions) directly the single particle spectral function $A(\mathbf{k}, \omega)$. In the following we discuss only those ARPES experiments which give evidence for the importance of the EPI in cuprates - see more in [11].

The *photoemission* measures a nonlinear response function of the electron system, and under some conditions it is analyzed in the so-called *three-step model*, where the total photoemission intensity $I_{tot}(\mathbf{k}, \omega) \approx I \cdot I_2 \cdot I_3$ is the product of three independent terms: (1) I - describes optical excitation of the electron in the bulk; (2) I_2 - describes the scattering probability of the travelling electrons; (3) I_3 - the transmission probability through the surface potential barrier. The central quantity in the three-step model is $I(\mathbf{k}, \omega)$ and it turns out that it can be written in the form (for $\mathbf{k} = \mathbf{k}_{\parallel}$) [11] $I(\mathbf{k}, \omega) \simeq I_0(\mathbf{k}, \nu) f(\omega) A(\mathbf{k}, \omega)$ with $I_0(\mathbf{k}, \nu) \sim |\langle \psi_f | \mathbf{pA} | \psi_i \rangle|^2$ and the quasi-particle spectral function $A(\mathbf{k}, \omega) = -\text{Im}G(\mathbf{k}, \omega)/\pi$

$$A(\mathbf{k}, \omega) = -\frac{1}{\pi} \frac{\text{Im}\Sigma(\mathbf{k}, \omega)}{[\omega - \xi(\mathbf{k}) - \text{Re}\Sigma(\mathbf{k}, \omega)]^2 + \text{Im}\Sigma^2(\mathbf{k}, \omega)}. \quad (36)$$

Here, $\langle \psi_f | \mathbf{pA} | \psi_i \rangle$ is the dipole matrix element which depends on \mathbf{k} , polarization and energy ν of the incoming photons. The knowledge of the matrix element is of a great importance and its calculation from first principles was done carefully in [76]. $f(\omega)$ is the Fermi function, G and $\Sigma = \text{Re}\Sigma + i\text{Im}\Sigma$ are the quasi-particle Green's function and the self-energy, respectively.

We summarize and comment here on some important ARPES results which were obtained recently and which

confirm the existence of the Fermi surface and importance of EPI in quasi-particle scattering [11].

ARPES in the normal state

(N1) There is a well defined Fermi surface in the metallic state with the topology predicted by the LDA. However, the bands are narrower than LDA predicts which points to a strong quasi-particle renormalization. (N2) The spectral lines are broad with $|\text{Im}\Sigma(\mathbf{k}, \omega)| \sim \omega$ (or $\sim T$ for $T > \omega$) which tells us that the quasi-particle liquid is a non-canonical Fermi liquid. (N3) There is a bilayer band splitting in $Bi2212$ (at least in the over-doped state). The previous experiments did not show this splitting and served for various speculations on some exotic non-Fermi liquid scenarios. (N4) At temperatures $T_c < T < T^*$ and in the under-doped cuprates there is a d-wave like pseudogap $\Delta_{pg}(\mathbf{k}) \sim \Delta_{pg,0}(\cos k_x - \cos k_y)$ in the quasi-particle spectrum where $\Delta_{pg,0}$ increases by lowering doping. We stress that the pseudogap phenomenon is not well understood at present and we shall discuss this problem in Part II. Its origin can be due to a precursor superconductivity or due to a competing order, such as spin- or charge-density wave or something similar. (N5) The ARPES self-energy gives clear evidence that EPI interaction is rather strong. For instance, at $T > T_c$ there are *kinks* in the quasi-particle dispersion $\omega(\xi_{\mathbf{k}})$ in the *nodal* direction (along the $(0, 0) - (\pi, \pi)$ line) at the characteristic phonon energy $\omega_{ph}^{(70)} \sim (60 - 70) \text{ meV}$ [48], see Fig. 13, and near the *anti-nodal point* $(\pi, 0)$ at 40 meV [77] - see Fig. 13.

That these kinks exist also above T_c excludes the scenario with the magnetic resonance peak in $\text{Im}\chi_s(\mathbf{Q}, \omega)$. Since the magnetic neutron scattering give small SFI coupling constant $\lambda^{sf} < 0.3$. The kinks cannot be due to SFI as we already discussed above. (N6) The position of the nodal kink is practically doping independent which points towards phonons as the scattering (gluing) boson. (N7) The quasi-particles (holes) couple practically to the whole spectrum of phonons since at least three group of phonons were extracted from the ARPES effective self-energy in $La_{2-x}Sr_xCuO_4$ [78] - Fig. 14.

This result is in a qualitative agreement with numerous tunnelling measurements [23]-[28] which apparently demonstrate that the broad spectrum of phonons couples with holes without preferring any particular phonons - see discussion below. (N8) Recent ARPES measurements in $B2212$ [49] show very different slope $d\omega/d\xi_{\mathbf{k}}$ of the quasi-particle energy $\omega(\xi_{\mathbf{k}})$ at very small $|\xi_{\mathbf{k}}| \ll \omega_{ph}$ and large energies $|\xi_{\mathbf{k}}| \gg \omega_{ph}$ - see Fig. 15. The theoretical analysis [79] of these results gives the total coupling constant $\lambda > 3$, the EPI one $\lambda^{ep} > 2$ while the Coulomb scattering (SFI is a part of it) is $\lambda^c \approx 1$ [79] - see Fig. 15. To this end let us mention some confusion related to the value of the EPI coupling constant extracted from ARPES. Namely, in [11], [80], [81] the EPI self-energy was obtained by subtracting the high energy slope of the quasi-particle spectrum $\omega(\xi_{\mathbf{k}})$ at $\omega \sim 0.3 \text{ eV}$. The latter is apparently due to the Coulomb interaction. Although the position of the low-energy kink is not affected by this

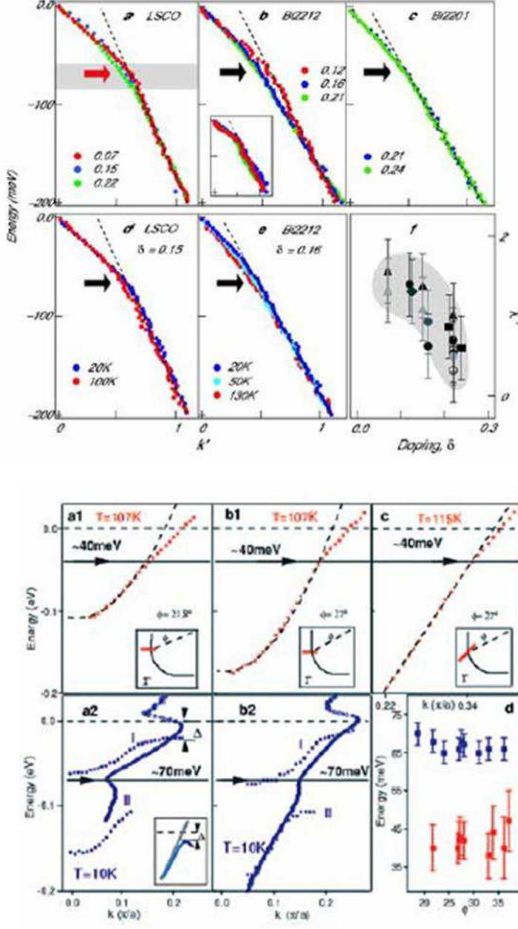


FIG. 13: (Top) Quasi-particle dispersion of *Bi2212*, *Bi2201* and *LSCO* along the *nodal* direction, plotted vs the momentum k for (a) – (c) different doping, and (d) – (e) different T ; black arrows indicate the kink energy; the red arrow indicates the energy of the $q = (\pi, 0)$ oxygen stretching phonon mode; inset of (e)- T -dependent Σ' for optimally doped *Bi2212*; (f) - doping dependence of the effective coupling constant λ' along $(0, 0) - (\pi, \pi)$ for the different HTSC oxides. From Ref. [48]. (Bottom) Quasi-particle dispersion $E(k)$ in the normal state (a1, b1, c), at 107 K and 115 K, along various directions ϕ around the *anti-nodal* point. The kink at $E = 40\text{meV}$ is shown by the horizontal arrow. (a2 and b2) is $E(k)$ in the superconducting state at 10 K with the shifted kink to 70meV . (d) kink positions as a function of ϕ in the anti-nodal region. From Ref. [77].

procedure (if $\omega_{ph}^{\max} \ll \omega_c$), the above (subtraction) procedure gives in fact an *effective EPI self-energy* $\Sigma_{eff}^{ep}(\mathbf{k}, \omega)$ and the *coupling constant* $\lambda_{z,eff}^{ep}(\mathbf{k})$ only. The latter is smaller than the real EPI coupling constant $\lambda_z^{ep}(\mathbf{k})$. The total self-energy is $\Sigma(\mathbf{k}, \omega) = \Sigma^{ep}(\mathbf{k}, \omega) + \Sigma^c(\mathbf{k}, \omega)$ where Σ^c is the contribution due to the Coulomb interaction. At very low energies $\omega \ll \omega_c$ one has usually $\Sigma^c(\mathbf{k}, \omega) = -\lambda_z^c(\mathbf{k})\omega$, where ω_c ($\sim 1\text{ eV}$) is the characteristic Coulomb energies and λ_z^c the Coulomb coupling con-

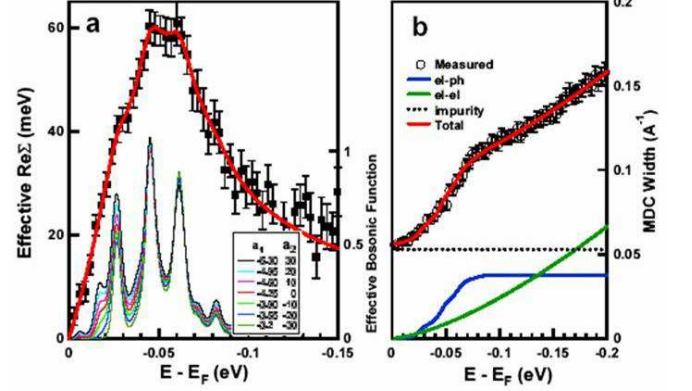


FIG. 14: (a) Effective real self-energy for the non-superconducting $La_{2-x}Sr_xCuO_4$, $x = 0.03$. Extracted $\alpha_{eff}^2(\omega)F(\omega)$ is in the inset. (b) Top: the total MDC width - open circles. Bottom: the EPI contribution shows saturation, impurity contribution - dotted black line. The residual part is growing $\sim \omega^{1.3}$. From [78].

stant. The quasi-particle spectrum $\omega(\mathbf{k})$ is determined from the condition

$$\omega - \xi(\mathbf{k}) - \text{Re}[\Sigma^{ep}(\mathbf{k}, \omega) + \Sigma^c(\mathbf{k}, \omega)] = 0, \quad (37)$$

where $\xi(\mathbf{k})$ is the bare band structure energy. At low energies $\omega < \omega_{ph}^{\max} \ll \omega_c$, Eq.(37) can be rewritten in the form

$$\omega - \xi^{ren}(\mathbf{k}) - \text{Re}\Sigma_{eff}^{ep}(\mathbf{k}, \omega) = 0, \quad (38)$$

$$\xi^{ren}(\mathbf{k}) = [1 + \lambda_z^c(\mathbf{k})]^{-1}\xi(\mathbf{k}) \quad (39)$$

$$\text{Re}\Sigma_{eff}^{ep}(\mathbf{k}, \omega) = \frac{\text{Re}\Sigma_{eff}^{ep}(\mathbf{k}, \omega)}{1 + \lambda_z^c(\mathbf{k})}. \quad (40)$$

Since at very low energies $\omega \ll \omega_{ph}^{\max}$, one has $\text{Re}\Sigma^{ep}(\mathbf{k}, \omega) = -\lambda_z^{ep}(\mathbf{k})\omega$ and $\text{Re}\Sigma_{eff}^{ep}(\mathbf{k}, \omega) = -\lambda_{z,eff}^{ep}(\mathbf{k})\omega$, then the real coupling constant is related to the effective one by

$$\lambda_z^{ep}(\mathbf{k}) = [1 + \lambda_z^c(\mathbf{k})]\lambda_{z,eff}^{ep}(\mathbf{k}) > \lambda_{z,eff}^{ep}(\mathbf{k}).$$

At higher energies $\omega_{ph}^{\max} < \omega < \omega_c$, which are less important for pairing, the EPI effects are suppressed and $\Sigma^{ep}(\mathbf{k}, \omega)$ stops growing, one has $\text{Re}\Sigma(\mathbf{k}, \omega) \approx \text{Re}\Sigma^{ep}(\mathbf{k}, \omega) - \lambda_z^c(\mathbf{k})\omega$. The measured $\text{Re}\Sigma^{exp}(\mathbf{k}, \omega)$ at $T = 10\text{ K}$ near and slightly away from the *nodal point* in the optimally doped *Bi2212* with $T_c = 91\text{ K}$ [83] is shown in Fig. 15.

It is seen that $\text{Re}\Sigma^{exp}(\mathbf{k}, \omega)$ has *two kinks* - the first one at *low energy* $\omega_1 \approx \omega_{ph}^{high} \approx 50 - 70\text{ meV}$ which is most probably of the phononic origin [11], [80], [81],

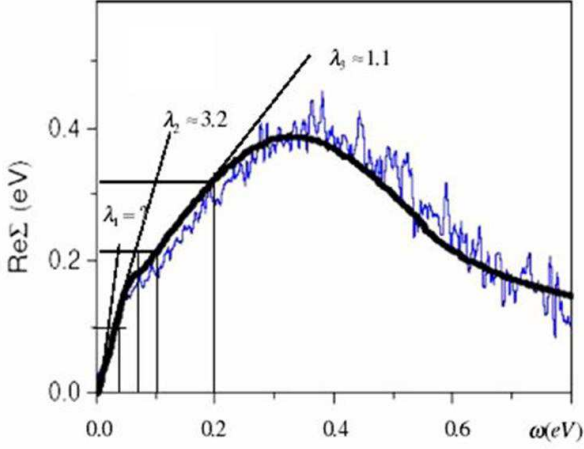


FIG. 15: Fig.4b from [83]: $Re\Sigma(\omega)$ measured in Bi2212 (thin line) and model $Re\Sigma(\omega)$ (bold line) obtained in [83]. The three thin lines ($\lambda_1, \lambda_2, \lambda_3$) are the slopes of $Re\Sigma(\omega)$ in different energy regions - see the text.

while the second kink at *higher energy* $\omega_2 \approx \omega_c \approx 350$ meV is probably due to the Coulomb interaction. However, the important results in Ref. [83] is that the slopes of $Re\Sigma^{exp}(\mathbf{k}, \omega)$ at low ($\omega < \omega_{ph}^{high}$) and high energies ($\omega_{ph}^{high} < \omega < \omega_c$) are *different*. The low-energy and high-energy slope *near the nodal point* are depicted and shown in Fig. 15 schematically (thin lines). From Fig. 15 it is obvious that EPI prevails at low energies $\omega < \omega_{ph}^{high}$. More precisely digitalization of $Re\Sigma^{exp}(\mathbf{k}, \omega)$ in the interval $\omega_{ph}^{high} < \omega < 0.4$ eV gives the Coulomb coupling $\lambda_z^c \approx 1.1$ while the same procedure at 20 meV $\approx \omega_{ph}^{low} < \omega < \omega_{ph}^{high} \approx 50 - 70$ meV gives the total coupling constant ($\lambda_2 \equiv \lambda_z = \lambda_z^{ep} + \lambda_z^c \approx 3.2$) and the EPI coupling constant $\lambda_z^{ep} (\equiv \lambda_{z,high}^{ep}) \approx 2.1 > 2\lambda_{z,eff}^{ep}(\mathbf{k})$, i.e. the EPI coupling is at least twice larger than in the previous analysis of ARPES results. This estimation tells us that at (and near) the nodal point, *the EPI interaction dominates* in the quasi-particle scattering at low energies since $\lambda_z^{ep} (\approx 2.1) \approx 2\lambda_z^c > 2\lambda_z^{sf}$, while at large energies (compared to ω_{ph}), the Coulomb interaction with $\lambda_z^c \approx 1.1$ dominates. We point out that EPI near the antinodal point can be even larger than in the nodal point, mostly due to the higher density of states near the antinodal point. (N8) Recent ARPES spectra in the optimally doped Bi2212 near the nodal and anti-nodal point [81] show a pronounced isotope effect in $Re\Sigma^{exp}(\mathbf{k}, \omega)$, thus pointing to the important role of EPI - see more in the part related to the isotope effect. The isotope effect in $Re\Sigma(\mathbf{k}, \omega)$ can be well described in the framework of the Migdal-Eliashberg theory for EPI [82] as it will be discussed in Part II. (N9) ARPES experiments on $Ca_2CuO_2Cl_2$ give strong evidence for the formation

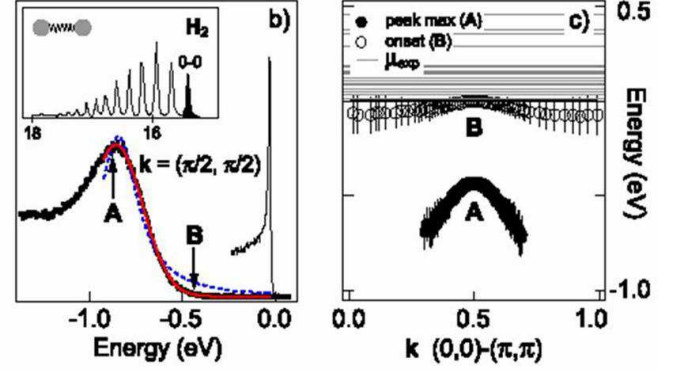


FIG. 16: (Left) The ARPES spectrum of undoped $Ca_2CuO_2Cl_2$ at $\mathbf{k} = (\pi/2, \pi/2)$. Gaussian shape - solid line, Lorentzian shape - dashed line. (Right) Dispersion of the polaronic band - A and of the quasi-particle band - B along the nodal direction. Horizontal lines are the chemical potentials for a large number of samples. From [84]

of *small polarons in undoped cuprates* which can be only due to phonons and strong EPI, while by doping quasi-particles appear and there are no small polarons [84]. Thus in [84], it a broad peak (around -0.8 eV) is observed at the top of the band ($\mathbf{k} = (\pi/2, \pi/2)$) with the dispersion similar to that predicted by the $t - J$ model - see Fig. 16.

However, the peak in Fig. 16 is of Gaussian shape and can be described only by coupling to bosons, i.e. this peak is a boson side band - see more in [5] and references therein. The theory based on the t-J model (in the antiferromagnetic state of the undoped compound) by including coupling to several (half-breathing, apical oxygen, low-lying) phonons, which is given in [85], explains successfully this broad peak of the boson side band by the formation of small polarons due to the EPI coupling ($\lambda^{ep} \approx 1.2$). Note that this λ^{ep} is for the polaron at the bottom of the band while in the case when the Fermi surface exists this coupling is even larger [85]. In [85] it was stressed that even when the electron-magnon interaction is stronger than the EPI one, the polarons are formed due to EPI. The latter involves excitation of many phonons at the lattice site (where the hole is seating), while it is possible to excite only one magnon at the given site.

(N10) Recent soft x-ray ARPES measurements on the *electron doped* HTSC $Nd_{1.85}Ce_{0.15}CuO_4$ [86], and $Sm_{(2-x)}Ce_xCuO_4$ ($x = 0.1, 0.15, 0.18$), $Nd_{1.85}Ce_{0.15}CuO_4$, $Eu_{1.85}Ce_{0.15}CuO_4$ [87] show kink at energies $50 - 70$ meV in the quasi-particle dispersion relation along both nodal and antinodal directions as it is shown in Fig. 17.

It is seen from this figure that the effective EPI coupling constant $\lambda_{eff}^{ep} (< \lambda^{ep})$ is isotropic and $\lambda_{eff}^{ep} \approx 0.8 - 1$. The kink in the electron-doped cuprates is due solely to

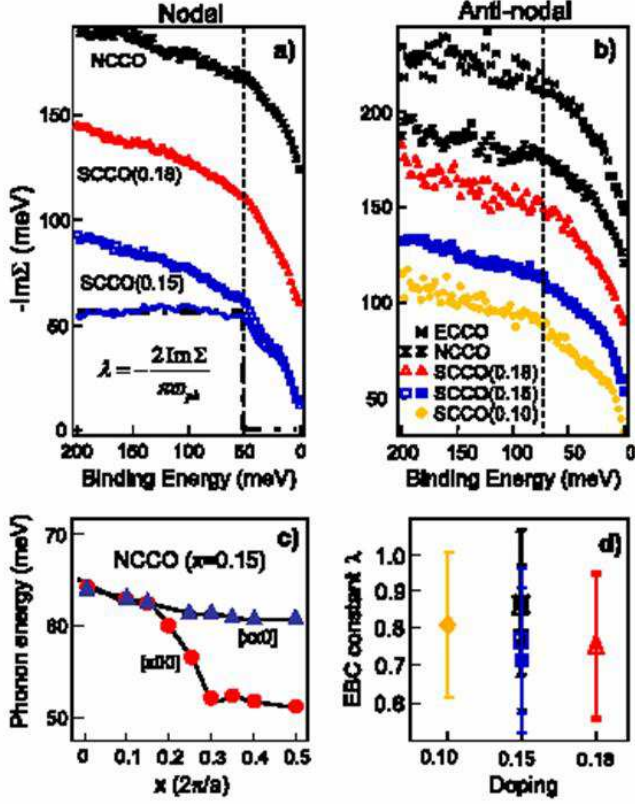


FIG. 17: NCCO electron-doped: (a) $Im\Sigma(\omega)$ measured in the nodal point. Curves are offsets by 50 meV for clarity. The change of the slope in the last bottom curve is at the phonon energy. (b) $Im\Sigma(\omega)$ for the antinodal direction with 30 meV offset. (c) Experimental phonon dispersion of the bond stretching modes. (d) Estimated λ_{eff}^{ep} from $Im\Sigma(\omega)$. From [87].

EPI and in that respect the situation is similar to the one in the hole-doped cuprates.

ARPES results in the superconducting state

(S1) There is an anisotropic superconducting gap in most HTSC compounds [11], which is predominately d-wave like, i.e. $\Delta_{sc}(\mathbf{k}) \sim \Delta_0(\cos k_x - \cos k_y)$ with $2\Delta_0/T_c \approx 5 - 6$. (S2) The kink at (60 – 70) meV in the quasi-particle energy around the nodal point is *not-shifted* in the superconducting state while the antinodal kink at $\omega_{ph}^{(40)} \sim 40$ meV is shifted in the superconducting state by $\Delta_0 (= (25 - 30)meV)$, i.e. $\omega_{ph}^{(40)} \rightarrow \omega_{ph}^{(40)} + \Delta_0 = (65 - 70)meV$ [11]. To remind the reader, in the standard Eliashberg theory the kink in the normal state at $\omega = \omega_{ph}$ should be shifted in the superconducting state to $\omega_{ph} + \Delta_0$ at any point at the Fermi surface. This puzzling result might be a smoking gun result since it makes a constraint on the quasi-particle interaction in cuprates. Until now there is only one plausible explanation [88] of this *shift-non-shift puzzle* which is based on an assumption of the

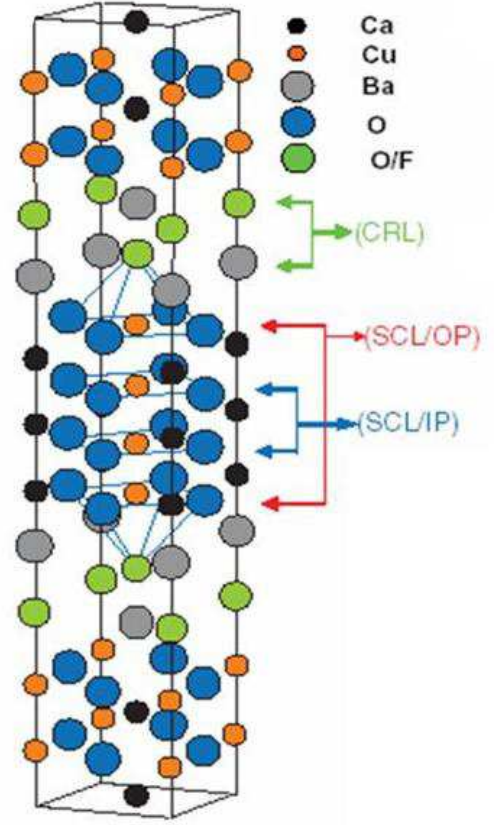


FIG. 18: Crystal structure of $Ba_2Ca_3Cu_4O_8(O_\delta F_{1-\delta})_2$. There are four CuO_2 layers in a unit cell with the outer having apical F atoms. From [89].

forward scattering peak (FSP) in EPI - see more in Part II. The FSP in EPI means that electrons scatter into a narrow region around the starting point in the k-space, so that at the most part of the Fermi surface, there is weak (or no) mixing of states with different signs of the order parameter $\Delta(\mathbf{k})$. (S3) The recent ARPES spectra [89] on an undoped single crystalline 4-layered cuprate with apical fluorine (F), $Ba_2Ca_3Cu_4O_8F_2$ (F0234) gives strong evidence against SFI - see Fig. 18.

Namely, F0234 is not a Mott insulator - as expected from valence charge counting which puts Cu valence as 2^+ , but it is a superconductor with $T_c = 60$ K. Moreover, the ARPES data [89] reveal at least two metallic Fermi-surface sheets with corresponding volumes equally below and above half-filling - see Fig. 19.

One of the Fermi-surfaces is due to the electron-like (N) band (with $20 \pm 6\%$ electron-doping) and the other

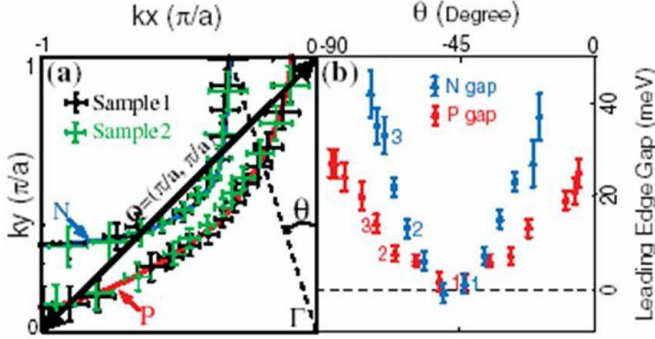


FIG. 19: (a) Fermi surface (FS) contours from two samples of F0234. n - electron-like; h - hole-like. Bold arrow is (π, π) scattering vector. Angle θ defines the horizontal axis in (b). (b) Leading gap edge along k-space angle from the two FS contours. From [89].

one due to the hole-like (P) band (with $20 \pm 8\%$ hole-doping) and their split along the nodal direction is significant and cannot be explained by the LDA (or DFA) method [90]. This electron and hole self-doping of inner and outer layers is in an appreciable contrast to other multilayered cuprates where there is only hole self-doping. For instance, in $\text{HgBa}_2\text{Ca}_n\text{Cu}_{n+1}\text{O}_{2n+2}$ ($n = 2, 3$) and $(\text{Cu,C})\text{Ba}_2\text{Ca}_n\text{Cu}_{n+1}\text{O}_{3n+2}$ ($n = 2, 3, 4$), the inner CuO_2 layers are less hole-doped than outer layers. It turns out, unexpectedly, that the superconducting gap on the N -band Fermi-surface is significantly larger than on the P -one, i.e. their ratio is anomalous ($\Delta_N/\Delta_P \approx 2$ and Δ_N is an order of magnitude larger than in the electron-doped cuprate $\text{Nd}_{2-x}\text{Ce}_x\text{CuO}_4$. Furthermore, the N -band Fermi-surface is rather far from the antinodal point at $(\pi/2, 0)$. This is an extremely important result which means that the antiferromagnetic spin fluctuations with the AF wave-vector $\mathbf{Q} = (\pi/2, \pi/2)$, as well as the van Hove singularity, are not important for the pairing in the N -band. To remind the reader, the SFI scenario assumes that the pairing is due to spin fluctuations with the wave-vector \mathbf{Q} which connects two antinodal points which are near the van Hove singularity at the hole-surface (at $(\pi/2, 0)$ and $(0, \pi/2)$) giving rise to large density of states. This is apparently not the case for the N -band Fermi-surface - see Fig. 19. The ARPES data give further that there is a kink at $\sim 85 \text{ meV}$ in the quasi-particle dispersion of both bands, while the kink in the N -band is stronger than that in the P -band. This result, together with the anomalous ratio ($\Delta_N/\Delta_P \approx 2$, strongly disfavors SFI as a pairing mechanism.

(S4) Despite the presence of significant elastic scattering in optimally doped Bi-2212, there are dramatic sharpening of the spectral function near the anti-nodal point $(\pi, 0)$ at $T < T_c$ [91]. This can be explained by

assuming that the small q -scattering (the forward scattering peak) dominates in the elastic impurity scattering [92], [93]. As a result, one finds that the impurity scattering rate in the superconducting state is almost zero, i.e. $\gamma_{imp}(\mathbf{k}, \omega) = \gamma_n(\mathbf{k}, \omega) + \gamma_a(\mathbf{k}, \omega) = 0$ for $|\omega| < \Delta_0$ for any kind of pairing (s - p - d -wave etc.) since the normal (γ_n) and the anomalous (γ_a) scattering rates compensate each other - the *collapse of the elastic scattering rate*. This result is a consequence of the Anderson-like theorem for unconventional superconductors which is due to the dominance of the small q -scattering [92]-[93]. In such a case d -wave pairing is weakly unaffected by impurities - there is small reduction in T_c [93], [94]. The physics behind this result is rather simple. The small q -scattering (forward scattering) means that electrons scatter into a small region in the k -space, so that at the most part of the Fermi surface there is no mixing of states with different signs of the order parameter $\Delta(\mathbf{k})$, and the detrimental effect of impurities is reduced. For states near the nodal points, there is mixing but since $\Delta(\mathbf{k})$ is small in this region, there is only small reduction in T_c [42]. This result points to the importance of strong correlations in the renormalization of the impurity scattering - see discussion in Part II.

In conclusion, in order to explain ARPES results in cuprates it is necessary to take into account: (1) EPI interaction since it dominates in the quasiparticle scattering in the energy region responsible for pairing; (2) effects of elastic nonmagnetic impurities with FSP; (3) the Coulomb interaction which dominates at higher energies $\omega > \omega_{ph}$. In this respect, the presence of ARPES kinks and the knee-like shape of the spectral width are serious constraints for the pairing theory.

D. Tunnelling spectroscopy and spectral function $\alpha^2 F(\omega)$

By measuring current-voltage $I - V$ characteristics in NIS (normal metal-insulator-superconductor) tunnelling junctions with large tunnelling barrier - see more below, one obtains from tunnelling conductance $G_{NS}(V) = dI/dV$ the so called tunnelling density of states in superconductors $N_T(\omega)$. Moreover, by measuring of $G_{NS}(V)$ at voltages $eV > \Delta$ it is possible to determine the Eliashberg spectral function $\alpha^2 F(\omega)$ and finally to confirm (definitely) the phonon mechanism of pairing in $LTSC$ materials, except heavy fermions. Four tunnelling techniques were used in the study of $HTSC$ cuprates: (1) vacuum tunneling by using the STM technique - scanning tunnelling microscope; (2) point-contact tunnelling; (3) break-junction tunnelling; (4) planar-junction tunnelling. Each of these techniques has some advantages although in principle the most potential one is the STM technique [95]. It should be stressed that there are still difficulties in understanding tunnelling experiments in $HTSC$ cuprates because of non-ideal tunnelling behavior of contacts [95]. Since tunnelling mea-

measurements probe a surface region of the order of superconducting coherence length ξ_0 , then this kind of measurements in *HTSC* materials with small coherence length ξ_0 ($\xi_{ab} \sim 20 \text{ \AA}$ in the $a-b$ plane and $\xi_c \sim 1-3 \text{ \AA}$ along the c -axis) depends strongly on the surface quality and sample preparation. Nowadays, many of these material problems in *HTSC* cuprates are understood and as a result consistent picture of tunnelling features is starting to emerge.

From tunnelling experiments one obtains the energy gap in the superconducting state. Since we have already discussed this problem in [2], we will only briefly mention some important result, that in most cases, $G_{NS}(V)$ has V-shape in all families of *HTSC* hole and electron doped cuprates. This is due to d -wave pairing with the gapless spectrum, which is definitely confirmed in the interference experiments on hole and electron doped cuprates [41]. Some experiments give the U-shape of $G_{NS}(V)$ which resembles s-wave pairing. This controversy is explained to be the property of the tunneling matrix element which filters out states with the maximal gap.

Here we are interested in the electron-boson spectral function $\alpha^2 F(\omega)$ in *HTSC* cuprates which can be extracted by using tunnelling spectroscopy. We inform the reader in advance, that the shape and the energy width of $\alpha^2 F(\omega)$, which are extracted from the second derivative $d^2 I/dV^2$ at voltages above the superconducting gap, in most *HTSC* cuprates resembles the phonon density of states $F(\omega)$. This result is strong evidence for the importance of *EPI* in the pairing potential of *HTSC* cuprates. For instance, plenty of break-junctions made from *Bi2212* single crystals [23] show that the negative peaks in $d^2 I/dV^2$ coincide with the peaks in the generalized phonon density of states $F_{ph}(\omega)$ measured by neutron scattering - see Fig. 20.

The tunnelling spectra in *Bi2212* break junctions [23], which are shown in Fig. 20, indicates that the spectral function $\alpha^2 F(\omega)$ is unchanged in magnetic field which disfavors SFI since in the latter case, this function should be sensitive to the magnetic field. The reported broadening of the peaks in $\alpha^2 F(\omega)$ are partly due to the gapless spectrum of d -wave pairing in *HTSC* cuprates. Additionally, the tunnelling density of states $N_T(\omega)$ at very low T show a pronounced gap structure and it was found that $2\bar{\Delta}/T_c = 6.2 - 6.5$, where $T_c = 74 - 85 \text{ K}$ and $\bar{\Delta}$ is some average value of the gap. In order to obtain $\alpha^2 F(\omega)$ the inverse procedure was used by assuming s -wave superconductivity and the effective Coulomb parameter $\mu^* \approx 0.1$ [23]. The obtained $\alpha^2 F(\omega)$ gives large *EPI* coupling constant $\lambda^{ep} \approx 2.3$. Although this analysis [23] was done in terms of s -wave pairing, it mimics qualitatively the case of d -wave pairing, since one expects that d -wave pairing does not change significantly the global structure of $d^2 I/dV^2$ at $eV > \Delta$ albeit introducing a broadening in it - see the physical meaning in Appendix A. We point out that the results obtained in [23] were reproducible on more than 30 junctions. In

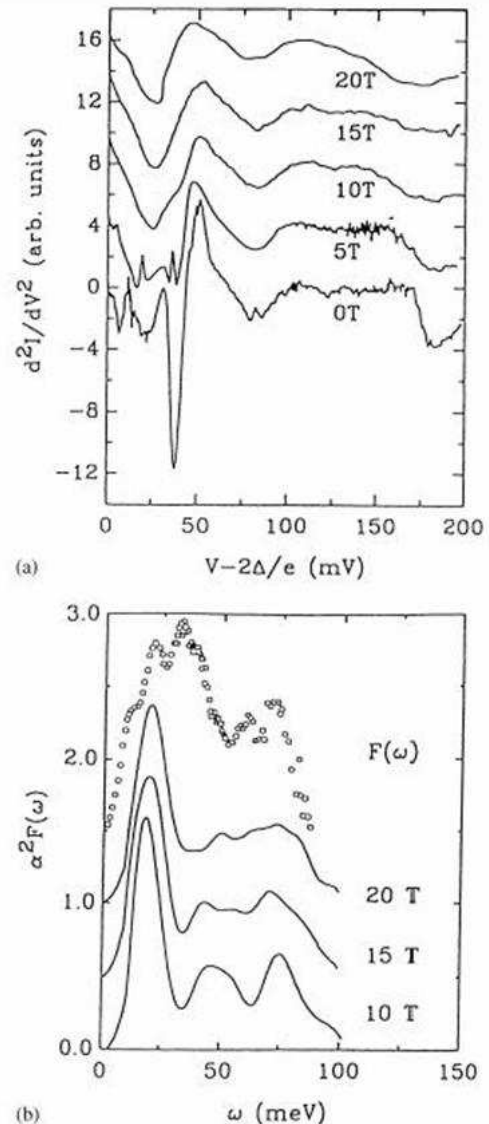


FIG. 20: (a) Second derivative of $I(V)$ for a *Bi2212* break junction in various magnetic fields. The structure of minima in $d^2 I/dV^2$ can be compared with the phonon density of states $F(\omega)$; (b) the spectral functions $\alpha^2 F(\omega)$ in various magnetic fields. From [23]

that respect very important results on slightly overdoped *Bi2212 - GaAs* and on *Bi2212 - Au* planar tunnelling junctions are obtained in [24] - see Fig. 21.

These results show very similar features to those obtained in [23] on break-junctions. It is worth mentioning that several groups [25], [26], [27] have obtained similar results for the shape of the spectral function $\alpha^2 F(\omega)$ from the $I-V$ measurements on various *HTSC* cuprates - see the comparison in Fig. 22. The latter results leave no much doubts about the importance of the *EPI* in

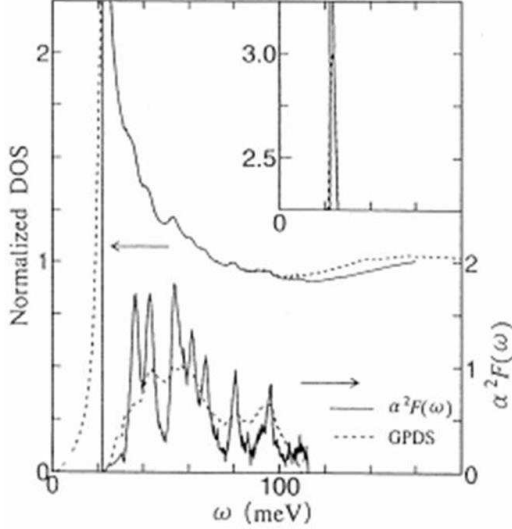


FIG. 21: The spectral functions $\alpha^2 F(\omega)$ and the calculated density of states at $0K$ (upper solid line) obtained from the conductance measurements the $Bi(2212) - Au$ planar junctions. From [24]

pairing mechanism of *HTSC* cuprates.

In that respect tunnelling measurements on *slightly overdoped* $Bi_2Sr_2CaCu_2O_8$ [24], [28] are impressive, since the Eliashberg spectral function $\alpha^2 F(\omega)$ was extracted from the measurements of d^2I/dV^2 and by solving the inverse problem. The extracted $\alpha^2 F(\omega)$ has several peaks in broad energy region up to $80 meV$ as it is seen in Fig. 21- 22, which coincide rather well with the peaks in the phonon density of states $F_{ph}(\omega)$. In [28] numerous peaks, from $P1 - P13$, in $\alpha^2 F(\omega)$ are discerned as shown in Fig.24, which correspond to various groups of phonon modes - laying in (and around) these peaks. Moreover, in [24], [28] are extracted the coupling constants for these modes and their contribution (ΔT_c) to T_c as it is seen in Fig. 23. Note, due to the nonlinearity of the problem, the sum of ΔT_c is not equal to T_c .

The next remarkable result is that the extracted *EPI* coupling constant is very large, i.e. $\lambda^{ep} (= 2 \int d\omega \alpha^2 F(\omega)/\omega) = \sum_i \lambda_i \approx 3.5$ - see Fig. 23. It is obvious from Figs. (23-24) that almost *all phonon modes contribute* to λ^{ep} and T_c , which means that on the average, each particular phonon mode is not too strongly coupled to electrons thus keeping the lattice stable. None of the modes has too large $\lambda_i < 1.3$, thus keeping the lattice stability.

For a better understanding of the the *EPI* coupling in these systems we show in Fig. 25 the total and partial density of phononic states. In Fig. 23 it is seen that lower

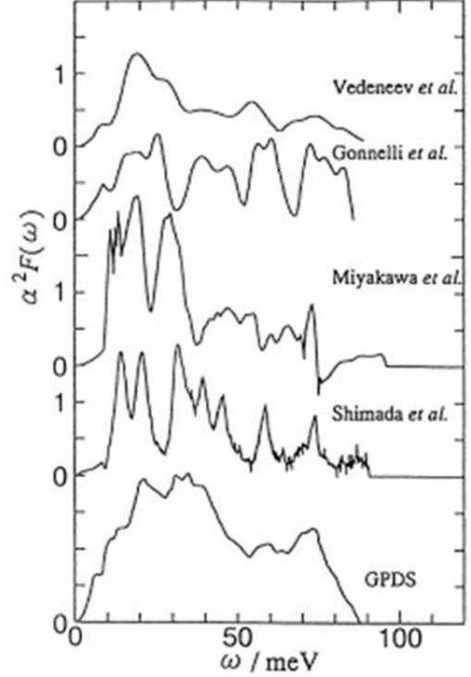


FIG. 22: The spectral functions $\alpha^2 F(\omega)$ from measurements of various groups: Vedeneev et al. [23], Gonnelli et al.[27], Miyakawa et al. [25], Shimada et al. [24]. The generalized density of states GPDS for $Bi2212$ is at the bottom. From [24].

frequency modes from $P1 - P3$, corresponding to Cu , Sr and Ca vibrations, are rather strongly coupled to electrons (with $\lambda_{\kappa} \sim 1$) and give appreciable contributions to T_c . It is also seen in Fig. 23 that the coupling constants λ_i of the high-energy phonons ($P9 - P13$ with $\omega \geq 70 meV$) have $\lambda_i \ll 1$ and give moderate contribution to T_c - around 10 %. These results confirm the *importance of modes which cause the change of the Madelung energy* in the ionic-metallic structure of *HTSC* cuprates, the idea also conveyed in [1], [2] - see more in *Part II*. If definitely confirmed, these results are in accordance with the moderate oxygen isotope effect in cuprates near the optimal doping. We stress that each peak $P1 - P13$ in $\alpha^2 F(\omega)$ corresponds to many modes. In order to get filling on the structure of vibrations possibly strongly involved in pairing, we show in Figs. 26-27 the structure of these vibrations at special points in the Brillouin zone. It is seen in Fig. 26 that the low-frequency phonons $P1 - P2$ are dominated by Cu , Sr , Ca vibrations.

It is seen in Fig. 23 that $P3$ modes are stronger coupled to electrons than $P4$ ones, although the density of state for the $P4$ modes is larger. The reason for such an anomalous behavior might be due to symmetries of corresponding phonons as it is shown in Fig. 27. Namely

No.peak	ω [meV]	λ_i	ΔT_c [K]
P1	14.3	1.26	7.4
P2	20.8	0.95	11.0
P3	31.7	0.48	10.5
P4	35.1	0.28	6.7
P5	39.4	0.24	7.0
P6	45.3	0.30	10.0
P7	58.3	0.15	6.5
P8	63.9	0.01	0.6
P9	69.9	0.07	3.6
P10	73.7	0.06	3.3
P11	77.3	0.01	0.8
P12	82.1	0.01	0.7
P13	87.1	0.03	1.8

FIG. 23: Table I - Phonon frequency ω , EPI coupling constant λ_i of the peaks $P1 - P13$ and contribution ΔT_c to T_c of each peak in $\alpha^2 F(\omega)$ -shown in Fig.24, obtained from the tunnelling conductance of $Bi_2Sr_2CaCu_2O_8$. ΔT_c is the decrease in T_c when the peak in $\alpha^2 F(\omega)$ is eliminated. From [28].

to the $P3$ peak contribute *axial vibrations* of O(1) in the Cu_2 plane which are odd under inversion, while in the $P4$ peak these modes are even. The in-plane modes of Ca and O(1) are present in $P3$ which are in-phase and out-of-phase modes, while in $P4$ they are all out-of-phase modes. For more information on other modes $P5 - P13$ see [28]. We stress that the Eliashberg equations based on the extracted $\alpha^2 F(\omega)$ of the slightly overdoped $Bi_2Sr_2CaCu_2O_8$ with the ratio $(2\Delta/T_c) \approx 6.5$ describe rather well numerous optical, transport and thermodynamic properties [28]. However, in underdoped systems with $(2\Delta/T_c) \approx 10$, where the pseudogap phenomena are pronounced, there are serious disagreements between experiments and the Eliashberg-like theory.

Similar conclusion, regarding the properties of the EPI spectral function $\alpha^2 F(\omega)$ in HTSC cuprates, comes out from tunneling measurements on the Andreev ($Z \ll 1$, low barrier)- and Giaever ($Z \gg 1$, high barrier) -type junctions in $La_{2-x}Sr_xCuO_4$ and YBCO compounds [97], where the extracted $\alpha^2 F(\omega)$ is in accordance with the phonon density of states $F_{ph}(\omega)$ see Fig. 28.

Note that the BTK parameter Z is related to the transmission and reflection coefficients for the normal metal $(1 + Z^2)^{-1}$ and $Z^2(1 + Z^2)^{-1}$ respectively.

Although most of the peaks in $\alpha^2 F(\omega)$ in HTSC cuprates coincide with the peaks in the phonon density of

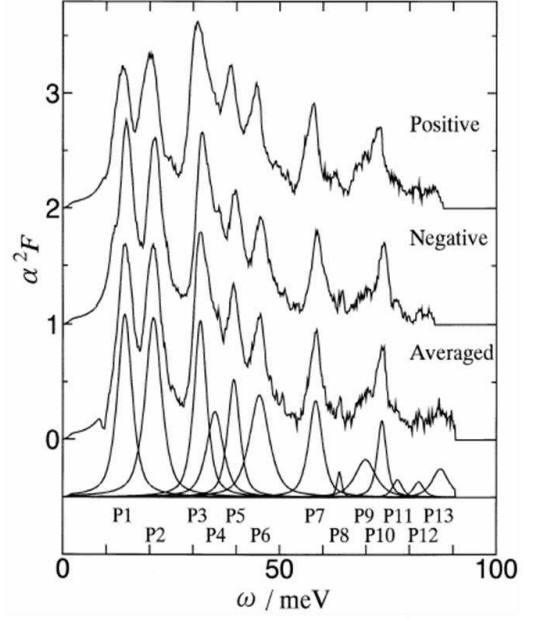


FIG. 24: The spectral functions $\alpha^2 F(\omega)$ from the tunnelling conductance of $Bi_2Sr_2CaCu_2O_8$ for the positive and the negative bias voltages, and the averaged one [24]. The averaged one is divided into 13 components. The origin of the ordinate is 2, 1, 0 and -0.5 from the top down. From [28], [24]

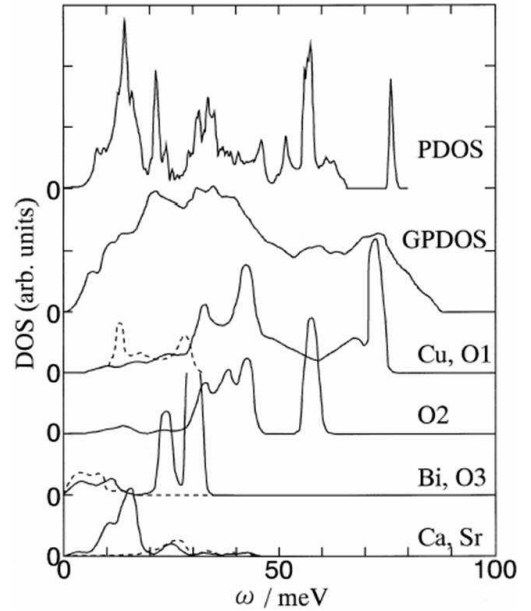


FIG. 25: The phonon density of states $F(\omega)$ (PDOS) of $Bi_2Sr_2CaCu_2O_8$ compared with the generalized density of states (GPDOS) [96]. Atomic vibrations: O1 - O in the CuO_2 plane; O2 - apical O; O3 - O in the BiO plane. From [24]

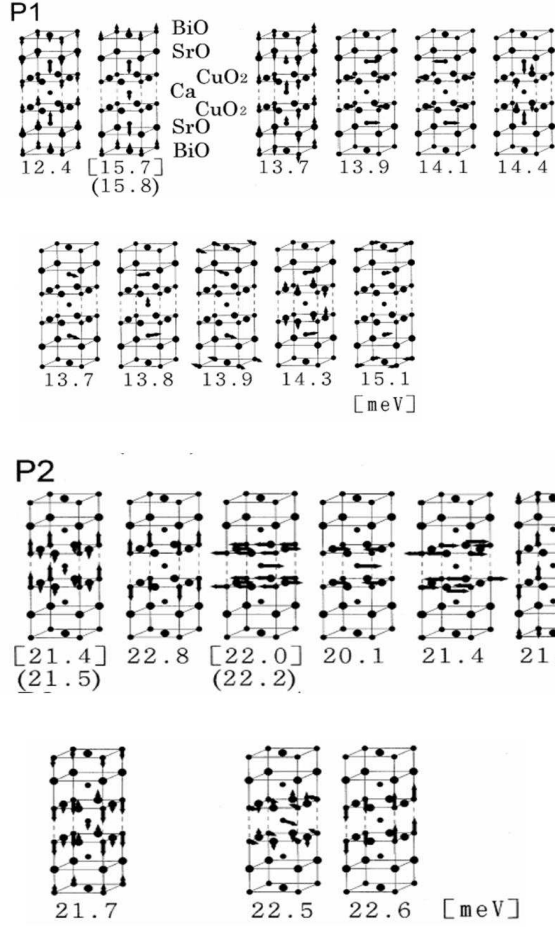


FIG. 26: Atomic polarization vectors and their frequencies (in meV) at special points in the Brillouin zone. The larger closed circles in the lattice are O-ions. $\Gamma - X$ is along the Cu-O-Cu direction. Arrows indicate displacements. The modes in square and round brackets are the transverse and longitudinal optical modes respectively. (Top) - modes of the P1 peak. (Bottom) - modes of the P2 peak. From [24], [28].

states it is legitimate to put the question - can the magnetic resonance in the superconducting state give contribution to the $\alpha^2 F(\omega)$? In that respect very important inelastic neutron scattering measurements of the magnetic resonance as a function of doping [98] give that the resonance energy E_r scales with T_c , i.e. $E_r = (5 - 6)T_c$ as shown in Fig.29. This means that if one of the peaks in $\alpha^2 F(\omega)$ is due to the magnetic resonance at $\omega = E_r$, then it shifts strongly with doping as it is observed in [98]. This is contrary to phonon peaks (energies) whose positions are doping independent. To this end, recent tunnelling experiments on Bi2212 [29] show clear *doping independence* of $\alpha^2 F(\omega)$ as it is seen in Fig. 30. This remarkable result is an additional and strong evidence in favor of EPI and against the SFI mechanism of pairing in HTSC cuprates.

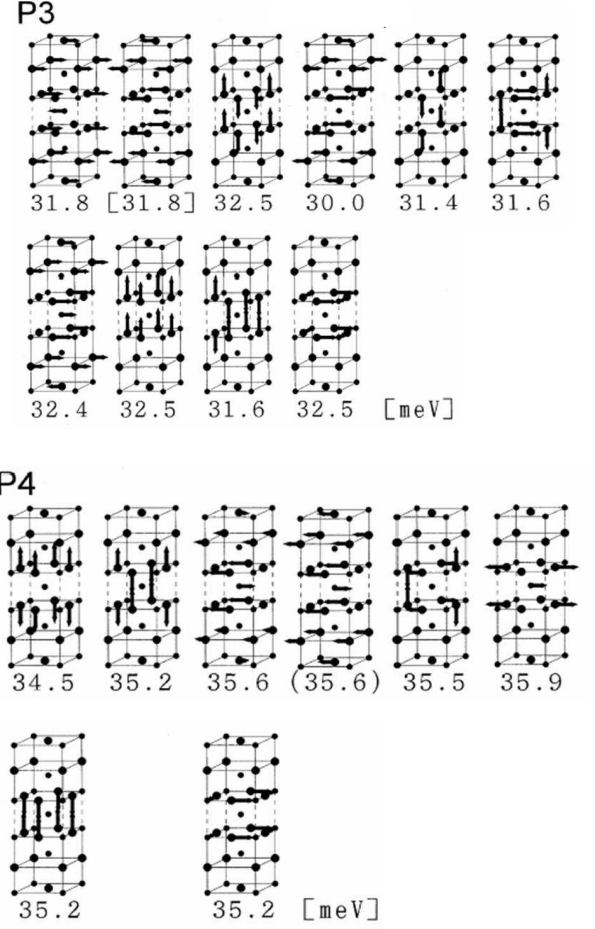


FIG. 27: Atomic polarization vectors and their frequencies (in meV) at special points in the Brillouin zone. The larger closed circles in the lattice are O-ions. $\Gamma - X$ is along the Cu-O-Cu direction. Arrows indicate displacements. The modes in square and round brackets are the transverse and longitudinal optical modes, respectively. (Top) - modes of the P3 peak. (Bottom) - modes of the P4 peak. From [24], [28].

It is interesting that in the vacuum tunneling *STM* measurements [99] the fine structure in $d^2 I/dV^2$ at $eV > \Delta$ was not seen below T_c , while the pseudogap structure is observed at temperatures near and above T_c . This result could mean that the *STM* tunnelling is likely dominated by the nontrivial structure of the tunnelling matrix element (along the c -axis), which is derived from the band structure calculations [100]. However, recent *STM* experiments on Bi2212 [30] give important information on possible nature of the bosonic mode which couples with electrons. In [30] the local conductance $dI/dV(\mathbf{r}, E)$ is measured where it is found that $d^2 I/dV^2(\mathbf{r}, E)$ has peak at $E(\mathbf{r}) = \Delta(\mathbf{r}) + \Omega(\mathbf{r})$ where $dI/dV(\mathbf{r}, E)$ has the maximal slope - see Fig. 31(a).

It turns out that the average phonon energy $\bar{\Omega}$ depends on the oxygen mass, i.e. $\bar{\Omega} \sim M_O^{-1/2}$, with $\bar{\Omega}_{16} = 52 meV$

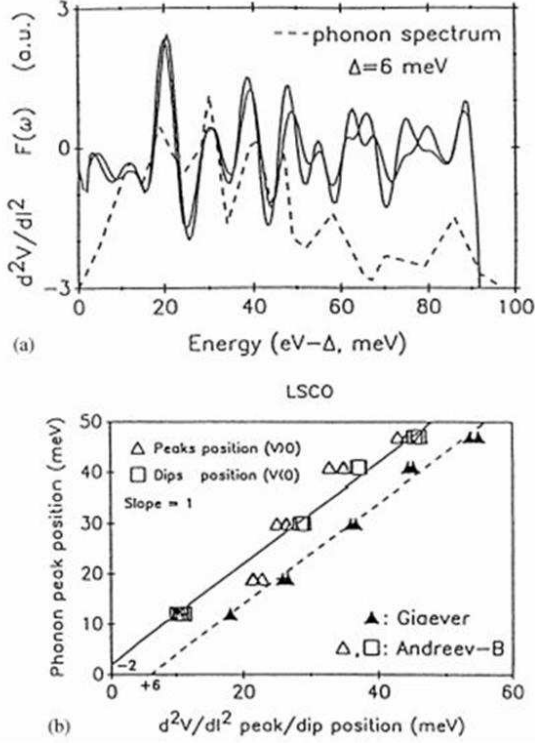


FIG. 28: (a) d^2I/dV^2 of a Giaever-like contact in $La_{2-x}Sr_xCuO_4$ - note the large structure below $50meV$; (b) d^2I/dV^2 of an Andreev- and Giaever-like contact compared to the peaks in the phonon density of states. From [97]

and $\bar{\Omega}_{18} \approx 48 meV$ - as it is seen in Fig. 31(b). This result is a convincing evidence that phonons are strongly involved in the quasi-particle scattering. A possible explanation is put forward in [30] by assuming that this isotope effect is due to the B_{1g} phonon which interacts with anti-nodal quasi-particles.

In our opinion the important message of tunnelling experiments in *HTSC* cuprates (by including $Ba_{1-x}K_xBiO_3$ too [101], [102]) is that there is strong evidence for the importance of EPI and that no particular phonon mode can be singled out in the spectral function $\alpha^2F(\omega)$ as being the only one which dominates in pairing mechanism. This important result means that the high T_c is not attributable to a particular phonon mode in the *EPI* mechanism, i.e. all phonon modes contribute to λ^{ep} . Having in mind that the phonon spectrum in *HTSC* cuprates is very broad (up to $80 meV$), then the large *EPI* constant ($\lambda^{ep} \gtrsim 2$) obtained in tunnelling experiments is not surprising at all.

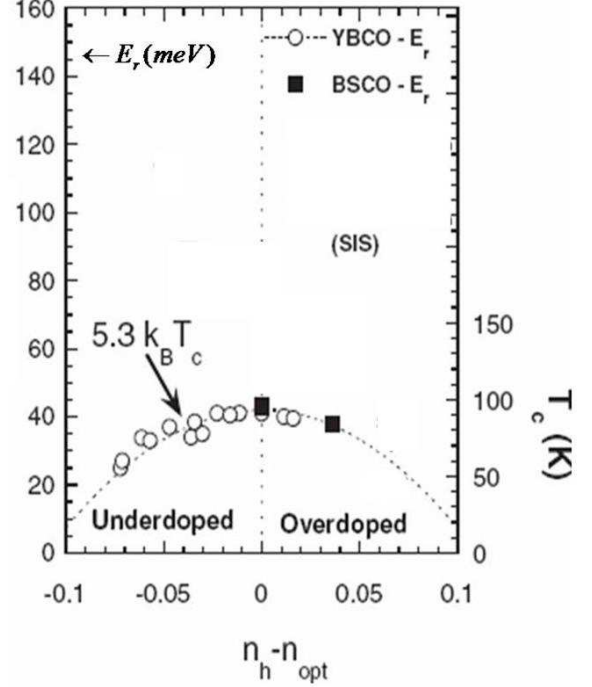


FIG. 29: Doping dependence of the energy E_r of the magnetic resonance peak at π, π in YBCO and Bi2212 measured at low temperatures by inelastic neutron scattering. From [98]

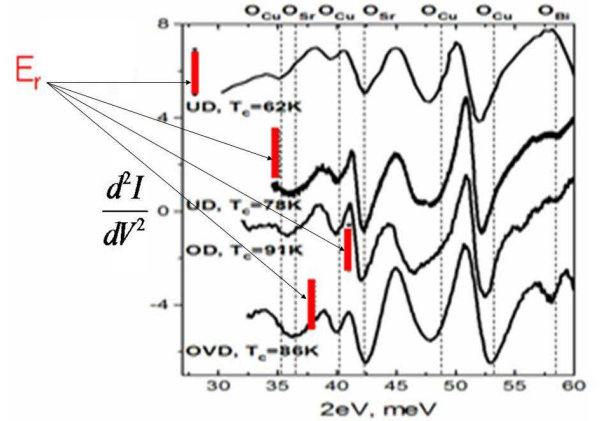


FIG. 30: Second derivative of $I(V)$ for a *Bi2212* tunnelling junctions for various doping: UD-underdoped; OD-optimally doped; OVD-overdoped system. The structure of minima in d^2I/dV^2 can be compared with the phonon density of states $F(\omega)$. The full and vertical lines mark the positions of the magnetic resonance energy $E_r \approx 5.4T_c$ for various doping taken from Fig.29. Red tiny arrows mark positions of the magnetic resonance E_r in various doped systems. Dotted vertical lines mark various phonon modes. From [29]

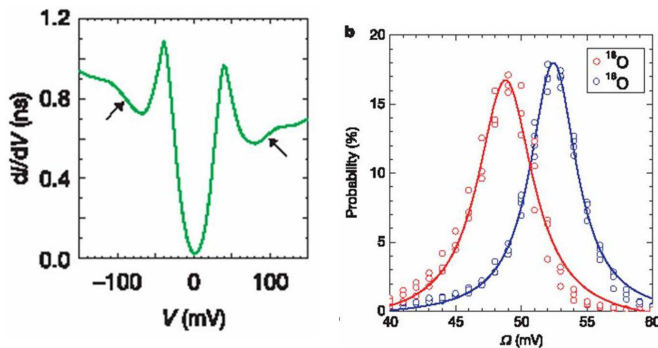


FIG. 31: (a) Typical conductance $dI/dV(\mathbf{r}, E)$. The ubiquitous feature at $eV > \Delta(\text{gap})$ with maximal slopes, which give peaks in $d^2I/dV^2(\mathbf{r}, E)$ are indicated by arrows. (b) The histograms of all values of $\Omega(\mathbf{r})$ for samples with O^{16} - right curve and with O^{18} - left curve. From [30]

E. Phonon spectra and EPI

Although experiments, such as inelastic neutron and Raman scattering, related to phonon spectra and their renormalization by *EPI* do not give directly $\alpha^2 F(\omega)$, as the tunnelling and optic spectra do, they nevertheless give useful information on the strength of *EPI* for some particular phonons. We stress in advance that the interpretation of experimental results in terms of *EPI* for weakly interacting electrons might be risky since in strongly correlated systems, such as HTSC cuprates, the phonon renormalization due to *EPI* is rather different from that in weakly correlated metals - see [103]. Since these questions are thoroughly studied in the excellent review [103] - see also *Part II*, we shall briefly enumerate the main points: (1) In strongly correlated systems, the *EPI* coupling for a number of phononic modes can be significantly larger than the LDA and Hartree-Fock methods predict. This is due to many-body effects [103]. (2) In strongly correlated systems the quasi-particle charge susceptibility, which enters the phonon self-energy $\Pi(\mathbf{q}, \omega) (\sim \chi_c(\mathbf{q}, \omega))$, is much more suppressed than in weakly correlated metals and these effects are out of the LDA possibilities [2], [104], [103]. This is one of the reasons that the analysis of experiments on phonon renormalizations in the framework of *LDA underestimates the EPI coupling constant significantly* - on all these questions, see more details in *Part II*.

1. The phonon Raman scattering

The *phonon* Raman scattering gives also evidence for appreciable *EPI* in cuprates [111], [112], [113]. We enumerate some of them - see more in [2] and References therein. (i) There is a pronounced asymmet-

ric line-shape (of the Fano resonance) in the metallic state. For instance, in $YBa_2Cu_3O_7$ two Raman modes at 115 cm^{-1} (Ba dominated mode) and at 340 cm^{-1} (O dominated mode in the CuO_2 planes) show pronounced asymmetry which is absent in $YBa_2Cu_3O_6$. This result points to appreciable interaction of Raman active phonons with continuum states (quasi-particles) [111], [112]. (ii) The phonon frequencies for some A_{1g} and B_{1g} are strongly renormalized in the superconducting state, between (6 – 10) %, pointing again to large *EPI* [113] - see also in [2], [44]. To this point we mention that the *electronic Raman scattering* in cuprates show a remarkable correlation between the Raman cross-section $\tilde{S}_{\text{exp}}(\omega)$ and the optical conductivity in the a-b plane $\sigma(\omega)$, i.e. $\tilde{S}_{\text{exp}}(\omega) \sim \sigma(\omega)$ [2]. It was argued above that *EPI* with the very broad spectral function $\alpha^2 F(\omega)$ explains in a natural way the ω and T dependence of $\sigma(\omega)$. This means that the electronic Raman spectra in cuprates can be explained by *EPI* in conjunction with strong correlations. This conclusion is supported by calculations of the Raman cross-section [105] which take into account *EPI* with $\alpha^2 F(\omega)$ extracted from tunnelling measurements in $YBa_2Cu_3O_{6+x}$ and $Bi_2Sr_2CaCu_2O_{8+x}$ [2], [23]-[28]. Quite similar properties (to cuprates) of the electronic Raman scattering, as well as of $\sigma(\omega)$, $R(\omega)$ and $\rho(T)$, were observed in experiments [62] on isotropic 3D metallic oxides $La_{0.5}Sr_{0.5}CoO_3$ and $Ca_{0.5}Sr_{0.5}RuO_3$ where there are no signs of antiferromagnetic fluctuations. This means that low-dimensionality and antiferromagnetic spin fluctuations cannot be a prerequisite for anomalous scattering of quasi-particles and *EPI* must be inevitably taken into account since it is present in all these compounds.

2. Neutron scattering, phonon spectra and EPI

The softening of numerous phonon modes has been observed in the normal state of cuprates giving important evidence for pronounced *EPI*. There are several important reviews on this subject [108] and here we discuss briefly two important examples which demonstrate in an impressive way the inefficiency of the LDA band structure calculations to treat quantitatively and qualitatively *EPI* in HTSC cuprates. Namely, by doping the Cu-O bond-stretching phonon mode shows a *substantial softening* at $\mathbf{q}_{hb} = (0.5, 0, 0)$ - called the *half-breathing phonon*, and a *large broadening* by 5 meV at 15% doping. While the softening can be partly described by the LDA method [109], it *predicts an order of magnitude smaller broadening* than the experimental one. The reason for this failure lies in strong correlations, which are not included in the LDA method as explained in [2], [5], [104], [103]. They give rise to an increase of the *EPI* coupling and to strong suppression of the charge fluctuations which enter the phonon self-energy via the charge susceptibility - see below and in *Part II*. The neutron scattering in $La_{1.85}Sr_{0.15}CuO_4$ gives evidence for large (30%) soften-

ing of the O_Z^Z with Λ_1 symmetry with the energy $\omega \approx 60$ meV, which is theoretically predicted in [106], and for the large line-width about 17 meV which also suggest strong EPI.

As it is discussed in the Introduction, there are recently several calculations of the EPI coupling constant λ^{ep} in the framework of DFT (or LDA), where very small $\lambda^{ep} \approx 0.3$ was obtained [13], [14]. However, the LDA method is inadequate for strongly correlated systems as it does not correctly take into account exchange-correlations and many-body effects, and therefore overestimates the screening in cuprates. If DFT is able to describe EPI correctly, it must also be able to calculate phonon renormalization, such as softening and broadening of the spectrum. In fact DFT completely fails to describe this renormalization for some important phonon modes and therefore fails to describe the effect of EPI on the electronic spectrum. The critique of LDA (DFT) results in HTSC cuprates is done in [2] and recently strongly argued in [5], [110] by its disagreement with neutron scattering measurements as it is shown in Fig. 32.

The point is that DFT (LDA) can reproduce the phonon softening in $La_{1.85}Sr_{0.15}CuO_4$ and $YBa_2Cu_3O_7$ rather good at low momenta $\mathbf{q} = (h, 0, 0)$ but predicts smooth softening at higher \mathbf{q} , while experiments show pronounced features for $h = 0.3$. At the same time DFT predicts an order of magnitude smaller line width than experiments [114].

In *Part II* we shall discuss some theoretical approaches related to EPI renormalization of phonons in strongly correlated systems. Here, we point out two results. *First*, there is an appreciable difference in the *phonon renormalization* in strongly and weakly correlated systems. Namely, the change of phonon frequencies in the presence of conduction electrons is proportional to the coupling constant $|g_{\mathbf{q}}|$ and charge susceptibility χ_c , i.e. $\delta\omega(\mathbf{q}) \sim |g_{\mathbf{q}}|^2 \text{Re} \chi_c$, while the line width is given by $\Gamma_{\omega(\mathbf{q})} \sim |g_{\mathbf{q}}|^2 |\text{Im} \chi_c|$. It turns out that in strongly correlated systems doped with hole concentration $\delta \ll 1$ the charge fluctuations are suppressed in which case the following sum-rule holds [5], [104]

$$\frac{1}{\pi N} \sum_{\mathbf{q} \neq 0} \int_{-\infty}^{\infty} |\text{Im} \chi_c(\mathbf{q})| d\omega = 2\delta(1 - \delta)N,$$

while in the LDA method one has

$$\frac{1}{\pi N} \sum_{\mathbf{q} \neq 0} \int_{-\infty}^{\infty} |\text{Im} \chi_c(\mathbf{q})|^{LDA} d\omega = (1 - \delta)N.$$

This means that for low doping $\delta \ll 1$ (note $n = 1 - \delta$), one has $|\text{Im} \chi_c| \ll |\text{Im} \chi_c^{LDA}|$ and LDA *strongly underestimates the coupling constant*, i.e. $|g_{\mathbf{q}}|_{LDA} \ll |g_{\mathbf{q}}|$. We stress that there is no such strong suppression in the quasi-particle self-energy [5].

Second, the theory gives that the coupling constant $|g_{\mathbf{q}}|$ in HTSC cuprates can be significantly larger than LDA predicts, which is due to some many-body effects

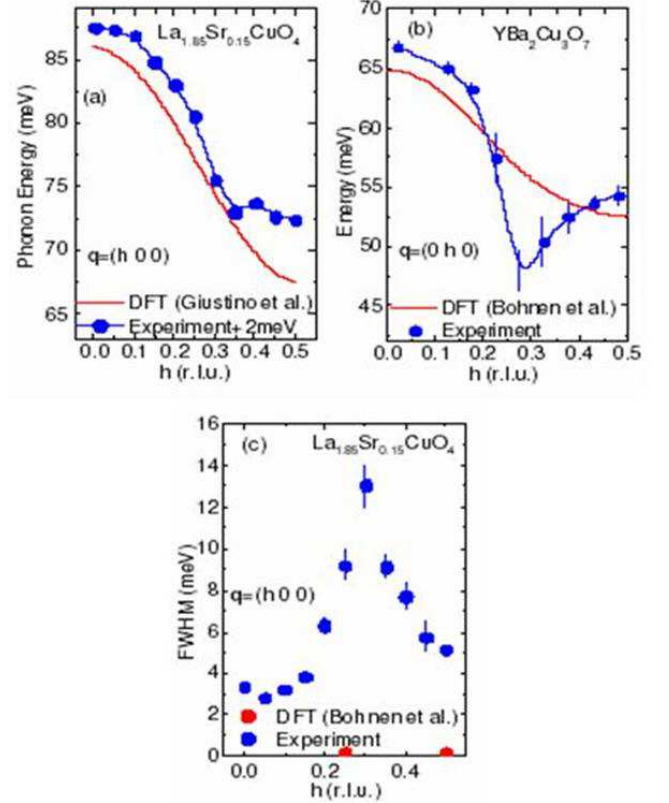


FIG. 32: Comparison of DFT calculations with experimental results:(a) in $La_{1.85}Sr_{0.15}CuO_4$; (b) in $YBa_2Cu_3O_7$. (c) Phonon line widths in $La_{1.85}Sr_{0.15}CuO_4$. DFT calculations [13] gives much smaller width than experiments [114]. From [110].

not present in the latter [5], [104]. It can be shown that for some phonon modes one has $|g_{\mathbf{q}}|^2 \gg |g_{\mathbf{q}}|_{LDA}^2$. For instance, for the half-breathing mode, one has $|g_{\mathbf{q}}|^2 \approx 3|g_{\mathbf{q}}|_{LDA}^2$ that is first calculated in [104]. These results point to inadequacy of LDA in calculations of EPI effects in HTSC cuprates.

F. Isotope effect for various doping

The isotope effect α_{T_c} in the critical temperature T_c was one of the very important proof for the EPI pairing in low-temperature superconductors (LTSC). As a curiosity the isotope effect in *LTSC* systems was measured almost exclusively in monoatomic systems and in few polyatomic systems: the hydrogen isotope effect in *PdH*, the *Mo* and *Se* isotope shift of T_c in Mo_6Se_8 , and the isotope effect in Nb_3Sn and MgB_2 . We point out that very small ($\alpha_{T_c} \approx 0$ in *Zr* and *Ru*) and even negative (in *PdH*) isotope effect in some polyatomic systems of *LTSC* ma-

materials are compatible with the *EPI* pairing mechanism but in the presence of substantial Coulomb interaction or lattice anharmonicity. The isotope effect α_{T_c} cannot be considered as the smoking gun since it is sensitive to numerous influences. For instance, in MgB_2 it is with certainty proved that the pairing is due to EPI and strongly dominated by the boron vibrations, but the boron isotope effect is significantly reduced, i.e. $\alpha_{T_c} \approx 0.3$. It is still unexplained. The situation in HTSC cuprates is much more complicated because they contain many-atoms in unit cell. Additionally, the situation is complicated with the presence of intrinsic and extrinsic inhomogeneities which can mask real effects. On the other hand new techniques such as ARPES, STM, μSR allow studies of the isotope effects in quasi-particle self-energies, i.e. α_Σ , which will be discussed below.

1. Isotope effect α_{T_c} in T_c

This problem will be discussed only briefly since more extensive discussion can be found in [2]. It is well known that in the pure EPI pairing mechanism, the total isotope coefficient α is given by

$$\alpha_{T_c} = \sum_{i,p} \alpha_i^{(p)} = - \sum_{i,p} \frac{d \ln T_c}{d \ln M_i^{(p)}}, \quad (41)$$

where $M_i^{(p)}$ is the mass of the i -th element in the p -th crystallographic position. Note that in the case when the screened Coulomb interaction is negligible, i.e. $\mu_c^* = 0$, one has $\alpha_{T_c} = 1/2$. From this formula one can deduce that the relative change of T_c , $\delta T_c/T_c$, for heavier elements is rather small - for instance it is 0.02 for $^{135}Ba \rightarrow ^{138}Ba$, 0.03 for $^{63}Cu \rightarrow ^{65}Cu$ and 0.07 for $^{138}La \rightarrow ^{139}La$. This means that measurements of α_i for heavier elements are at/or beyond the ability of present day experimental techniques. Therefore most isotope effect measurements were done by substituting light atoms ^{16}O by ^{18}O only. It turns out that in most optimally doped HTSC cuprates α_O is small. For instance $\alpha_O \approx 0.02 - 0.05$ in $YBa_2Cu_3O_7$ with $T_{c,max} \approx 91 K$, but it is appreciable in $La_{1.85}Sr_{0.15}CuO_4$ with $T_{c,max} \approx 35 K$ where $\alpha_O \approx 0.1 - 0.2$. In $Bi_2Sr_2CaCu_2O_8$ with $T_{c,max} \approx 76 K$ one has $\alpha_O \approx 0.03 - 0.05$ while $\alpha_O \approx 0.03$ and even negative (-0.013) in $Bi_2Sr_2Ca_2Cu_2O_{10}$ with $T_{c,max} \approx 110 K$. The experiments on $Tl_2Ca_{n-1}BaCu_nO_{2n+4}$ ($n = 2, 3$) with $T_{c,max} \approx 121 K$ are still unreliable and α_O is unknown: In the electron-doped $(Nd_{1-x}Ce_x)_2CuO_4$ with $T_{c,max} \approx 24 K$ one has $\alpha_O < 0.05$ while in the underdoped materials α_O increases. The largest α_O is obtained even in the optimally doped compounds like in systems with substitution, such as $La_{1.85}Sr_{0.15}Cu_{1-x}M_xO_4$, $M = Fe, Co$, where $\alpha_O \approx 1.3$ for $x \approx 0.4$ %. In $La_{2-x}M_xCuO_4$ there is a Cu isotope effect which is of the order of the oxygen one, i.e. $\alpha_{Cu} \approx \alpha_O$ giving $\alpha_{Cu} + \alpha_O \approx 0.25 - 0.35$ for optimally doped systems ($x = 0.15$). In case when

$x = 0.125$ with $T_c \ll T_{c,max}$ one has $\alpha_{Cu} \approx 0.8 - 1$ with $\alpha_{Cu} + \alpha_O \approx 1.8$ [107]. The appreciation of copper isotope effect in $La_{2-x}M_xCuO_4$ tells us that vibrations other than oxygen ions are important in giving high T_c . In that sense one should have in mind the tunnelling experiments discussed above, which tell us that all phonons contribute to the Eliashberg pairing function $\alpha^2 F(\mathbf{k}, \omega)$ and according to these results the oxygen modes give moderate contribution to T_c [28]. Having these facts in mind, then the small oxygen isotope effect $\alpha_{T_c}^{(O)}$ in optimally doped cuprates, if it is intrinsic property, does not exclude the EPI mechanism of pairing.

2. Isotope effect α_Σ in the self-energy

The fine structure of the quasi-particle self-energy $\Sigma(\mathbf{k}, \omega)$, such as kinks, can be resolved in ARPES measurements and in some respect in STM. It turns out that there is an isotope effect in the self-energy in the optimally doped $Bi2212$ samples [81], [115], [116]. In the first paper on this subject [81], there is a red shift $\delta\omega_{k,70} \sim -(10 - 15) meV$ of the nodal kink at $\omega_{k,70} \simeq 70 meV$ for the $^{16}O \rightarrow ^{18}O$ substitution. This isotope shift of the self-energy $\delta\Sigma = \Sigma_{16} - \Sigma_{18} \sim 10 meV$ is more pronounced at large energies $\omega = 100 - 300 meV$. However, there is a dispute on the latter result which is not confirmed experimentally [115], [116]. The isotope effect in $Re\Sigma(\mathbf{k}, \omega)$ [115], [116] can be well described in the framework of the Migdal-Eliashberg theory for EPI [82] which is in accordance with the recent ARPES measurements with low-energy photons $\sim 7 eV$ [117]. The latter allowed very good precision in measuring the isotope effect in the nodal point of $Bi2212$ with $T_c^{16} = 92.1 K$ and $T_c^{18} = 91.1 K$ [117]. They observed shift in the maximum of $Re\Sigma(\mathbf{k}_N, \omega)$ - at $\omega_{k,70} \approx 70 meV$ which corresponds to the half-breathing or breathing phonon, by $\delta\omega_{k,70} \approx 3.4 \pm 0.5 meV$ as shown in Fig. 33.

By analyzing the shift in $Im\Sigma(\mathbf{k}_N, \omega)$ - shown in Fig. 33, one finds similar result $\delta\omega_{k,70} \approx 3.2 \pm 0.6 meV$. The similar shift was obtained in STM measurements [30] which is shown in Fig. 31(b) and can have its origin in different phonons. We would like to stress two points: (i) in compounds with $T_c \sim 100 K$ the isotope effect in T_c is moderate, i.e. $\alpha_{T_c}^{(O)} \lesssim 0.1$, [117]. If we consider this value to be intrinsic then it is not in conflict with the tunnelling experiments in [28] which give evidence that vibrations of heavier ions contribute significantly to T_c - see the above discussion on the tunnelling spectroscopy; (ii) the extracted value in [117] of the effective EPI coupling constant $\lambda_{eff}^{ep} \sim 0.6$, which is smaller than the real λ^{ep} - see above the discussion on ARPES, is significantly larger than the LDA theory predicts $\lambda_{LDA}^{ep} < 0.3$ [13], [14]. This again points that the LDA method does not pick up the many-body effects due to strong correlations - see Part II.

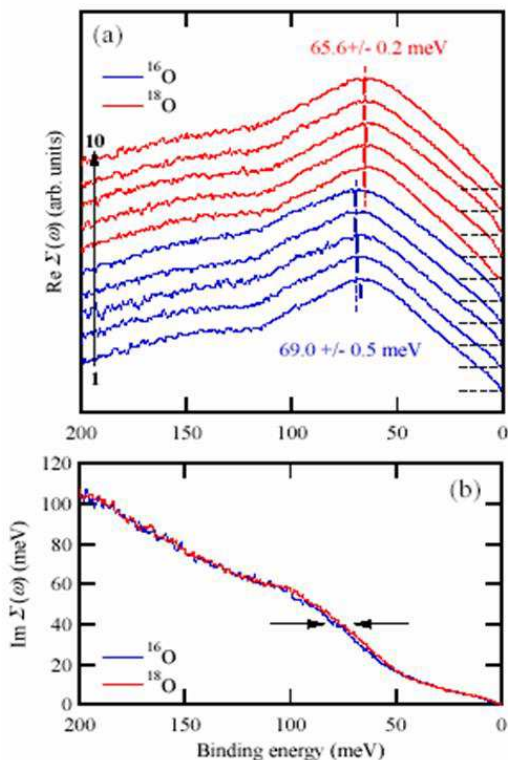


FIG. 33: (a) Effective $Re\Sigma$ for five samples for O^{16} (blue) and O^{18} (red) along the nodal direction. (b) Effective $Im\Sigma$ determined from MDC full widths. An impurity term is subtracted at $\omega = 0$. From [117].

IV. SUMMARY OF PART I

The analysis of experimental data in HTSC cuprates which are related to optics, tunnelling and ARPES *measurements near the optimal doping* give evidence for the large electron-phonon interaction with the coupling constant $1 < \lambda^{ep} < 3.5$. The analysis is done in the framework of the Migdal-Eliashberg theory which is a reliable approach for systems near the optimal doping. The spectral function averaged over the Fermi surface $\alpha^2 F(\omega)$ is extracted from various tunnelling measurements and it contains peaks at the same positions as the phonon density of states. The energy width of $\alpha^2 F(\omega)$ is the same as the width of the phonon density of states $F(\omega)$. This is an unambiguous proof for the important role which EPI plays in the pairing mechanism of cuprates. The optical IR reflectivity data provide additional support for this finding since the transport spectral function has the width and global properties similar to $F(\omega)$. These findings are additionally and strongly supported by ARPES measurements on BISCO compounds. The ARPES kinks in the quasi-particle self-energy can be explained exclusively by EPI and there is no much room for spin fluctuations (SFI) effects. The weakness of SFI is unambigu-

ously proved in magnetic neutron scattering on YBCO where the imaginary part of the susceptibility is drastically reduced in the low energy region by going from slightly underdoped toward optimally doped systems, while T_c is practically unchanged. This implies that the SFI coupling constant is limited to the value $\lambda^{sf} \lesssim 0.3$. All these results do not leave doubts on the significance of EPI and weakness of SFI. The obtained total EPI coupling constant is rather large, i.e. $1 < \lambda^{ep} < 3.5$, while the transport coupling constant is $\lambda_{tr} \sim \lambda/3$. The different renormalization of the quasi-particle and transport self-energies by the Coulomb interaction and strong correlations points to dominance of the small-momentum scattering in EPI. This will be discussed in *Part II*.

Inelastic neutron scattering measurements in cuprates show that the broadening of phonon lines is by an order of magnitude larger than the LDA (DFA) method predicts. Since the phonon line-widths depend on the EPI coupling and the charge susceptibility it is evident that calculations of both quantities are beyond the range of applicability of LDA. As a consequence, LDA overestimates electronic screening and thus underestimates the EPI coupling. This means that LDA is suitable only for weakly correlated systems, while many-body effects due to strong correlations are not contained in this mean-field type theory.

In spite of the very promising and encouraging results about the dominance of EPI in cuprates the theory is still confronted with the task of obtaining sufficiently large coupling constant in the d-channel in order that EPI conforms with d-wave pairing. At present we do not have such a detailed microscopic theory although some concepts, such as the dominant EPI scattering at small transfer momenta, are understood at least qualitatively. These set of problems and questions will be discussed in *Part II*.

Acknowledgement. We are thankful to Vitalii Lazarevich Ginzburg for his permanent interest in our work and for support in many respects over many years. One of us (M. L. K.) is thankful to Karl Bennemann for inspiring discussions on many subjects related to physics of HTSC cuprates. We thank Godfrey Akpojotor for careful reading of the manuscript. M. L. K. is thankful to the Max-Born-Institut für Nichtlineare Optik und Kurzzeitspektroskopie, Berlin for the hospitality and financial support during his stay where part of this work has been done.

V. APPENDIX - SPECTRAL FUNCTIONS

A. Spectral functions $\alpha^2 F(\mathbf{k}, \mathbf{k}', \omega)$ and $\alpha^2 F(\omega)$

Before discussing experimental results in cuprate superconductors which are related to various spectral functions, we introduce the reader briefly into the subject. The quasiparticle-bosonic (Eliashberg) spectral function $\alpha^2 F(\mathbf{k}, \mathbf{k}', \omega)$ and its Fermi surface aver-

age $\alpha^2 F(\omega) = \langle \langle \alpha^2 F(\mathbf{k}, \mathbf{k}', \omega) \rangle \rangle_{\mathbf{k}, \mathbf{k}'}$ enter the quasi-particle self-energy $\Sigma(\mathbf{k}, \omega)$, while the transport spectral function $\alpha^2 F_{tr}(\omega)$ enters the transport self-energy $\Sigma_{tr}(\mathbf{k}, \omega)$ and dynamical conductivity $\sigma(\omega)$. Since the Migdal-Eliashberg theory for EPI is well defined we define the spectral functions for this case and the generalization to other electron-boson interaction is straightforward. In the superconducting state the Matsubara Green's function $\hat{G}(\mathbf{k}, \omega_n)$ and $\hat{\Sigma}(\mathbf{k}, \omega_n)$ are 2×2 matrices with the diagonal elements $G_{11} \equiv G(\mathbf{k}, \omega_n)$, G_{22} , $\Sigma_{11} \equiv \Sigma(\mathbf{k}, \omega_n)$, Σ_{22} and off-diagonal elements $G_{12} \equiv F(\mathbf{k}, \omega_n)$, G_{21} , $\Sigma_{12} \equiv \Phi(\mathbf{k}, \omega_n)$, Σ_{21} which describe superconducting pairing. By defining $i\omega_n [1 - Z(\mathbf{k}, \omega_n)] = [\Sigma(\mathbf{k}, \omega_n) - \Sigma(\mathbf{k}, -\omega_n)]/2$ and $\chi(\mathbf{k}, \omega_n) = [\Sigma(\mathbf{k}, \omega_n) + \Sigma(\mathbf{k}, -\omega_n)]/2$, the Eliashberg functions for EPI in the presence of the Coulomb interaction (in the pairing channel) read [118], [119], [120]

$$Z(\mathbf{k}, \omega_n) = 1 + \frac{T}{N} \sum_{\mathbf{p}, m} \frac{\lambda_{\mathbf{k}\mathbf{p}}^Z(\omega_n - \omega_m) \omega_m}{N(\mu) \omega_n} \frac{Z(\mathbf{p}, \omega_m)}{D(\mathbf{p}, \omega_m)}, \quad (42)$$

$$\chi(\mathbf{k}, \omega_n) = -\frac{T}{N} \sum_{\mathbf{p}, m} \frac{\lambda_{\mathbf{k}\mathbf{p}}^Z(\omega_n - \omega_m)}{N(\mu)} \frac{\epsilon(\mathbf{p}) - \mu + \chi(\mathbf{p}, \omega_m)}{D(\mathbf{p}, \omega_m)}, \quad (43)$$

$$\Phi(\mathbf{k}, \omega_n) = \frac{T}{N} \sum_{\mathbf{p}, m} \left[\frac{\lambda_{\mathbf{k}\mathbf{p}}^\Delta(\omega_n - \omega_m)}{N(\mu)} - V_{\mathbf{k}\mathbf{p}} \right] \frac{\Phi(\mathbf{p}, \omega_m)}{D(\mathbf{p}, \omega_m)}, \quad (44)$$

where $N(\mu)$ is the density of states at the Fermi surface, $\omega_n = \pi T(2n+1)$, $\Phi(\mathbf{k}, \omega_n) \equiv Z(\mathbf{k}, \omega_n) \Delta(\mathbf{k}, \omega_n)$ and $D = \omega_m^2 Z^2 + (\epsilon - \mu + \chi)^2 + \Phi^2$. (For studies of optical properties - see below, it is useful to introduce the renormalized frequency $i\tilde{\omega}_n(i\omega_n) (\equiv i\omega_n Z(\omega_n)) = \omega_n - \Sigma(\omega_n)$ (or its analytical continuation $\tilde{\omega}(\omega) = Z(\omega)\omega = \omega - \Sigma(\omega)$). These equations are supplemented with the electron number equation $n(\mu)$ (μ is the chemical potential)

$$\begin{aligned} n(\mu) &= \frac{2T}{N} \sum_{\mathbf{p}, m} G(\mathbf{p}, \omega_m) e^{i\omega_m 0^+} \\ &= 1 - \frac{2T}{N} \sum_{\mathbf{p}, m} \frac{\epsilon(\mathbf{p}) - \mu + \chi(\mathbf{p}, \omega_m)}{D(\mathbf{p}, \omega_m)}. \end{aligned} \quad (45)$$

Note that in the case of EPI one has $\lambda_{\mathbf{k}\mathbf{p}}^\Delta(\nu_n) = \lambda_{\mathbf{k}\mathbf{p}}^Z(\nu_n) (\equiv \lambda_{\mathbf{k}\mathbf{p}}(\nu_n))$ (with $\nu_n = \pi T n$) where $\lambda_{\mathbf{k}\mathbf{p}}(\nu_n)$ is defined by

$$\lambda_{\mathbf{k}\mathbf{p}}(\nu_n) = 2 \int_0^\infty \frac{\nu \alpha_{\mathbf{k}\mathbf{p}}^2 F(\nu) d\nu}{\nu^2 + \nu_n^2} \quad (46)$$

$$\alpha_{\mathbf{k}\mathbf{p}}^2 F(\nu) = N(\mu) \sum_{\kappa} |g_{\kappa, \mathbf{k}\mathbf{p}}^{ren}|^2 B_{\kappa}(\mathbf{k} - \mathbf{p}, \nu) \quad (47)$$

where $B_{\kappa}(\mathbf{k} - \mathbf{p}; \nu)$ is the phonon spectral function of the κ -th phonon mode related to the phonon propagator

$$D_{\kappa}(\mathbf{q}, i\nu_n) = - \int_0^\infty \frac{\nu}{\nu^2 + \nu_n^2} B_{\kappa}(\mathbf{q}, \nu) d\nu. \quad (48)$$

The renormalized coupling constant $g_{\kappa, \mathbf{k}\mathbf{p}}^{ren} (\approx g_{\kappa, \mathbf{k}\mathbf{p}}^0 \epsilon^{-1} \gamma)$ comprises the screening effect due to long-range Coulomb interaction ($\sim \epsilon^{-1}$ - the inverse electronic dielectric function) and short-range strong correlations ($\sim \gamma$ - the vertex function) - see more in *Part II*. Usually in the case of low-temperature superconductors (LTS) with s-wave pairing the anisotropy is rather small (or in the presence of impurities it is averaged out) which allows an averaging of the Eliashberg equations [118], [119], [120]

$$Z(\omega_n) = 1 + \frac{\pi T}{\omega_n} \sum_m \frac{\lambda(\omega_n - \omega_m) \omega_m}{\sqrt{\omega_m^2 + \Delta^2(\omega_m)}}, \quad (49)$$

$$\begin{aligned} Z(\omega_n) \Delta(\omega_n) &= \pi T \sum_m [\lambda(\omega_n - \omega_m) \\ &- \mu(\omega_c) \theta(\omega_c - |\omega_m|)] \frac{\Delta(\omega_m)}{\sqrt{\omega_m^2 + \Delta^2(\omega_m)}}, \end{aligned} \quad (50)$$

$$\lambda(\omega_n - \omega_m) = \int_0^\infty d\nu \frac{2\nu \alpha^2 F(\nu)}{\nu^2 + (\omega_n - \omega_m)^2}. \quad (51)$$

Here $\alpha^2 F(\omega) = \langle \langle \alpha^2 F(\mathbf{k}, \mathbf{k}', \omega) \rangle \rangle_{\mathbf{k}, \mathbf{k}'}$, where $\langle \langle \dots \rangle \rangle_{\mathbf{k}, \mathbf{k}'}$ is the average over the Fermi surface. The above equations can be written on the real axis by the analytical continuation $i\omega_m \rightarrow \omega + i\delta$ where the gap function is complex i.e. $\Delta(\omega) = \Delta_R(\omega) + i\Delta_I(\omega)$. The solution for $\Delta(\omega)$ allows the calculation of the current-voltage characteristic $I(V)$ and *tunnelling conductance* $G_{NS}(V) = dI_{NS}/dV$ in the superconducting state of the *NIS* tunneling junction where $I_{NS}(V)$ is given by

$$I_{NS}(V) = 2e \sum_{\mathbf{k}, \mathbf{p}} |T_{\mathbf{k}, \mathbf{p}}|^2 \int_{-\infty}^\infty \frac{d\omega}{2\pi}$$

$$A_N(\mathbf{k}, \omega) A_S(\mathbf{p}, \omega + eV) [f(\omega) - f(\omega + eV)]. \quad (52)$$

Here, $A_{N,S}(\mathbf{k}, \omega) = -2ImG_{N,S}(\mathbf{k}, \omega)$ are the spectral functions of the normal metal and superconductor, respectively and $f(\omega)$ is the Fermi distribution function. Since the angular and energy dependence of the tunnelling matrix elements $|T_{\mathbf{k}, \mathbf{p}}|^2$ is practically unimportant for *s-wave* superconductors, then in that case the relative conductance $\sigma_{NS}(V) \equiv G_{NS}(V)/G_{NN}(V)$ is proportional to the tunnelling density of states $N_T(\omega) = \int A_S(\mathbf{k}, \omega) d^3k / (2\pi)^3$, i.e. $\sigma_{NS}(\omega) \approx N_T(\omega)$ where

$$N_T(\omega) = Re \left\{ \frac{\omega + i\tilde{\gamma}(\omega)}{\sqrt{(\omega + i\tilde{\gamma}(\omega))^2 - \tilde{Z}^2(\omega) \Delta(\omega)^2}} \right\}. \quad (53)$$

Here, $\tilde{Z}(\omega) = Z(\omega)/\text{Re}Z(\omega)$, $\tilde{\gamma}(\omega) = \gamma(\omega)/\text{Re}Z(\omega)$, $Z(\omega) = \text{Re}Z(\omega) + i\gamma(\omega)/\omega$ and the *quasi-particle scattering rate* in the superconducting state $\gamma_s(\omega, T) = -2\text{Im}\Sigma(\omega, T)$ is given by

$$\gamma_s(\omega, T) = 2\pi \int_0^\infty d\nu \alpha^2 F(\nu) N_s(\nu + \omega) \{2n_B(\nu) + n_F(\nu + \omega) + n_F(\nu - \omega)\} + \gamma^{imp}, \quad (54)$$

where $N_s(\omega) = \text{Re}\{\omega/(\omega^2 - \Delta^2)^{1/2}\}$ is the quasi-particle density of states in the superconducting state, $n_{B,F}(\nu)$ are Bose and Fermi distribution function respectively. Since the structure of phononic spectrum is contained in $\alpha^2 F(\omega)$, it is reflected on $\Delta(\omega)$ for $\omega > \Delta_0$ (the real gap obtained from $\Delta_0 = \text{Re}\Delta(\omega = \Delta_0)$) which gives the structure in $G_S(V)$ at $V = \Delta_0 + \omega_{ph}$. On the contrary one can extract the spectral function $\alpha^2 F(\omega)$ from $G_{NS}(V)$ by the inversion procedure proposed by McMillan and Rowell [121], [2]. It turns out that in low-temperature superconductors, negative peaks of d^2I/dV^2 at $eV_i = \Delta + \omega_{ph,i}$, correspond to the peak positions of $\alpha^2 F(\omega)$ and $F(\omega)$. However, we would like to point out that in HTSC cuprates the gap function is unconventional and very anisotropic, i.e. $\Delta(\mathbf{k}, i\omega_n) \sim \cos k_x a - \cos k_y a$. Since in this case the extraction of $\alpha^2 F(\mathbf{k}, \mathbf{k}', \omega)$ is extremely difficult and at present rather unrealistic task, then an "average" $\alpha^2 F(\omega)$ is extracted from the experimental curve $G_S(V)$. There is belief that it gives relevant information on the real spectral function such as the energy width of the bosonic spectrum ($0 < \omega < \omega_{\max}$) and positions and distributions of peaks due to bosons. It turns out that even such an approximate procedure gives valuable information in HTSC cuprates - see discussion in *Section III D*.

Note that in the case of spin-fluctuation interaction (the SFI model) one should make difference between $\lambda_{\mathbf{k}\mathbf{p}}^Z(i\nu_n)$ and $\lambda_{\mathbf{k}\mathbf{p}}^\Delta(i\nu_n)$ since they differ by sign i.e. $\lambda_{\mathbf{k}\mathbf{p}}^Z(i\nu_n) = -\lambda_{\mathbf{k}\mathbf{p}}^\Delta(i\nu_n) > 0$ since SFI is repulsive in the pairing-channel - see Eqs. (7-8).

1. Inversion of tunnelling data

Phonon features in the conductance $\sigma_{NS}(V)$ at $eV = \Delta_0 + \omega_{ph}$ makes the tunnelling spectroscopy a powerful method in obtaining the Eliashberg spectral function $\alpha^2 F(\omega)$. Two methods were used in the past for extracting $\alpha^2 F(\omega)$.

The *first method* is based on solving the *inverse problem* of the nonlinear Eliashberg equations. Namely, by measuring $\sigma_{NS}(V)$, one obtains the tunnelling density of states $N_T(\omega) (\sim \sigma_{NS}(\omega))$ and by the inversion procedure one gets $\alpha^2 F(\omega)$ [121]. In reality the method is based on the iteration procedure - the McMillan-Rowell (MR) inversion, where in the first step an initial $\alpha^2 F_{ini}(\omega)$, μ_{ini}^*

and $\Delta_{ini}(\omega)$ are inserted into Eliashberg equations (for instance $\Delta_{ini}(\omega) = \Delta_0$ for $\omega < \omega_0$ and $\Delta_{ini}(\omega) = 0$ for $\omega > \omega_0$) and then $\sigma_{ini}(V)$ is calculated. In the second step the functional derivative $\delta\sigma(\omega)/\delta\alpha^2 F(\omega)$ ($\omega \equiv eV$) is found in the presence of a small change of $\alpha^2 F_{ini}(\omega)$ and then the iterated solution $\alpha^2 F_{(1)}(\omega) = \alpha^2 F_{ini}(\omega) + \delta\alpha^2 F(\omega)$ is obtained, where the correction $\delta\alpha^2 F(\omega)$ is given by

$$\delta\alpha^2 F(\omega) = \int d\nu \left[\frac{\delta\sigma_{ini}(V)}{\delta\alpha^2 F(\nu)} \right]^{-1} [\sigma_{exp}(\nu) - \sigma_{ini}(\nu)]. \quad (55)$$

The procedure is iterated until $\alpha^2 F_{(n)}(\omega)$ and $\mu_{(n)}^*$ converge to $\alpha^2 F(\omega)$ and μ^* which reproduce the experimentally obtained conductance $\sigma_{NS}^{exp}(V)$. In such a way the obtained $\alpha^2 F(\omega)$ for *Pb* resembles the phonon density of states $F_{Pb}(\omega)$, that is obtained from neutron scattering measurements. Note that the method depends explicitly on μ^* but on the contrary it requires only data on $\sigma_{NS}(V)$ up to the voltage $V_{\max} = \omega_{ph}^{\max} + \Delta_0$ where ω_{ph}^{\max} is the maximum phonon energy ($\alpha^2 F(\omega) = 0$ for $\omega > \omega_{ph}^{\max}$) and Δ_0 is the zero-temperature superconducting gap. One pragmatical feature for the interpretation of tunnelling spectra (and for obtaining the spectral pairing function $\alpha^2 F(\omega)$) in *LTS* and *HTSC* cuprates is that the negative peaks of d^2I/dV^2 are at the peak positions of $\alpha^2 F(\omega)$ and $F(\omega)$. This feature will be discussed later on in relation with experimental situation in cuprates.

The *second method* has been invented in [122] and it is based on the combination of the Eliashberg equations and dispersion relations for the Greens functions - we call it GDS method. First, the tunnelling density of states is extracted from the tunneling conductance in a more rigorous way [123]

$$N_T(V) = \frac{\sigma_{NS}(V)}{\sigma_{NN}(V)} - \frac{1}{\sigma^*(V)} \int_0^V du \times \frac{d\sigma^*(u)}{du} [N_T(V-u) - N_T(V)] \quad (56)$$

where $\sigma^*(V) = \exp\{-\beta V\} \sigma_{NN}(V)$ and the constant β is obtained from $\sigma_{NN}(V)$ at large biases - see [122]. $N_T(V)$ under the integral can be replaced by the BCS density of states. Since the second method is used in extracting $\alpha^2 F(\omega)$ in a number of LTS as well as in HTSC cuprates - see below, we describe it briefly for the case of isotropic EPI at T=0 K. In that case the Eliashberg equations are [118], [119], [120], [122]

$$Z(\omega)\Delta(\omega) = \int_{\Delta_0}^\infty d\omega' \text{Re} \left[\frac{\Delta(\omega')}{[\omega'^2 - \Delta^2(\omega')]^{1/2}} \right] \times [K_+(\omega, \omega')] - \mu^* \theta(\omega_c - \omega) \quad (57)$$

$$Z(\omega) = \frac{1}{\omega} \int_{\Delta_0}^\infty d\omega' \text{Re} \left[\frac{\omega'}{[\omega'^2 - \Delta^2(\omega')]^{1/2}} \right] K_-(\omega, \omega') \quad (58)$$

where

$$K_{\pm}(\omega, \omega') = \int_{\Delta_0}^{\omega_{ph}^{\max}} d\nu \alpha^2 F(\nu) \left(\frac{1}{\omega' + \omega + \nu + i0^+} \right. \\ \left. \pm \frac{1}{\omega' - \omega + \nu - i0^+} \right). \quad (59)$$

Here μ^* is the Coulomb pseudopotential, the cutoff ω_c is approximately $(5 - 10) \omega_{ph}^{\max}$, $\Delta_0 = \Delta(\Delta_0)$ is the energy gap. Now by using the dispersion relation for the matrix Greens functions $G(\mathbf{k}, \omega_n)$ one obtains [122]

$$\text{Im } S(\omega) = \frac{2\omega}{\pi} \int_{\Delta_0}^{\infty} d\omega' \frac{N_T(\omega') - N_{BCS}(\omega')}{\omega^2 - \omega'^2} \quad (60)$$

where $S(\omega) = \omega / [\omega^2 - \Delta^2(\omega)]^{1/2}$. From Eqs. (57-58) one obtains

$$\int_0^{\omega - \Delta_0} d\nu \alpha^2 F(\omega - \nu) \text{Re} \left\{ \Delta(\nu) [\nu^2 - \Delta^2(\nu)]^{1/2} \right\} \\ = \frac{\text{Re } \Delta(\omega)}{\omega} \int_0^{\omega - \Delta_0} d\nu \alpha^2 F(\nu) N_T(\omega - \nu) + \frac{\text{Im } \Delta(\omega)}{\pi} \\ + \frac{\text{Im } \Delta(\omega)}{\pi} \int_0^{\infty} d\omega' N_T(\omega') \int_0^{\omega_{ph}^{\max}} d\nu \frac{2\alpha^2 F(\nu)}{(\omega' + \nu)^2 - \omega^2}. \quad (61)$$

Based on Eqs. (56-61) one obtains the scheme for extracting $\alpha^2 F(\omega)$

$$\sigma_{NS}(V), \sigma_{NN}(V) \rightarrow N_T(V) \\ \rightarrow \text{Im } S(\omega) \rightarrow \Delta(\omega) \rightarrow \alpha^2 F(\omega).$$

The advantage in this method is that the explicit knowledge of μ^* is not required [122]. However, the integral equation for $\alpha^2 F(\omega)$ is linear Fredholm equation of the first kind which is ill-defined - see the discussion in Section II.B.2.

2. Phonon effects in $N_T(\omega)$

We briefly discuss the physical origin for the phonon effects in $N_T(\omega)$ by considering a model with only one peak, at ω_0 , in the phonon density of states $F(\omega)$ by assuming for simplicity $\mu^* = 0$ and neglecting the weak structure in $N_T(\omega)$ at $n\omega_0 + \Delta_0$, which is due to the nonlinear structure of the Eliashberg equations [125]. In Fig.34 it is seen that the real gap $\Delta_R(\omega)$ reaches a maximum at $\omega_0 + \Delta_0$ then decreases, becomes negative and zero, while $\Delta_I(\omega)$ is peaked slightly beyond $\omega_0 + \Delta_0$ that is the consequence of the effective electron-electron interaction via phonons.

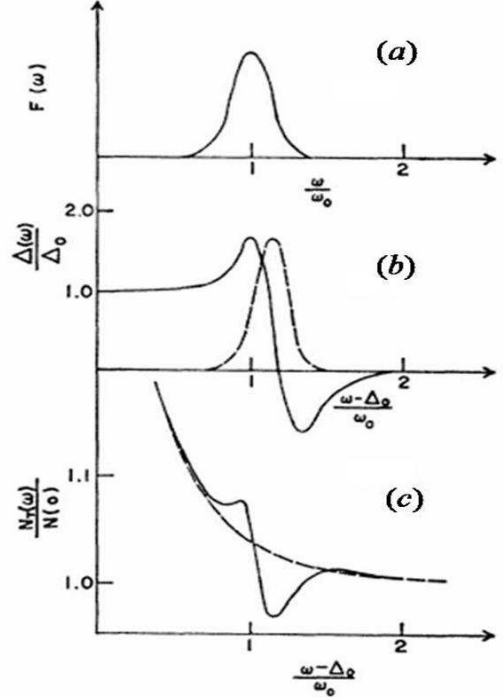


FIG. 34: (a) Model phonon density of states $F(\omega)$ with the peak at ω_0 . (b) The real (solid) Δ_R and imaginary part Δ_I (dashed) of the gap $\Delta(\omega)$. (c) The normalized tunnelling density of states $N_T(\omega)/N(0)$ (solid) compared with the BCS density of states (dashed). From [125].

It follows that for $\omega < \omega_0 + \Delta_0$ most phonons have higher energies than the energy ω of electronic charge fluctuations and there is over-screening of this charge by ions giving rise to attraction. For $\omega \approx \omega_0 + \Delta_0$ charge fluctuations are in resonance with ion vibrations giving rise to the peak in $\Delta_R(\omega)$. For $\omega_0 + \Delta_0 < \omega$ the ions move out of phase with respect to charge fluctuations giving rise to repulsion and negative $\Delta_R(\omega)$. This is shown in Fig. 34(b). The structure in $\Delta(\omega)$ is reflected on $N_T(\omega)$ as shown in Fig. 34(c) which can be reconstructed from the approximate formula for $N_T(\omega)$ expanded in powers of Δ/ω

$$\frac{N_T(\omega)}{N(0)} \approx 1 + \frac{1}{2} \left[\left(\frac{\Delta_R(\omega)}{\omega} \right)^2 - \left(\frac{\Delta_I(\omega)}{\omega} \right)^2 \right].$$

As $\Delta_R(\omega)$ increases above Δ_0 this gives $N_T(\omega) > N_{BCS}(\omega)$, while for $\omega \gtrsim \omega_0 + \Delta_0$ the real value $\Delta_R(\omega)$ decreases while $\Delta_I(\omega)$ rises and $N_T(\omega)$ decreases giving rise for $N_T(\omega) < N_{BCS}(\omega)$.

B. Transport spectral function $\alpha_{tr}^2 F(\omega)$

The spectral function $\alpha_{tr}^2 F(\omega)$ enters the dynamical conductivity $\sigma_{ij}(\omega)$ ($i, j = a, b, c$ axis in HTS systems)

which generally speaking is a tensor quantity given by the following formula

$$\sigma_{ij}(\omega) = -\frac{e^2}{\omega} \int \frac{d^4q}{(2\pi)^4} \gamma_i(q, k+q) \times G(k+q) \Gamma_j(q, k+q) G(q), \quad (62)$$

where $q = (\mathbf{q}, \nu)$ and $k = (\mathbf{k} = 0, \omega)$ and the bare current vertex $\gamma_i(q, k+q; \mathbf{k} = 0)$ is related to the Fermi velocity $v_{F,i}$, i.e. $\gamma_i(q, k+q; \mathbf{k} = 0) = v_{F,i}$. The vertex function $\Gamma_j(q, k+q)$ takes into account the renormalization due to all scattering processes responsible for finite conductivity [124]. In the following we study only the in-plane conductivity at $\mathbf{k} = 0$. The latter case is realized due to the long penetration depth in HTSC cuprates and the skin depth in the normal state are very large. In the *EPI* theory, $\Gamma_j(q, k+q) \equiv \Gamma_j(\mathbf{q}, i\omega_n, i\omega_n + i\omega_m)$ is a solution of an approximative integral equation written in the symbolic form [68]

$$\Gamma_j = v_j + V_{eff} G \Gamma_j \quad (63)$$

where the effective potential V_{eff} (due to EPI) is given by $V_{eff} = \sum_{\kappa} |g_{\kappa}^{ren}|^2 D_{\kappa}$, where D_{κ} is the phonon Green's function. In such a case the Kubo theory predicts $\sigma_{ii}^{intra}(\omega)$ ($i = x, y, z$)

$$\sigma_{ii}(\omega) = \frac{\omega_p^2}{4i\pi\omega} \left\{ \int_{-\omega}^0 d\nu th\left(\frac{\omega+\nu}{2T}\right) S^{-1}(\omega, \nu) + \int_0^{\infty} d\nu [th\left(\frac{\omega+\nu}{2T}\right) - th\left(\frac{\nu}{2T}\right)] S^{-1}(\omega, \nu) \right\}, \quad (64)$$

where $S(\omega, \nu) = \omega + \Sigma_{tr}^*(\omega + \nu) - \Sigma_{tr}(\nu) + i\gamma_{tr}^{imp}$, and γ_{tr}^{imp} is the impurity contribution. In the following we

omit the tensor index ii in $\sigma_{ii}(\omega)$. In the presence of several bosonic scattering processes the transport self-energy $\Sigma_{tr}(\omega) = Re\Sigma_{tr}(\omega) + iIm\Sigma_{tr}(\omega)$ is given by

$$\Sigma_{tr}(\omega) = -\sum_l \int_0^{\infty} d\nu \alpha_{tr,l}^2 F_l(\nu) [K_1(\omega, \nu) + iK_2(\omega, \nu)], \quad (65)$$

$$K_1(\omega, \nu) = Re\left[\Psi\left(\frac{1}{2} + i\frac{\omega+\nu}{2\pi T}\right) - \Psi\left(\frac{1}{2} + i\frac{\omega-\nu}{2\pi T}\right)\right], \quad (66)$$

$$K_2(\omega, \nu) = \frac{\pi}{2} [2cth\left(\frac{\nu}{2T}\right) - th\left(\frac{\omega+\nu}{2T}\right) + th\left(\frac{\omega-\nu}{2T}\right)] \quad (67)$$

Here $\alpha_{tr,l}^2 F_l(\nu)$ is the *transport spectral function* which measures the strength of the l -th (bosonic) scattering process and Ψ is the digamma function. The index l enumerates EPI, charge and spin-fluctuation scattering processes. Like in the case of EPI, the transport bosonic spectral function $\alpha_{tr,l}^2 F(\Omega)$ is given explicitly by

$$\alpha_{tr,l}^2 F(\omega) = \frac{1}{N^2(\mu)} \int \frac{dS_{\mathbf{k}}}{v_{F,\mathbf{k}}} \int \frac{dS_{\mathbf{k}'}}{v_{F,\mathbf{k}'}} \times \left[1 - \frac{v_{F,\mathbf{k}}^i v_{F,\mathbf{k}}^i}{(v_{F,\mathbf{k}}^i)^2} \right] \alpha_{\mathbf{k}\mathbf{k}',l}^2 F(\omega). \quad (68)$$

We stress that in the phenomenological SFI theory [6] one assumes $\alpha_{\mathbf{k}\mathbf{k}'}^2 F(\omega) \approx N(\mu) g_{sf}^2 \text{Im}\chi(\mathbf{k} - \mathbf{p}, \omega)$, which, as we have repeated several times, can be justified only for small g_{sf} , i.e. $g_{sf} \ll W_b$ (the band width).

In case of weak coupling ($\lambda < 1$), $\sigma(\omega)$ can be written in the generalized (extended) Drude form as discussed in Section III.B.

-
- [1] E. G. Maksimov, Uspekhi Fiz. Nauk **170**, 1033 (2000); V. L. Ginzburg, E. G. Maksimov, Physica **C 235-240**, 193 (1994); Superconductivity (in Russian) **5**, 1505 (1992)
- [2] M. L. Kulić, Phys. Reports **338**, 1-264 (2000)
- [3] C. Falter, phys. stat. solidi (b) **242**, 118 (2005)
- [4] A. S. Alexandrov, arXiv:0808.3520; T. M. Hardy, J. P. Hague, J. H. Samson, A. S. Alexandrov, arXiv:0806.2810
- [5] O. Gunnarsson, O. Rösch, J. Phys: Condens. Matter **20**, 043201 (2008); O. Rösch, J. E. Hahn, O. Gunnarsson, V. H. Crespi, phys. stat. solidi (b) **242**, 78 (2005)
- [6] A. J. Millis, H. Monien, D. Pines, Phys. Rev. **B 42**, 167 (1990); P. Monthoux and D. Pines, Phys. Rev. Lett. **69**, 961 (1992); Phys. Rev. B **47**, 6069 (1993); B. P. Stojković, D. Pines, Phys. Rev. **B56**, 11931 (1997); D. Pines, preprint CNSL Newsletter, LALP-97-010, No. 138, June 1997; Physica **B163**, 78 (1990)
- [7] P. A. Lee, N. Nagaosa, C.-G. Wen, Rev. Mod. Phys. **78**, 17 (2006)
- [8] T. Ami, M. Imada, J. Phys. Soc. Jpn. **76**, 113708 (2007)
- [9] D. J. Scalapino, S. R. White, S. C. Zhang, Phys. Rev. Lett. **68**, 2830 (1992)
- [10] L. Pryadko, S. Kivelson, O. Zachar, Phys. Rev. Lett. **92**, 067002 (2004)
- [11] A. Damascelli, Z. Hussain, Z. -X. Shen, Rev. Mod. Phys. **75**, 473 (2003); J. C. Campuzano, M. R. Norman, M. Randeria, cond-mat/0209476 (2002)
- [12] J. Hwang et al., Phys. Rev. Lett. **100**, 137005 (2008)
- [13] R. Heid et al., Phys. Rev. Lett. **100**, 137001 (2008)
- [14] F. Giustino et al., Nature **452**, 975 (2008)
- [15] E. G. Maksimov, M. L. Kulić, O. V. Dolgov, G. Akpojotor, in preparation
- [16] Ph. Bourges, in *The Gap Symmetry and Fluctua-*

- tions in *High Temperature Superconductors*, J. Bok, G. Deutscher, D. Pavuna, S. A. Wolf, Eds. (Plenum, New York, 1998), pp. 349-371; preprint cond-mat/9901333 (1999)
- [17] P. B. Allen, *Phys. Rev.* **B3**, 305 (1971)
- [18] O. V. Dolgov, S. V. Shulga, *J. of Superconductivity* **8**, 611 (1995); S. V. Shulga, O. V. Dolgov, E. G. Maksimov, *Physica* **C178**, 266 (1991), O. V. Dolgov, E. G. Maksimov, S. V. Shulga, in *Electron-Phonon Interaction in Oxide Superconductors*, ed. R. Baquero, World Scien., p.30 (1991)
- [19] S. V. Shulga, in *High- T_c Superconductors and Related Materials*, p. 323 (2001), eds. S.-L. Drechsler, T. Mishonov, Kluwer Academic Publishers
- [20] A. E. Karakozov, E. G. Maksimov, O. V. Dolgov, *Sol. St. Comm.* **124**, 119 (2002)
- [21] A. E. Karakozov, E. G. Maksimov, *Solid St. Commun.* **139**, 80 (2006)
- [22] P. Kusar et al., arXiv: 0805.0536v2
- [23] L. N. Bulaevskii, O. V. Dolgov, I.P. Kazakov, S.N. Maksimovskii, M.O. Ptitsyn, V.A. Stepanov, S.I. Vedeneev, *Supercond. Science & Technology*, **1**, 205 (1988); S. I. Vedeneev, A. G. M. Jensen, P. Samuely, V. A. Stepanov, A. A. Tsvetkov and P. Wyder, *Phys. Rev.* **49**, 9823 (1994); S. I. Vedeneev, A. G. M. Jansen, A. A. Tsvetkov, P. Wyder, *Phys. Rev.* **B 51**, 16380 (1995); S. I. Vedeneev, A. G. M. Jensen and P. Wyder, *Physica* **B 218**, 213 (1996)
- [24] D. Shimada, Y. Shiina, A. Mottate, Y. Ohyagi and N. Tsuda, *Phys. Rev.* **B 51**, 16495 (1995); N. Miyakawa, A. Nakamura, Y. Fujino, T. Kaneko, D. Shimada, Y. Shiina and N. Tsuda, *Physica C* 282-287, 1519 (1997);
- [25] N. Miyakawa, Y. Shiina, T. Kaneko and N. Tsuda, *J. Phys. Soc. Jpn.* **62**, 2445 (1993); N. Miyakawa, Y. Shiina, T. Kido and N. Tsuda, *J. Phys. Soc. Jpn.* **58**, 383 (1989)
- [26] Y. Shiina, D. Shimada, A. Mottate, Y. Ohyagi and N. Tsuda, *J. Phys. Soc. Jpn.* **64**, 2577 (1995); Y. Ohyagi, D. Shimada, N. Miyakawa, A. Mottate, M. Ishinabe, K. Yamauchi and N. Tsuda, *J. Phys. Soc. Jpn.* **64**, 3376 (1995)
- [27] R. S. Gonnelli, F. Asdente and D. Andoreone, *Phys. Rev.* **B 49**, 1480 (1994)
- [28] D. Shimada et al., *Physica C* **298**, 195 (1998); N. Tsuda et al., in *New Research on Superconductivity*, Ed. Barry P. Martinis, pp. 105-141, 2007 Nova Science Publishers, Inc.
- [29] Y. G. Ponomarev et al., in Proc. of the Intern. Conf. on Strongly Correlated Systems, Houston, Texas, USA, May 13-17, 2007, p. 190; *Physica C* (2008)
- [30] K. McElroy, R. W. Simmonds, J. E. Hoffman, D. H. Lee, K. M. Lang, J. Orenstein, H. Eisaki, S. Uchida, J. C. Davis, *Nature* **422**, 592 (2003); J. Lee et al., *Bull. Am. Phys. Soc.* **50**, 299 (2005); J. C. Davis et al., *Bull. Am. Phys. Soc.* **50**, 1223 (2005)
- [31] F. Marsiglio et al., *Phys. Rev.* **B50**, 7023 (1994)
- [32] O. Klein et al., *Phys. Rev.* **B50**, 6307 (1994)
- [33] D. G. Hinks, J. D. Jorgensen, *Physica C***385**, 98 (2003)
- [34] J. C. Phillips, *phys. stat. solidi (b)* **242**, 51 (2005)
- [35] M. L. Cohen, P. W. Anderson, *Superconductivity in d and f band metals*, AIP Conference Proceedings (ed. D. H. Douglass) New York, p.17 (1972); reprint in P.W. Anderson A Career in Theoretical Physics (World Scientific, 1994) p. 288
- [36] O. V. Dolgov, E. G. Maksimov, *Uspekhi Fiz. Nauk* **177**, 983 (2007) (*Phys.-Uspekhi*, 50, 933 (2007))
- [37] D. A. Kirzhnits, in *High Temperature Superconductivity*, eds. V. L. Ginzburg and D. Kirzhnits, Consultant Bureau New York, London, 1982; D. A. Kirzhnits, Chapter 2 in: "Dielectric Function of Condensed Systems", eds. L.V.Keldysh, D.A.Kirzhnits, A.A.Maradudin, Elsevier Publ., Amsterdam (1989)
- [38] O. V. Dolgov, D. A. Kirzhnits, E. G. Maksimov, *Rev. Mod. Phys.* **53**, 81 (1981); O.V. Dolgov, D.A. Kirzhnits, E.G. Maksimov, Chapter 2 in: "Superconductivity, Superdiamagnetism and Superfluidity", ed. by V.L.Ginzburg, MIR Publ., Moscow (1987) (in English); O.V. Dolgov, E.G.Maksimov, Chapter 4 in: "Dielectric Function of Condensed Systems", eds. L.V.Keldysh, D.A.Kirzhnits, A.A.Maradudin, Elsevier Publ., Amsterdam (1989)
- [39] J. E. Moussa, M. L. Cohen, *Phys. Rev.* **B 74**, 094520 (2006)
- [40] P. W. Anderson, *Science* **316**, 1705 (2007)
- [41] C. C. Tsuei, J. R. Kirtley, *Rev. Mod. Phys.* **72**, 969 (2000)
- [42] A. I. Lichtenstein, M. L. Kulić, *Physica C* **245**, 186 (1995)
- [43] D. J. Scalapino, *Physics Reports* **250**, 329(1995)
- [44] M. L. Kulić, *AIP Conference Proceedings Volume* **715**, 75 (2004), Lectures On The Physics Of Highly Correlated Electron Systems; M. L. Kulić, O. V. Dolgov, *phys. stat. solidi (b)* **242**, 151 (2005)
- [45] M. L. Kulić, R. Zeyher, *Phys. Rev.* **B 49**, 4395 (1994); *Physica C* **199-200**, 358 (1994); *Physica C* **235-240**, 358 (1994)
- [46] H. Y. Kee, S. A. Kivelson, G. Aeppli, *Phys. Rev. Lett.* **88**, 257002 (2002)
- [47] M. L. Kulić, I. M. Kulić, *Physica* **391**, 42 (2003)
- [48] A. Lanzara et al., *Nature* **412**, 510 (2001)
- [49] T. Valla et al., *Science* **285**, 2110 (1999)
- [50] I. Božović, *Phys. Rev.* **B 42**, 1969 (1990)
- [51] Z. Schlesinger et al., *Phys. Rev. Lett.* **65**, 801 (1990)
- [52] D. B. Romero et al., *Phys. Rev. Lett.* **68**, 1590 (1992); D. B. Romero et al., *Sol. St. Comm.* **82**, 183 (1992)
- [53] A. V. Puchkov, D. N. Basov, T. Timusk, *J. Phys.: Condens. Matter* **8**, 10049 (1996); J. Hwang, T. Timusk, G. D. Gu, *Nature* **427**, 714 (2004); M. Norman, *Nature* **427**, 692 (2004).
- [54] F. Gao et al., *Phys. Rev.* **B47**, 1036 (1993)
- [55] A. V. Boris et al., *Science* **304**, 708 (2004).
- [56] H. J. Kaufmann, Ph. D. Thesis, Uni. Cambridge, February 1999
- [57] J. Schutzmann et al., *Phys. Rev.* **B46**, 512 (1992)
- [58] K. Kamaras et al., *Phys. Rev. Lett.* **64**, 84 (1990)
- [59] E. Schachinger, J. P. Carbotte, *Phys. Rev.* **B 64**, 094501 (2001)
- [60] J. Hwang et al., *Phys. Rev.* **B75**, 144508 (2007); J. Hwang et al., *Nature (London)* **427**, 714 (2004)
- [61] B. Vignolle et al., *Nature Phys.* **3**, 163 (2007)
- [62] I. Božović, J. H. Kim, J. S. Harris, Jr., C. B. Eom, J. M. Phillips, J. T. Cheung, *Phys. Rev. Lett.*, **73**, 1436 (1995)
- [63] J. E. Hirsch, *Physica* **201**, 347 (1992)
- [64] P. F. Maldague, *Phys. Rev.* **B16**, 2437 (1977)
- [65] F. Carbone et al., *Phys. Rev.* **B74**, 024502 (2006); F. Carbone et al., *Phys. Rev.* **B74**, 064510 (2006)
- [66] H. J. Molegraaf et al., *Science* **295**, 2239 (2002)

- [67] G. Deutscher et al., Phys. Rev. **B72**, 095504 (2005)
- [68] H. J. Kaufmann, E. G. Maksimov, E. K. H. Salje, J. of Supercond. **11**, 755 (1998)
- [69] I. I. Mazin, O. V. Dolgov, Phys. Rev. **B45**, 2509 (1992)
- [70] T. A. Friedman et al., Phys. Rev. **B42**, 6217 (1990)
- [71] P. B. Allen, Nature **412**, 494 (2001)
- [72] A. F. Santander-Syro et al., Europhys. Lett. **62**, 568 (2003)
- [73] R. Zeyher, M. L. Kulić, Phys. Rev. **B53**, 2850 (1996); R. Zeyher, M. L. Kulić, Phys. Rev. **B54**, 8985 (1996); M. L. Kulić and R. Zeyher, Mod. Phys. Lett. **B 11**, 333 (1997)
- [74] D. Mihailović, V. V. Kabanov, Struct Bond (2005) **114**, p. 331-364, Springer-Verlag Berlin-Heidelberg 2005
- [75] V. V. Kabanov et al., Phys. Rev. Lett. **95**, 147002 (2005)
- [76] A. Bansil, M. Lindros, Phys. Rev. Lett. **83**, 5154 (1999)
- [77] T. Cuk et al., Phys. Rev. Lett. **93**, 117003 (2004)
- [78] X. J. Zhou et al., Phys. Rev. Lett. **95**, 117001 (2005)
- [79] M. L. Kulić, O. V. Dolgov, Phys. Rev. **B 76**, 132511 (2007)
- [80] T. Cuk et al., phys. stat. solidi (b) **242**, 11 (2005)
- [81] G.-H. Gweon et al., Nature **430**, 187 (2004)
- [82] E. G. Maksimov, O. V. Dolgov, M. L. Kulic, Phys. Rev. **B72**, 212505 (2005)
- [83] T. Valla, T. E. Kidd, Z.-H. Pan, A. V. Fedorov, W.-G. Yin, G. D. Gu, P. D. Johnson, Phys. Rev. Lett. **98**, 167003 (2007)
- [84] K. M. Shen et al., Phys. Rev. Lett. **93**, 267002 (2004)
- [85] O. Rösch et al., Phys. Rev. Lett. **95**, 227002 (2005); A. S. Mishenko, N. Nagaosa, Phys. Rev. Lett. **93**, 036402 (2004); S. Ciuchi et al., Phys. Rev. **B 56**, 4494 (1997)
- [86] M. Tsunekawa, New Journal of Physics **10**, 073005 (2008)
- [87] S. R. Park et al., Phys. Rev. Lett. **101**, 117006 (2008)
- [88] M. L. Kulić, O. V. Dolgov, Phys. Rev. **B 71**, 092505 (2005)
- [89] Y. Chen et al., Phys. Rev. Lett. **97**, 23640 (2006)
- [90] W. Xie et al., Phys. Rev. Lett. **98**, 047001 (2007)
- [91] L. Zhu, P. J. Hirschfeld, D. J. Scalapino, Phys. Rev. **B70**, 214503 (2004)
- [92] M. L. Kulić, V. Oudovenko, Solid State Comm. **104**, 731 (1997)
- [93] M. L. Kulić, O. V. Dolgov, Phys. Rev. **B60**, 13062(1999)
- [94] H. -Y. Kee, Phys. Rev. **B64**, 012506(2001)
- [95] J. Kirtley et al., in Superconductivity I, eds. J. Kettersson, K. H. Bennemann, 2008 Springer Verlag, Berlin
- [96] B. Renker et al., Z. Phys. **B77**, 65 (1989)
- [97] G. Deutscher et al., J. Supercond. **7**, 371 (1994)
- [98] Y. Sidis et al., phys. stat. sol. (b) **241**, 1204 (2004) and References therein
- [99] O. Fischer et al., Rev. Mod. Phys. **79**, 353 (2007)
- [100] O. K. Andersen, O. Jepsen, A. I. Lichtenstein, I. I. Mazin, Phys. Rev. **B49**, 4145 (1994)
- [101] Q. Huang, J. F. Zasadinski, N. Tralshawala, K. E. Gray, D. Hinks, J. L. Peng and R. L. Greene, Nature (London) **347**, 389 (1990)
- [102] P. Samuely, N. L. Bobrov, A. G. N. Jansen, P. Wyder, S. N. Barilo, S. V. Shiryayev, Phys. Rev. **B48**, 13904 (1993); P. Samuely, P. Szabo, A. G. N. Jansen, P. Wyder, J. Marcus, C. Escribe-Filippini, M. Afronte, Physica **B 194-196**, 1747 (1994)
- [103] O. Rösch, O. Gunnarsson, Phys. Rev. Lett. **92**, 146403 (2004)
- [104] K. J. Szczepanski, K. W. Becker, Z. Phys. **B89**, 327 (1992); G. Khaliullin, P. Horsch, Phys. Rev. **B54**, R9600 (1996)
- [105] S. N. Rashkeev and G. Wendin, Phys. Rev. **B47**, 11603 (1993)
- [106] T. Bauer, C. Falter, arXiv:0808.2765
- [107] J. F. Franck, in *Physical Properties of High Temperature Superconductors V*, ed. D. M. Ginsberg, (World Scientific, Singapore, 1994); Physica **C282-287**, 198 (1997)
- [108] L. Pintschovius, phys. stat. solidi (b) **242**, 30 (2005)
- [109] K. -P. Bohnen, R. Heid, M. Kraus, Europhys. Lett. **64**, 104 (2003)
- [110] D. Reznik et al., Nature **455**, E6 (2008)
- [111] C. Thomsen, M. Cardona, B. Gegenheimer, R. Liu and A. Simon, Phys. Rev. **B 37**, 9860 (1988)
- [112] C. Thomsen and M. Cardona, in Physical Properties of High Temperature Superconductors I, ed. by D. M. Ginzberg (World Scientific, Singapore, 1989), pp. 409; R. Feile, Physica **C 159**, 1 (1989); C. Thomsen, in Light Scattering in Solids VI, ed. by M. Cardona and G. Guentherodt (Berlin, Heidelberg, New York, Springer, 1991), pp. 285
- [113] V. G. Hadjiev, X. Zhou, T. Strohm, M. Cardona, Q. M. Lin, C. W. Chu, Phys. Rev. **B 58**, 1043 (1998)
- [114] D. Reznik et al., Nature **440**, 1170 (2006); D. Reznik et al., J. Low Temp. Phys. **147**, 353 (2007); L. Pintschovius et al., Phys. Rev. **B69**, 214506 (2004)
- [115] J. F. Douglas et al., Nature **446**, E5 (2007)
- [116] H. Iwasawa et al., Physica **C463-465**, 52 (2007)
- [117] H. Iwasawa et al., arXiv: 0808.1323
- [118] P.B. Allen, B. Mitrović, Solid State Physics, ed. H. Ehrenreich, F. Seitz, D. Turnbull, Academic, New York, **V37**, p. 1, (1982)
- [119] O. V. Dolgov, E. G. Maksimov, Uspekhi Fiz. Nauk **138**, 95 (1982); O.V. Dolgov, E.G.Maksimov, Chapter 1 in: "Thermodynamics and Electrodynamics of Superconductors", ed. by V.L.Ginzburg, Nova Science Publ., N.Y.(1987)
- [120] F. Marsiglio, J. P. Carbotte, in Superconductivity I, eds. J. Kettersson, K. H. Bennemann, 2008 Springer Verlag, Berlin
- [121] W. L. McMillan and J. M. Rowell, Phys. Rev. Lett. **14**, 108 (1965)
- [122] A. A. Galkin, A. I. Dyashenko, V. M. Svistunov, Zh. Eksp. Teor. Fiz., **66**, 2262 (1974); V. M. Svistunov et al, J. Low Temp. Phys. **31**, 339 (1978)
- [123] Yu. M. Ivanshenko, Yu. V. Medvedev, Fiz. Nizkih Temp., **2**, 143 (1976)
- [124] J. R. Schrieffer, *Theory of Superconductivity*, New York, (1964)
- [125] D. J. Scalapino, J. R. Schrieffer, J. W. Wilkins, Phys. Rev. **148**, 263 (1966)